



ADAPTATION OF THE AIR WEATHER SERVICE FO
MODEL TO FORECAST RADIATION FOG EVENTS
IN THE SOUTHEAST UNITED STATES

THESIS

Andrew C. Goodnite, Captain, USAF

DISTRIBUTION STATEMENT A

Approved for public release;
Distribution Unlimited

DEPARTMENT OF THE AIR FORCE
AIR UNIVERSITY
AIR FORCE INSTITUTE OF TECHNOLOGY

Wright-Patterson Air Force Base, Ohio

DTIC QUALITY INSPECTED 1

AFIT/GM/ENP/97M-06

ADAPTATION OF THE AIR WEATHER SERVICE FOG
MODEL TO FORECAST RADIATION FOG EVENTS
IN THE SOUTHEAST UNITED STATES

THESIS

Andrew C. Goodnite, Captain, USAF

AFIT/GM/ENP/97M-06

Approved for public release; distribution unlimited

19970402 079

The views expressed in this thesis are those of the
author and do not reflect the official policy or position
of the Department of Defense of the U. S. Government

AFIT/GM/ENP/97M-06

ADAPTATION OF THE AIR WEATHER SERVICE FOG MODEL TO FORECAST
RADIATION FOG EVENTS IN THE SOUTHEAST UNITED STATES

THESIS

Presented to the Faculty of the Graduate School of Engineering

Air Education and Training Command

In Partial Fulfillment of the

Requirements for the Degree of

Master of Science in Meteorology

Andrew C. Goodnite, B.S.

Captain, USAF

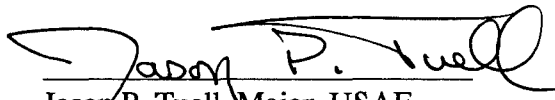
March 1997

Approved for public release, distribution unlimited


ADAPTATION OF THE AIR WEATHER SERVICE FOG MODEL TO FORECAST
RADIATION FOG EVENTS IN THE SOUTHEAST UNITED STATES

Andrew C. Goodnite, B.S.
Captain, USAF

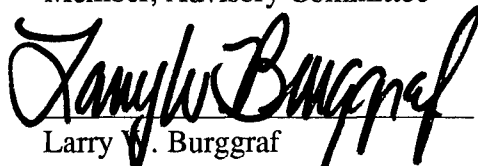
Approved:


Jason P. Tuell, Major, USAF
Chairman, Advisory Committee

7 March 97
date


Michael K. Walters, Lt Col, USAF
Member, Advisory Committee

7 March 97
date


Larry V. Burggraf
Member, Advisory Committee

10 Mar 97
date

Acknowledgments

I would like to take this opportunity to thank the many people who have helped me in this research and preparation of this thesis.

First, I must thank James O'Sullivan from St. Louis University. Your assistance in providing the fog model program and your answers to my many questions were a tremendous help with my research project.

Next, I would like to thank my thesis advisor Dr. Jason Tuell. Our stimulating conversations and your supportive answers gave me the right amount of assistance when I needed it.

Last, but certainly not least, I must thank the three people who have sacrificed the most through this whole time. My children, Jessica and Amy, who loved daddy even when his temper tantrums were both loud and frequent, and my best friend, (who also happens to be my wife), Regina. You are always there for me through better or worse. May the better begin now.

Table of Contents

Acknowledgments	iii
List of Figures	vii
List of Tables.....	xi
Table of Symbols.....	xii
Abstract.....	xiv
1. Background and Statement of the Problem	1
1.1 Background.....	1
1.2 Statement of the Problem.....	2
1.3 Organization.....	4
2. Radiation Fog Formation Processes and Modeling of these Processes	5
2.1 Fundamental Processes Responsible for Fog Formation.....	5
2.2 Observational Studies and Modeling Attempts	7
2.3 Development and Structure of the AWS Fog Model	15
2.4 Adaptation of AWS Fog Model to the Southeast United States	18
3. Data Analysis.....	21
3.1 Method of Limiting Observational Data	21

3.2 Parameterization of Soil Moisture	23
3.3 Analysis of Temperature and Dewpoint.....	27
3.4 Analysis of Wind Speed	30
3.5 Analysis of Wind Direction	31
3.6 Regression Analysis of Fog Model Input Variables.....	32
4. Verification and Sensitivity Study of the AWS Fog Model	34
4.1 Statistics used in Verification Study	34
4.2 SLU Version Verification	36
4.2.1 SLU Version Verification Results for Summer Season.....	37
4.2.2 SLU Version Verification Results for Fall Season.....	42
4.2.3 SLU Version Verification Results of a Single Summer Fog Event.....	46
4.2.4 SLU Version Verification Results of a Single Fall Non-Fog Event.....	53
4.3 Sensitivity Study	57
4.3.1 Sensitivity Tests on Soil Type	58
4.3.2 Sensitivity Tests on Soil Relative Humidity (RH).....	59
4.3.3 Sensitivity Tests on Wind Speed.....	60
4.3.4 Sensitivity Tests on Temperature and Dewpoint	60
4.3.5 Results of Sensitivity Study of Longwave Parameter, Shortwave Parameter, and Height of Observation Level.....	61
4.3.6 Results of Sensitivity Study of Lapse Rate.....	62
4.4 Verification Study of Adapted Version.....	65

4.4.1 Adapted Version Verification Results for Summer Season.....	65
4.4.2 Adapted Version Verification Results for Fall Season	66
4.5 Suggestions for Operational Use of the AWS Fog Model.....	74
5. Conclusions and Recommendations for Future Work	77
5.1 Summary of Conclusions	77
5.2 Recommendations for Future Research	82
Bibliography	84
Appendix.....	86
Vita.....	120

List of Figures

Figure 2.1. Vertical Representation of Fog Model.....	16
Figure 2.2. Example of longwave surface cooling	18
Figure 3.1. Scatter plot parameterization of soil moisture versus visibility	25
Figure 3.2. Predicted 10 m temperature and dewpoint with soil RH set to 30 %.....	26
Figure 3.3. Predicted 10 m temperature and dewpoint with soil RH set to 50 %.....	26
Figure 3.4. Predicted 10 m temperature and dewpoint with soil RH set to 70%.....	27
Figure 3.5. Scatter plot dewpoint depression versus visibility	29
Figure 3.6 Scatter plot 22 UTC dewpoint depression versus 11 UTC visibility	29
Figure 3.7. Scatter plot wind speed versus visibility	30
Figure 3.8. Scatter plot wind direction versus visibility.....	31
Figure 4.1. Mean temperature difference between observed temperature and model 10 meter temperature for 61 summer radiation cooling events.....	41
Figure 4.2. Mean dewpoint difference between observed dewpoint and 10 meter model dewpoint for 61 summer radiation cooling events.....	41
Figure 4.3. Visibility at 11 UTC for 61 summer radiation cooling events.....	42
Figure 4.4. Mean temperature difference between observed temperature and model 10 meter temperature for 61 fall radiation cooling events.	45
Figure 4.5. Mean dewpoint difference between observed dewpoint and 10 meter model dewpoint for 61 fall radiation cooling events.	45
Figure 4.6. Visibility at 11 UTC for 61 fall radiation cooling events.	46

Figure 4.7. Hourly observations of temperature and dewpoint from 28 - 29 August	
1985	48
Figure 4.8. Predicted surface temperature and dewpoint based on 22 UTC 28 August	
1985 data using SLU version of model.....	49
Figure 4.9. Predicted 10 meter temperature and dewpoint based on 22 UTC 28 August	
1985 data using SLU version of model.....	49
Figure 4.10. Predicted 200 meter temperature and dewpoint based on 22 UTC 28 August	
1985 data using SLU version of model.....	50
Figure 4.11. Comparison of observed temperature and predicted surface temperature	
based on 22 UTC 28 August 1985 data using SLU version of model.....	50
Figure 4.12. Comparison of observed temperature and predicted 10 meter temperature	
based on 22 UTC 28 August 1985 data using SLU version of model.....	51
Figure 4.13. Comparison of observed dewpoint and predicted 10 meter dewpoint based	
on 22 UTC 28 August 1985 data using SLU version of model	51
Figure 4.14. Comparison of observed visibility and predicted 10 meter visibility based on	
22 UTC 28 August 1985 data using SLU version of model.	52
Figure 4.15. Hourly observations of temperature and dewpoint from 9 - 10 November	
1985	54
Figure 4.16. Predicted surface temperature and dewpoint based on 22 UTC 9 November	
1985 data using SLU version of model.....	54
Figure 4.17. Predicted 10 meter temperature and dewpoint based on 22 UTC 9	
November 1985 data using SLU version of model.....	55

Figure 4.18. Predicted 200 meter temperature and dewpoint based on 22 UTC 9 November 1985 data using SLU version of model.....	55
Figure 4.19. Comparison of observed temperature and predicted 10 meter temperature based on 22 UTC 9 November 1985 data using SLU version of model.....	56
Figure 4.20. Comparison of observed dewpoint and predicted 10 meter dewpoint based on 22 UTC 9 November 1985 data using SLU version of model.	56
Figure 4.21. Comparison of observed visibility and predicted 10 meter visibility based on 22 UTC 9 November 1985 data using SLU version of model.	57
Figure 4.22. Visibility at 11 UTC for 61 summer radiation cooling events using adapted model	70
Figure 4.23. Visibility at 11 UTC for 61 fall radiation cooling events using adapted model	70
Figure 4.24. Comparison of observed and predicted 10 meter temperature based on 22 UTC 28 August 1985 data using adapted version of model.	71
Figure 4.25. Comparison of observed dewpoint and predicted 10 meter dewpoint based on 22 UTC 28 August 1985 data using adapted version of model.....	71
Figure 4.26. Comparison of observed visibility and predicted 10 meter visibility based on 22 UTC 28 August 1985 data using adapted version of model.	72
Figure 4.27. Comparison of observed temperature and predicted 10 meter temperature based on 22 UTC 9 November 1985 data using adapted version of model.....	72
Figure 4.28. Comparison of observed dewpoint and predicted 10 meter dewpoint based on 22 UTC 9 November 1985 data using adapted version of model.....	73

Figure 4.29. Comparison of observed visibility and predicted 10 meter visibility based on	
22 UTC 9 November 1985 using adapted version of model	73

List of Tables

Table 3.1. Precipitation Data Parameterization.....	24
Table 4.1. SLU Version Verification Results for Summer Season.....	40
Table 4.2. SLU Version Verification Results for Fall Season.....	44
Table 4.3. Results of Sensitivity Tests using SLU Version.....	63
Table 4.4. Adapted Version Verification Results for Summer Season.....	68
Table 4.5. Adapted Version Verification Results for Fall Season	69

Table of Symbols

Bias	the ratio of the number of times fog was forecasted to the number of times fog occurred
C	rate of condensation per unit mass of air
c_p	specific heat of air at constant pressure
FAR	false alarm rate
F_{NL}	net long-wave radiative flux, positive downwards
G	gravitational setting flux of liquid water, positive downwards
g	gravity
K_h, K_q, K_w	exchange coefficients for heat, water vapor and liquid water respectively (assumed equal)
k_{Mol}	molecular diffusion coefficient
k'	Von Karman's constant
L	latent heat of condensation
n	time step
PC	proportion correct
POD	probability of detection
Q	the atmospheric variable being considered
q	humidity mixing ratio
q_l	liquid water content
R	stability parameter
SS	persistence based skill score
S	sources and sinks of the property Q
T	temperature of air
T_s	surface temperature
t	time (in seconds)
u, v	components of the wind velocity along the x and y axis
\underline{V}	the horizontal wind vector
W	the number of times the event was not predicted and did not occur

X	the number of times the event was predicted and occurred
Y	the number of times the event was not predicted but occurred
Z	the number of times the event was predicted but did not occur
z	height coordinate
∇	the horizontal ∇ operator
w	liquid water mixing ratio
ρ	density of air
θ	potential temperature

Abstract

This research examined the performance of the Air Weather Service (AWS) Fog Model and the potential for using it in the Southeast United States for predicting fog. This task was accomplished in four separate steps. First, a correlation study was performed by comparing different weather elements in observations that met radiational cooling conditions to the observed visibility. This correlation study showed that the 22 UTC dewpoint depression was correlated (0.60) with early morning fog and no other weather elements that are commonly observed had significant correlation with early morning fog. Second, a verification study was conducted on the Saint Louis University (SLU) version of the fog model. This verification study showed that the fog model has an underforecasting bias in the summer season and an overforecasting bias in the fall season and that persistence forecasts beats fog model forecasts for both seasons. Third, a sensitivity study was conducted on the fog model. The sensitivity study showed that the fog model is sensitive to the value input for wind speed; the fog model predicts more fog events as the wind speed is increased. Finally, the SLU version of the AWS Fog Model was modified to adapt it to the Southeast United States and another verification study was conducted. The fog model was adjusted to remove the summer underforecasting bias and the fall overforecasting bias. After this adjustment, the fog model verification scores showed a slight improvement over the verification of the SLU version of the fog model.

ADAPTATION OF THE AIR WEATHER SERVICE FOG MODEL TO FORECAST RADIATION FOG EVENTS IN THE SOUTHEAST UNITED STATES

1. Background and Statement of the Problem

1.1 Background

Numerical modeling of radiation fog has received a great deal of attention over the past thirty years. Forecasting fog formation using operational synoptic scale models has not made much progress in recent years. This is because fog forecasting requires an accurate representation of the nocturnal boundary layer, radiative cooling near the surface and turbulence in stratified layers, a high resolution vertical grid close to the surface since fog rarely exceeds 100 m in height, and a parameterization of soil - atmosphere interactions (Bergot and Guedalia 1994). The current operational synoptic scale models lack many of these features.

There are several types of fog, for example radiation, advection, sea, upslope, etc., all of which form by different mechanisms. This work focuses on the use of a one dimensional (1D) model to forecast radiation fog in the Southeast United States.

Radiation fog forms when the surface cools during night and causes the adjacent air layer to reach saturation through turbulent heat and moisture exchange (O'Sullivan 1996). Since radiation fog can be described as a vertical phenomena which occurs over a limited horizontal area, and operational synoptic scale models lack many of the necessary processes which control fog formation, several 1D models have been developed for predicting fog.

1.2 Statement of the Problem

Air Weather Service (AWS), in conjunction with St. Louis University (SLU), has developed one of these 1D fog forecasting models for use by Air Force bases in California. Air Force weather stations in the southeastern part of the United States have requested assistance in improving their ability to forecast radiation fog. Some changes and adjustments were made to the SLU version of the AWS Fog Model to adapt it to the Southeast United States. The revised model also requires verification before it can be used operationally in this area. Forecasting the onset, intensity, and duration of fog events accurately is critical to Air Force operations. Correct fog forecasting gives the mission planners enough time to plan the next day's missions around limitations imposed by the weather. Also, accurate fog forecasts allow air traffic controllers and flight planners to plan and coordinate flights around airfields that are expected to be unusable

due to fog. In a wartime situation forecasting fog and low stratus clouds can significantly add to the effectiveness of flight and ground operations. For example, the detection and lock-on ranges for IR and TV sensors are very dependent on visibility over the target. A fog or stratus layer between the target and sensor will greatly reduce the detection and lock-on ranges of the sensors. Accurate forecasting of fog and stratus will allow mission planners to plan missions over targets that are not obscured by fog or stratus.

The purpose of this research is to verify performance of the AWS Fog Model and adapt it for use as a forecast tool to aid Air Force forecasters in predicting radiation fog events in the Southeast United States. This task was accomplished in four steps. First, a correlation study was performed by comparing the different variables in observations that met certain radiational cooling conditions (see Chapter 3) to the observed visibility. This correlation study was necessary to establish the importance of each input variable of the model. Second, a verification study was conducted on the SLU version of the AWS Fog Model. This verification study established the forecast accuracy of the SLU version to predict fog in the Southeast United States. Third, a sensitivity study was conducted on the SLU version of the fog model. This sensitivity study was used to adjust and revise the SLU version of the fog model for application in the Southeast United States. Fourth, the SLU version of the fog model was revised using the results of the sensitivity and verification study. Finally, another verification study was conducted after model parameters were adapted to the Southeast United States.

1.3 Organization

Chapter 2 examines the fundamental processes responsible for fog formation, covers some of the related efforts in the field of numerical fog prediction, describes the development and structure of the SLU version of the AWS Fog Model, and covers the changes made to the SLU version to adapt it the Southeast United States. Chapter 3 describes the method used to limit the observational data, explains the parameterization of the soil moisture input variable, and gives a detailed analysis of the correlation of temperature, dewpoint, wind speed and wind direction to visibility. Chapter 4 contains the verification and sensitivity study of the SLU version of the fog model, and the verification study done after model parameters were adapted to the Southeast United States. Finally, Chapter 5 presents conclusions and recommendations for future work. An appendix is provided for the entire adapted (AFIT) version of the AWS Fog Model (FORTRAN code). This research effort is concerned with tuning the AWS Fog Model to obtain the best possible forecasts of radiation fog in the Southeast. It is not an attempt to criticize or justify the current SLU version of the fog model but to adapt and revise the SLU version to fit the needs of Air Force forecasters in the Southeast.

2. Radiation Fog Formation Processes and Modeling of these Processes

2.1 Fundamental Processes Responsible for Fog Formation

Radiation fog is caused by cooling air from below due to the net loss of longwave radiation at the surface to a temperature below its dewpoint. This can happen during clear windless nights when the ground is cooled by radiation. Advection fog which is caused by the cooling of air below its dewpoint when warm moist air moves over an area with over colder surfaces (Wallace and Hobbs 1977), is not forecasted by the fog model.

The processes that bring about supersaturation and fog formation are defined by Fleagle and Businger (1980) as follows:

- a. mixing of parcels of saturated, or nearly saturated, air at different temperatures and vapor densities may produce a supersaturated mixture,
- b. divergence of net irradiance may result in cooling air below its dewpoint, radiation fog is formed in this way,
- c. adiabatic cooling accompanying upward motion or falling pressure may result in supersaturation and condensation, e.g. upslope fog,
- d. condensation may occur on giant hygroscopic nuclei at relative humidities below 100%, and,
- e. the molecular diffusion coefficient for water vapor in air exceeds the thermal diffusivity coefficient so that water vapor may evaporate so rapidly from warm

surfaces that supersaturation is confined to a laminar layer adjacent to the surface.

According to Meyer and Rao (1995), the job of forecasting low ceilings and visibilities is straightforward: we need simply to predict the diurnal behavior of air mass temperatures and dewpoints near the surface of the earth. Unfortunately, the task is complicated because low ceilings and visibilities are often a race between dew and fog. If the moisture is deposited on the ground as dew faster than it condenses in the air, fog will not form. Experienced forecasters are familiar with the practical problems associated with this race. For example, a heavy early morning dew (or frost) can completely ruin an otherwise perfectly good fog forecast. As a result, when faced with the task in the late afternoon or evening of preparing an early morning fog forecast, forecasters must decide if the moisture available in the late afternoon will be deposited on the ground overnight as dew or will develop into an early morning fog. This delicate balance is explained by Monteith (1957) from observations of dew deposition. He inferred that a drop in wind speed below a certain level may result in a virtual cessation of turbulence. The mechanism for dew deposition thus ceases, so that a saturated atmosphere which continues to cool radiatively is ultimately forced to condense excess water into the air in the form of fog (Roach and Brown 1976).

An important first step in improving one's ability to forecast air mass fog is to improve the understanding of the physical processes responsible for fog, and, for dew or frost. The meteorological processes operating in the air mass must serve to bring the air mass temperature and dewpoints together. The processes can accomplish this by cooling

the air mass (to lower its temperature to its dewpoint) or by moistening the air mass (to elevate its dewpoint to its temperature).

The local processes involved are:

- a. cooling due to long-wave radiation from the surface and clouds,
- b. turbulent mixing of heat and moisture which is a function wind speed and the strength of the inversion, and,
- c. condensational heating of air near the surface due to the formation of dew.

The regional processes involved are:

- a. temperature and moisture advection, and,
- b. upslope cooling or downslope warming.

The physical laws required:

- a. heat moves along the gradient of temperature from the hotter to the colder air, and,
- b. water vapor moves along the gradient of moisture from wetter to dryer air.

2.2 Observational Studies and Modeling Attempts

One of the first attempts at numerical prediction of fog and stratus was made by Fisher and Caplan (1963). The first objective of their study was to determine what kind of observations are needed to forecast fog and stratus. They initially considered the following factors to be most important in affecting the temperature, water vapor content, and liquid water content of a vertical column of air:

- a. the vertical eddy diffusion of these properties,
- b. the horizontal advection, and,
- c. the latent heat associated with the condensation and evaporation.

Their model assumes that the temperature, specific humidity, and liquid water content of a vertical column of the atmosphere obey the following equation:

$$\frac{\partial Q}{\partial t} = \frac{\partial}{\partial z} K_Q \left(\frac{\partial Q}{\partial z} \right) - \underline{V} \cdot \nabla Q + S \quad (2.1)$$

where

Q = the atmospheric variable being considered,

K_Q = coefficient of eddy diffusivity of that property,

\underline{V} = the horizontal wind vector,

∇ = the horizontal ∇ operator, and,

S = sources and sinks of the property Q .

The important processes of radiational cooling of the surface, radiational cooling of the fog and stratus, and the deposition of dew onto the surface were not considered in this early modeling attempt. Fisher and Caplan determined that while their model lacked several important processes to accurately model the nocturnal boundary layer, a model of this type might eventually be brought to a sufficient state of completion to be useful. They also determined that observations of the vertical profiles of specific humidity, liquid water, temperature, and wind are essential for model initialization (Fisher and Caplan 1963).

One of the next attempts at fog modeling was by Zdunkowski and Nielsen (1969). They predicted diurnal changes in temperature and specific humidity, given the following assumptions:

- a. the exchange coefficient is only a function of height,
- b. water vapor and water droplets are the only radiative agents,
- c. the total moisture content of the air (liquid plus water vapor) is conserved, and,
- d. the advection of air is not taken into account.

These assumptions were very restrictive in that the exchange coefficient should also be a function of stability and wind shear. Also, the important process of radiational cooling in the air layer was ignored and the gravitational settling of fog droplets was neglected. This work was improved upon by Zdunkowski and Barr (1972). They parameterized the exchange coefficients as a function of stability, wind shear, and height as follows:

$$K_H = R \left[\left(\frac{\partial u}{\partial z} \right)^2 + \left(\frac{\partial v}{\partial z} \right)^2 - f(\theta) \right] (k'z)^2 + k_{Mol} \quad (2.2)$$

where the quantity, $f(\theta)$ is defined by

$$f(\theta) = \frac{gR}{T} \frac{\partial \theta}{\partial z}, \quad (2.3)$$

and inside of fog $\frac{\partial \theta}{\partial z}$ is defined by

$$\frac{\partial \theta}{\partial z} = \frac{\theta}{T} \left(\frac{\partial T}{\partial z} + \gamma_m \right), \quad (2.4)$$

where,

R = stability parameter,

u, v = components of the wind velocity along the x and y axis,

z = height coordinate,

θ, T = potential and air temperatures,

k' = Von Karman's constant,

k_{Mol} = molecular diffusion coefficient,

g = gravity, and,

γ_m = moist adiabatic lapse rate.

Zdunkowski and Barr (1972) assumed that the geostrophic wind is constant with height and time throughout the boundary layer and that advection effects can be disregarded. The exchange coefficient described above approaches the molecular diffusion coefficient at $z = 0$ as the atmosphere becomes very stable under radiative cooling conditions. The testing of this exchange coefficient parameterization formed the bulk of their research.

A field study of radiation fog published by Roach and Brown (1976) produced the following observations about the physics of radiation fog.

1. Periods of strong cooling and significant fog development occurred primarily when wind speeds dropped below $0.5 - 1 \text{ m s}^{-1}$. Conversely, increasing wind to greater than 2 m s^{-1} appeared to be associated with fog dispersal. Standard airfield anemometers have a stopping speed of about 2 m s^{-1} and such an instrument will record a flat calm throughout most fog events. This feature is consistent with the inferences from observations of dew deposition made by Monteith (1957).

2. The liquid water content of the fog was a small fraction of the total water condensed. Most of the water condensed appears to have been deposited on the ground. This observation highlights a significant mechanism not modeled before Roach and Brown (1976) - the gravitational settling of fog droplets. Gravitational settling reduces liquid water concentrations to approximately $0.1\text{--}0.3\text{ g m}^{-3}$.
3. Radiative cooling as deduced from radiative flux divergence measurements was generally greater than the actual cooling. Roach and Brown (1976) observed that radiative cooling is about twice the observed cooling, the difference is made up by the release of latent heat of condensation and by convergence of eddy heat flux.
4. Developing fog radiatively shields the surface. When this occurs, the radiation inversion migrates to the fog top and is accompanied by the establishment of a convective regime with a slight super-adiabatic lapse rate in the lower part of the fog. The fog top then becomes the effective 'surface' from a radiative and, possibly also from a boundary layer turbulence, view-point. The super-adiabatic lapse rate established in the lowest few meters is probably associated with the upward transfer of soil heat flux (Roach and Brown 1976).

Turton and Brown (1987) published a revised version of the Roach and Brown (1976) model that incorporated the momentum equations and allowed the exchange coefficients to vary with stability. The basic equations used in their model are as follows:

$$\frac{\partial \theta}{\partial t} = \frac{\partial}{\partial z} \left(K_h \frac{\partial \theta}{\partial z} \right) + \frac{\theta}{T} \frac{L}{c_p} C + \frac{1}{\rho c_p} \frac{\theta}{T} \frac{\partial F_{NL}}{\partial z} \quad (2.5)$$

$$\frac{\partial q}{\partial t} = \frac{\partial}{\partial z} \left(K_q \frac{\partial q}{\partial z} \right) - C \quad (2.6)$$

$$\frac{\partial w}{\partial t} = \frac{\partial}{\partial z} \left(K_w \frac{\partial w}{\partial z} \right) + C + \frac{\partial G}{\partial z} \quad (2.7)$$

where

θ = potential temperature of air,

T = temperature of air,

ρ = density of air,

c_p = specific heat of air at constant pressure,

F_{NL} = net long-wave radiative flux, positive downwards,

z = height coordinate with origin at the earth's surface,

K_h, K_q, K_w = exchange coefficients for heat, water vapor and liquid water respectively (assumed equal),

L = latent heat of vaporization,

C = rate of condensation per unit mass of air,

q = humidity mixing ratio,

w = liquid water mixing ratio, and,

G = gravitational setting flux of liquid water, positive downwards.

The above equations were the same as used by Roach and Brown (1976). The temperature distribution within the soil was given by

$$\frac{\partial T_s}{\partial t} = \frac{1}{\rho_s c_s} \frac{\partial}{\partial z} \left(k_s \frac{\partial T}{\partial z} \right) \quad (2.8)$$

where T_s is the soil temperature and ρ_s , c_s , k_s are the density, specific heat, and thermal conductivity of the soil respectively. The one-dimensional momentum equations are

$$\frac{\partial u}{\partial t} = fv + \frac{\partial}{\partial z} \left(k_m \frac{\partial u}{\partial z} \right) \quad (2.9)$$

$$\frac{\partial v}{\partial t} = f(U_g - u) + \frac{\partial}{\partial z} \left(k_m \frac{\partial v}{\partial z} \right) \quad (2.10)$$

where u , v are orthogonal components of the horizontal wind parallel and perpendicular to the direction of the geostrophic wind, respectively, f is the Coriolis parameter, K_m is the exchange coefficient for momentum and U_g is the geostrophic wind, assumed constant with height.

The exchange coefficients are made a function of the local gradient Richardson number (Ri) using the level-2 formulation of Mellor and Yamada (1974):

$$K_m = l^2 \left\{ \left(\frac{\partial u}{\partial z} \right)^2 + \left(\frac{\partial v}{\partial z} \right)^2 \right\}^{1/2} S_m \quad (2.11)$$

$$K_h = l^2 \left\{ \left(\frac{\partial u}{\partial z} \right)^2 + \left(\frac{\partial v}{\partial z} \right)^2 \right\}^{1/2} S_h \quad (2.12)$$

where l is the mixing length (Turton and Brown 1987). The functions S_m and S_h depend upon Ri and are given by Mellor and Yamada (1974) as follows:

$$S_M = 15.0^{1/2} \left(1 - R_f \right)^{1/2} \tilde{S}_M^{3/2} \quad (2.13)$$

$$S_H = 15.0^{1/2} (1 - R_f)^{1/2} \tilde{S}_M^{1/2} \tilde{S}_H \quad (2.14)$$

where \tilde{S}_M and \tilde{S}_H may be determined as functions of the gradient Richardson number,

$$Ri \equiv \left[\beta g \frac{\partial \theta}{\partial z} \right] \times \left[\left(\frac{\partial u}{\partial z} \right)^2 + \left(\frac{\partial v}{\partial z} \right)^2 \right]^{-1} \quad (2.15)$$

and

$$R_f = 0.725 \left[Ri + 0.18 - \left(Ri^2 - 0.316 Ri + 0.0346 \right)^{1/2} \right] \quad (2.16)$$

Recently, Bergot and Guedalia (1994) modified the COBEL (Counche Brouillard Eau Liquide) one-dimensional model of radiation fog to be forced with mesoscale terms of geostrophic horizontal advection of temperature and water vapor. Using this model, Bergot and Guedalia (1994) tested the model's sensitivity to the input variables of temperature, dewpoint, height of the mixing layer, and geostrophic wind.

One of the most interesting observations was the effect of geostrophic wind on fog formation. Bergot and Guedalia (1994) carried out different simulations, under identical initial conditions ($T = 10^\circ\text{C}$ and $q = 6 \text{ g kg}^{-1}$), with the geostrophic wind varying between 2 and 10 m s^{-1} . They noted not much difference between the time of fog formation for winds taken between 2 and 6 m s^{-1} . However, fog forms 2 hours later when the geostrophic wind is increased to 10 m s^{-1} . Bergot and Guedalia observed that the stronger the geostrophic wind, the longer fog formation will be postponed. The fog may even be prevented from forming, but once formed the vertical development (fog depth) will be increased by the stronger geostrophic wind.

2.3 Development and Structure of the AWS Fog Model

The Air Weather Service Fog Model was originally developed by Dr. W. Dale Meyer, AWS/XOX, on an Excel spreadsheet and later converted into the Mathematica[®] computer language. This version has been described in Meyer and Rao (1995). The Mathematica[®] model was then translated into FORTRAN as described by O'Sullivan (1996). The FORTRAN version is currently being upgraded by SLU to include a soil model. The Mathematica version is not being upgraded and will most likely be replaced with the FORTRAN version. Consequently, the current SLU FORTRAN version will be adapted for use by Air Force forecasters in the Southeast United States.

The AWS Fog Model is a one dimensional model, which requires input of initial conditions for one location. From these initial conditions, the model produces forecasts of diurnal temperature changes, dewpoint changes, wind speed changes, and visual range as a function of time using a finite centered difference scheme. The model runs over a 24 hour period in 1 minute time steps. The initial conditions for the SLU version are location (latitude, longitude), date (Julian Day), observed surface temperature at sunset, observed dewpoint at sunset, observed wind speed at sunset, soil type, soil moisture, and the lapse rate of the atmosphere. The model has a staggered vertical resolution with a surface level of 0 meters, a fog level of 10 meters, a stratus cloud level of 200 meters, and an upper boundary of 1000 meters. Temperature and dewpoint are held constant at the upper boundary, but not at 200 meters, 10 meters or the surface.

The architecture of the SLU version of the model is shown in Figure 2.1:

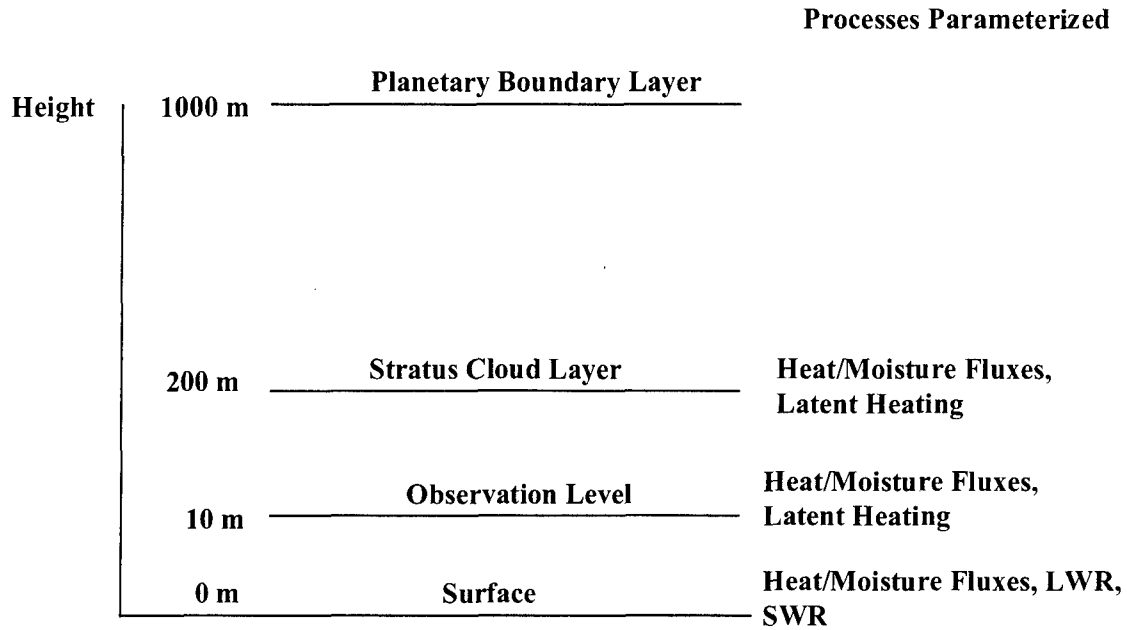


Figure 2.1. Vertical Resolution of the AWS Fog Model (not to scale). Height of layer to left. LWR- longwave radiation; SWR - shortwave radiation.

O'Sullivan (1996) gives a very detailed description of the prognostic equations and parameterizations. In brief, from O'Sullivan (1996) prognostic equations are used for change of temperature and change of moisture, while diurnal wind, longwave terrestrial cooling, longwave cooling of atmospheric levels, and solar heating are parameterized.

The prognostic equation for temperature at 10 m and 200 m is as follows:

$$T(n+1) = T(n-1) + \frac{1}{2} \left[\frac{\partial T}{\partial t_n} + \frac{\partial T}{\partial t_{n-1}} \right] \Delta t + \frac{L}{c_p} \Delta q \quad (2.17)$$

while at the surface

$$T_s(n+1) = T_s(n-1) + \frac{1}{2} \left[\frac{\partial T_s}{\partial t_n} + \frac{\partial T_s}{\partial t_{n-1}} \right] \Delta t \quad (2.18)$$

where

T = temperature at either 10 m or 200 m,

T_s = surface temperature,

n = time step,

t = time (in seconds),

L = latent heat of condensation,

c_p = specific heat capacity of air, and,

q = specific humidity at either 10 m or 200 m.

The local change of temperature in this model arises from turbulent heating (or cooling), longwave terrestrial cooling, and solar heating.

The prognostic equation for moisture at the surface, 10 m, and 200 m is as follows:

$$q(n+1) = q(n-1) + \frac{1}{2} \left[\frac{\partial q}{\partial t_n} + \frac{\partial q}{\partial t_{n-1}} \right] \Delta t \quad (2.19)$$

where the local change of specific humidity is due to turbulent fluxes and condensation at each level.

The parameterization of longwave terrestrial cooling used takes the form following Haltiner and Martin (1957):

$$T_1 - T = \frac{2}{\sqrt{\pi}} \frac{F_{N1}}{S} \sqrt{t} \quad (2.20)$$

T_1 is the initial temperature of the surface model initialization and T is the temperature at time t . F_{N1} is the initial radiation used as a starting value to create the curve shown in Figure 2.2. S represents the information from the soil, including the thermal conductivity, density, and thermal diffusivity (O'Sullivan 1996).

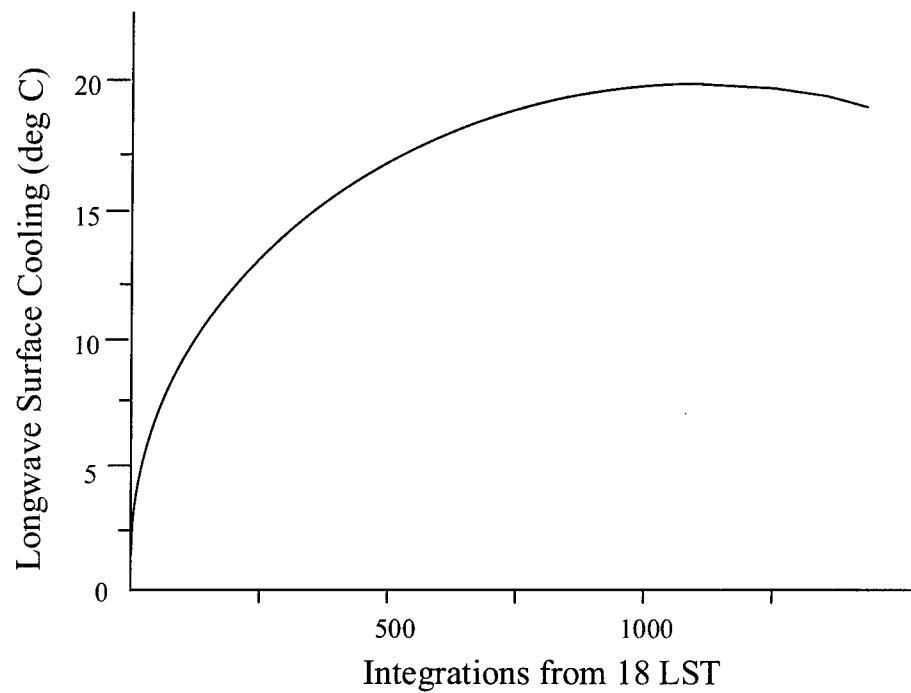


Figure 2.2. Example of longwave surface cooling obtained by model using formulation following Brunt (1932) and Groen (1947).

O'Sullivan (1996) also describes the parameterization of longwave radiation at fog and stratus levels and the parameterization of surface evaporation even though they weren't used in the SLU version.

2.4 Adaptation of AWS Fog Model to the Southeast United States

The SLU model was modified for this research. Modifications were made for four reasons: to correct errors in the code; to improve documentation; to provide additional input variables; and, to provide parameterization of new physical processes. The SLU FORTRAN version contained many array size errors. Most of the array size errors were simple typographical errors in the FORTRAN code. Each of the areas where array size errors appeared were corrected and annotated in the revised model FORTRAN code (see appendix). A list of variable descriptions was included in the revised version to aid making changes to the model in the future.

The model now allows the temperature and dewpoint at 200 meters and 1000 meters to be input if available. If this data is not available, then the model uses the default value of 90% of the adiabatic lapse rate to compute the temperature and dewpoints at 200 and 1000 meters.

A parameterization of visibility from Bergot and Guedalia (1994) was added to allow for visibility comparisons between actual observations and model output. As soon as the mixing ratio q reaches the saturation value q_{sat} , the excess condenses as liquid water q_l . The dewpoint is decreased to match the saturation dewpoint at that level and the mixing ratio q are then calculated. The horizontal visibility in meters, is computed from the liquid water content by the relation (Roach and Brown 1976):

$$vis = \frac{3.9}{144.7(\rho q_l)^{0.88}} \quad (2.21)$$

where

ρ = density of air, and,

q_l = liquid water content.

Using the results of the verification and sensitivity study done on the SLU version of the fog model, fog model parameters changed as follows. For the summer season, the underforecasting bias was removed by increasing the soil relative humidity parameter from 50 % to 53 %. For the fall season, the overforecasting bias was removed by decreasing the soil relative humidity parameter from 50 % to 43 %.

3. Data Analysis

3.1 Method of Limiting Observational Data

The data used in this thesis is from a ten year database of hourly surface weather observations from Pope Air Force Base (Pope AFB) North Carolina. Pope AFB is located on the relatively flat coastal plain in the Southeast United States about 90 miles inland from the Atlantic Ocean, at 35.17° N latitude and 79.02° W longitude. The observation area overlooks the military concrete runway, which is surrounded by grass covered sandy soil. The area surrounding Pope AFB is the mostly tree covered Fort Bragg Army Post.

A FORTRAN program was written to select only observations that met the conditions described below.

A. No large changes in wind speed or direction

1. Wind speed between 0 UTC and 13 UTC (20L to 9L) 12 knots or less
2. No wind direction change greater than 60 degrees between 0 UTC and 13 UTC, except for wind speeds of 5 knots or less

B. No large changes (except diurnal) in temperature

Exclude all cases where temperature increases from 0 UTC to 13 UTC

C. No large changes in dewpoint

Exclude cases where the dewpoint increases or decreases more than 7 degrees F (4 °C) between 0 UTC and 13 UTC

D. No cloud cover

Exclude cases where more than scattered clouds are present before
visibility starts to decrease between 0 UTC and 13 UTC

E. No large changes in sea level pressure

Exclude cases where sea level pressure increases or decreases more than 10
mb between 0 UTC and 13 UTC

F. No reduced visibility except reductions caused by fog

1. No reduced visibility of any kind between 22 UTC and 02 UTC
2. Select only cases with visibility obstruction codes of FG or BR between
the hours of 02 UTC and 13 UTC
3. Also select cases with no visibility obstruction codes and no reduction
to visibility

To eliminate advection fog events, rain/fog events, frontal fog events, etc., only the observations that met the criteria above were used in this study. The weather events reflected in the observations that met all the criteria above are termed “synoptically calm” weather events. They were used for an in-depth data analysis to investigate the relationships between reduction to visibility due to fog and the input parameters of the fog model which are temperature, dewpoint, wind speed, and soil moisture. The 11 UTC observations were selected from each synoptically calm weather event for use in the data analysis. The 11 UTC (7 am local) observations were chosen because this is usually the time of lowest visibility due to fog and the time of lowest temperature due to diurnal temperature changes.

3.2 Parameterization of Soil Moisture

The fog model requires an ill defined input variable called Soil Relative Humidity (SoilRH). SoilRH is ill defined because it is not reported in a standard of weather observation. The soil moisture was parameterized by scaling the precipitation data to a scale from zero to eighteen as shown in Table 3.1. This parameterization was tested to determine whether the observed visibility is sensitive to the amount of moisture in the soil.

The precipitation parameterization scale is defined to correlate the amount of precipitation to the available soil moisture. The precipitation parameterization was compared to the visibility for each event to see if the model's sensitivity to soil moisture is reflected in the visibility observations. Figure 3.1 shows that the reduction of visibility due to fog events are not correlated to this soil moisture parameterization. The correlation was 0.071 which is very low.

The low correlation of soil moisture to visibility suggests that the development of fog does not depend significantly on the moisture of the soil, as reflected in this parameterization. This result is contrary to the work done by O'Sullivan (1996). In his study, O'Sullivan stated that the initial soil wetness had a major role in influencing the onset time of fog. In his research, he ran the model three times with SoilRH set up 30%, 50%, and 70%, respectively, and compared each of the three model outputs to an actual fog event.

Table 3.1: Precipitation data parameterization.

Scale	Precipitation Data
0	One inch or more of precipitation within 12 hours prior to the 22 UTC forecast time
1	Between one half and one inch of precipitation within the 12 hours prior to the 22 UTC forecast time
2	One inch or more of precipitation within 24 hours prior to the 22 UTC forecast time
3	Trace to one half inch of precipitation within the 12 hours prior to the 22 UTC forecast time
4	Between one half and one inch of precipitation within the 24 hours prior to the 22 UTC forecast time
5	One inch or more of precipitation within 36 hours prior to the 22 UTC forecast time
6	Trace to one half inch of precipitation within the 24 hours prior to the 22 UTC forecast time
7	Between one half and one inch of precipitation within the 36 hours prior to the 22 UTC forecast time
8	One inch or more of precipitation within 48 hours prior to the 22 UTC forecast time.
9	Trace to one half inch of precipitation within the 36 hours prior to the 22 UTC forecast time
10	Between one half and one inch of precipitation within the 48 hours prior to the 22 UTC forecast time
11	One inch or more of precipitation within 60 hours prior to the 22 UTC forecast time
12	Trace to one half inch of precipitation within the 48 hours prior to the 22 UTC forecast time
13	Between one half and one inch of precipitation within the 60 hours prior to the 22 UTC forecast time
14	One inch or more of precipitation within 72 hours prior to the 22 UTC forecast time
15	Trace to one half inch of precipitation within the 60 hours prior to the 22 UTC forecast time
16	Between one half and one inch of precipitation within the 72 hours prior to the 22 UTC forecast time
17	Trace to one half inch of precipitation within the 72 hours prior to the 22 UTC forecast time
18	No precipitation within the 72 hours prior to the 22 UTC forecast time

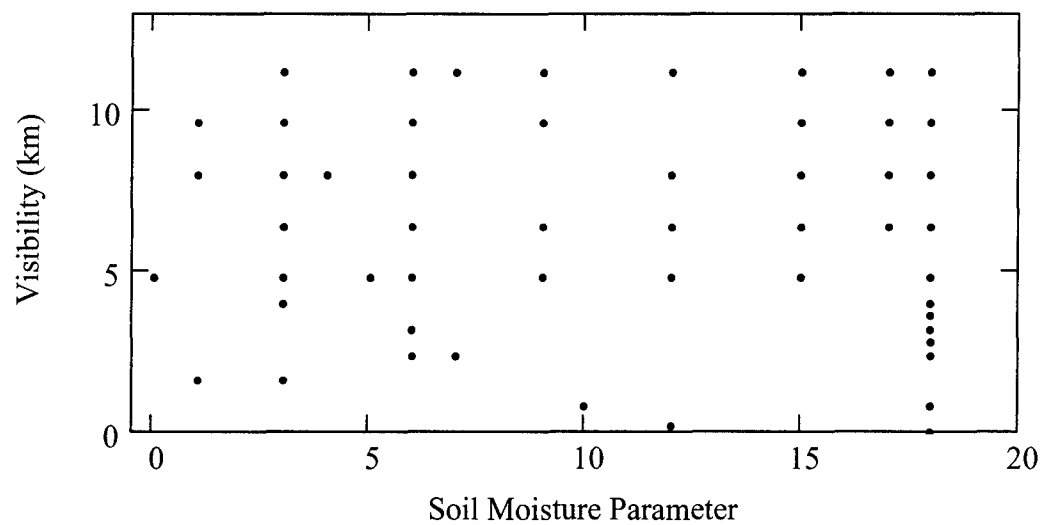


Figure 3.1. Scatter plot of the soil moisture parameterization versus 11 UTC visibility. Data from “synoptically calm” weather events selected from a ten year database of hourly surface weather observations from Pope AFB.

O’Sullivan’s results showed that for SoilRH equal to 30%, the air moisture in the model output was too dry; no saturated conditions existed in the model output (Figure 3.2). For SoilRH equal to 50%, the model output of air moisture that was about right; saturated conditions existed in the model output for about the same time frame as reductions to visibility were observed at Mather Air Force Base (Figure 3.3). For SoilRH equal to 70%, the model output was too moist; saturated conditions existed long before and after reductions to visibility were observed at Mather Air Force Base (Figure 3.4). Therefore, O’Sullivan concluded that soil moisture has a major role in influencing the onset of fog. However, O’Sullivan should have concluded that the fog model is very sensitive to soil moisture. Actual observations of visibility, as shown in the correlation analysis above, do not reflect this sensitivity. This calls into question the physics of the parameterization of soil moisture used in the AWS Fog Model.

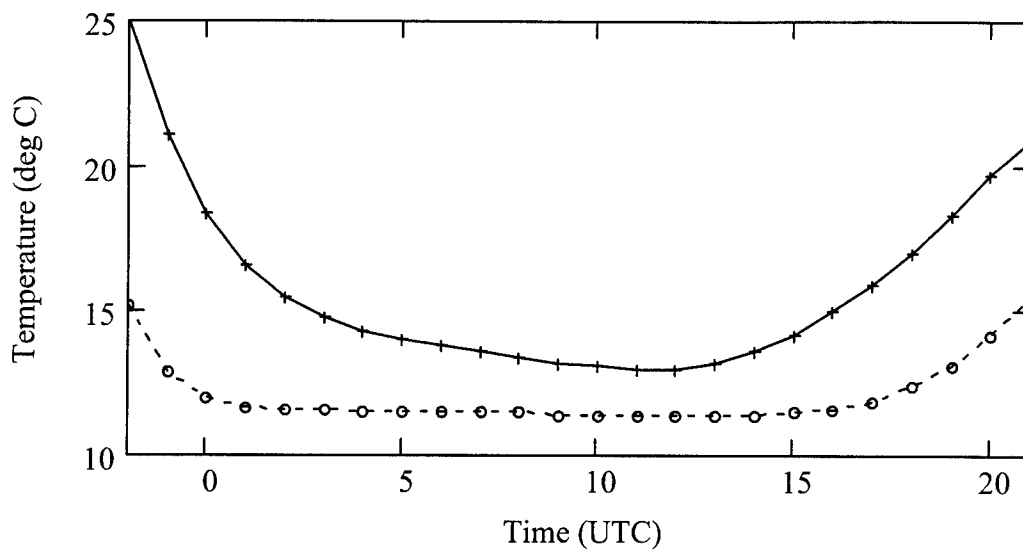


Figure 3.2. Predicted 10 m temperature (—+—), and dewpoint (---o---) with soil RH set to 30%. Reproduced using SLU version of AWS Fog Model, based on 1800 PST 17 July 1993 Mather Air Force Base data as presented by O'Sullivan (1996).

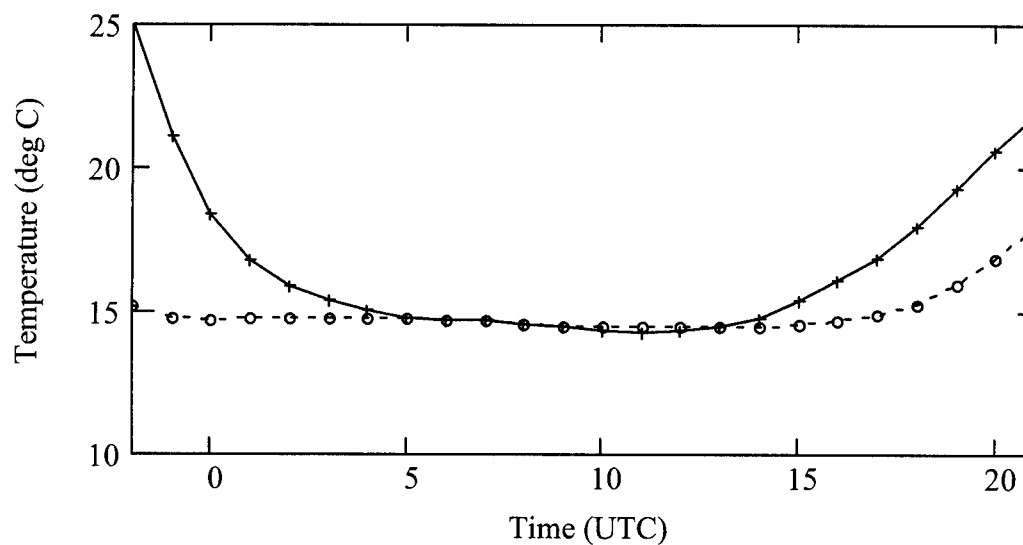


Figure 3.3. Predicted 10 m temperature (—+—), and dewpoint (---o---) with soil RH set to 50%. Reproduced using SLU version of AWS Fog Model, based on 1800 PST 17 July 1993 Mather Air Force Base data as presented by O'Sullivan (1996).

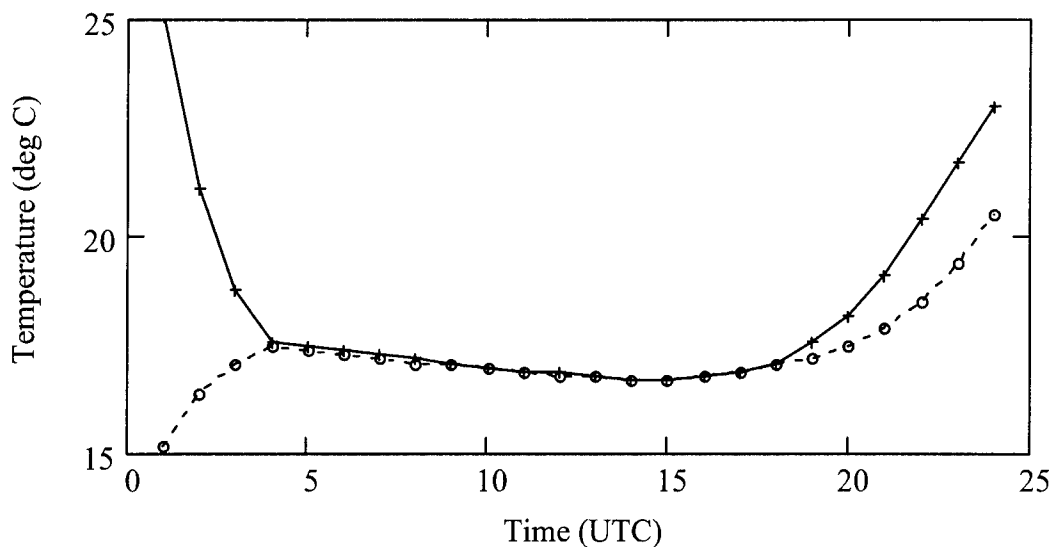


Figure 3.4. Predicted 10 m temperature (—+—), and dewpoint (---o---) with soil RH set to 70%. Reproduced using SLU version of AWS Fog Model, based on 1800 PST 17 July 1993 Mather Air Force Base data as presented by O'Sullivan (1996).

3.3 Analysis of Temperature and Dewpoint

Observations of temperature and dewpoint were combined into the single parameter called dewpoint depression (DPP). Dewpoint depression was also compared to the visibility for each event to test an assumption made by O'Sullivan (1996). O'Sullivan assumed fog was formed when the dry bulb temperature and dewpoint approach each other to within 2.2 °C (4.0 °F) or less. Figure 3.5 shows that the reduction of visibility due to fog events is not well correlated to dewpoint depression. The correlation was 0.13, which is low. The low correlation of dewpoint depression to visibility suggests that even through all occurrences of fog are at dewpoint depressions of 2.2 °C or less, not all occurrences of dewpoint depressions of 2.2 °C or less are accompanied by an occurrence of fog. The fog model must be able not only to compute diurnal changes in temperature

and dewpoint, but also be able to handle the liquid water that is condensed out of the air. As discussed in Chapter 2, the condensed liquid water can either be deposited on the ground overnight as dew or will develop into an early morning fog. The formation of fog versus dew depends almost entirely on wind speed. Under very light wind conditions as the radiative inversion sets up, the winds above the inversion become uncoupled from the winds below the inversion. The winds below the inversion decrease due to high static stability to a level that results in a virtual cessation of turbulence. The mechanism for dew deposition ceases, and a fog layer starts to form. Under stronger wind conditions as the radiative inversion sets up, the winds below the inversion decrease, but not to a level that stops the turbulence transfer process, thus dew deposition continues and fog does not form. The AWS Fog Model does a good job of modeling the diurnal changes in temperature and dewpoint, but lacks the necessary vertical resolution and stability parameterization to accurately model the decreasing wind speed during the night. In fact the model predicts more occurrences of fog under strong wind conditions than under light winds (see sensitivity tests on wind speed in Chapter 4). Figure 3.6 shows that the reduction of visibility due to fog events at 11 UTC has a good correlation to the dewpoint depression at 22 UTC. The correlation was 0.60 which is almost exactly the same as the percentage of events that were correctly forecasted at 11 UTC in the verification study (Table 4.1).

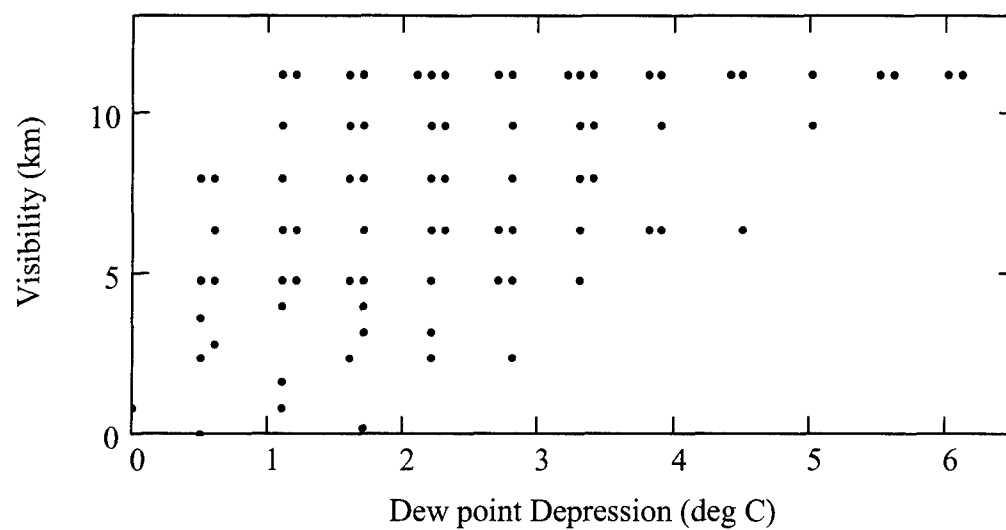


Figure 3.5. Scatter plot of the 11 UTC dewpoint depression versus 11 UTC visibility. Data from “synoptically calm” weather events selected from a ten year database of hourly surface weather observations from Pope AFB.

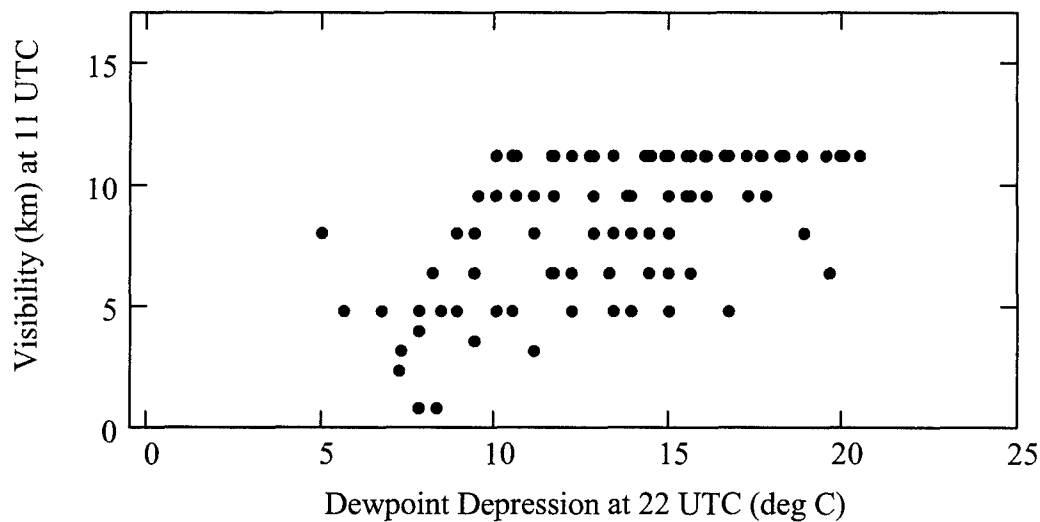


Figure 3.6 Scatter plot of the 22 UTC dewpoint depression versus 11 UTC visibility. Data from “synoptically calm” weather events selected from a ten year database of hourly surface weather observations from Pope AFB.

3.4 Analysis of Wind Speed

Observations of wind speed were compared to the visibility for each event to determine if there was a correlation between visibility and wind speed. Figure 3.7 shows that the reduction of visibility due to fog events are not well correlated to wind speed. The correlation was 0.08, which is very low.

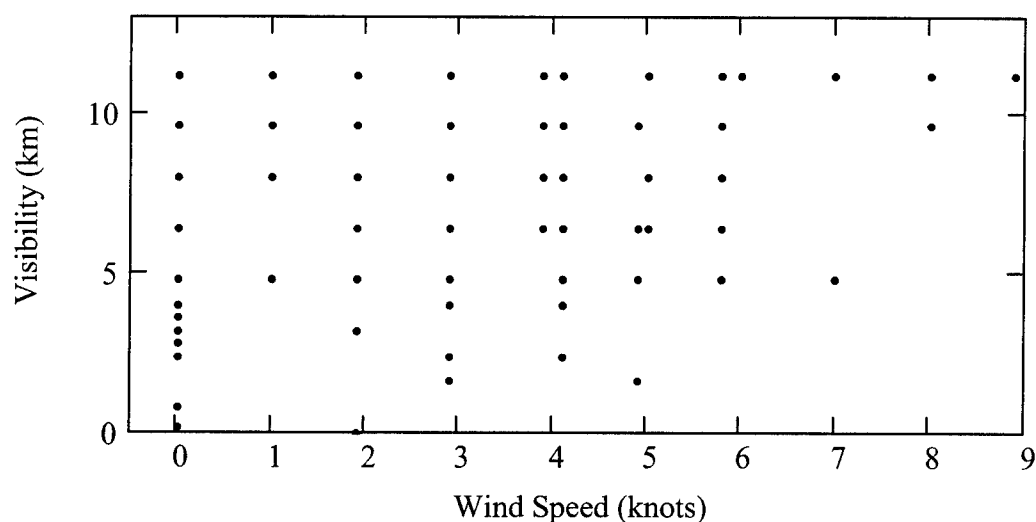


Figure 3.7. Scatter plot of 22 UTC wind speed versus 11 UTC visibility. Data from “synoptically calm” weather events selected from a ten year database of hourly surface weather observations from Pope AFB.

The low correlation of wind speed to visibility suggests that even though more occurrences of fog occur at low wind speeds, advection fog being an exception, low speeds do not guarantee fog formation. The low correlation of wind speed to visibility would most likely be higher if more precise observations of wind speed were available. The wind speed measurements used in this correlation analysis were taken from standard airfield anemometers that according to Monteith (1957) have a stopping speed of around 2 m s^{-1} . Such an instrument will record a flat calm throughout most radiational cooling

events. Significant fog development appears to occur when winds speeds drop below 2 knots. Due to this instrumentation limitation wind speed did not correlate well with visibility even though it is very important in fog formation.

3.5 Analysis of Wind Direction

Observations of wind direction were also compared to the visibility for each event to see if there is a correlation between visibility and wind direction. Figure 3.8 shows an interesting correlation. Notice the visibilities for wind directions in the range from 150 degrees to 250 degrees are disproportionately low. This occurs because low level moisture is advected into the station when the winds are from the southeast to southwest.

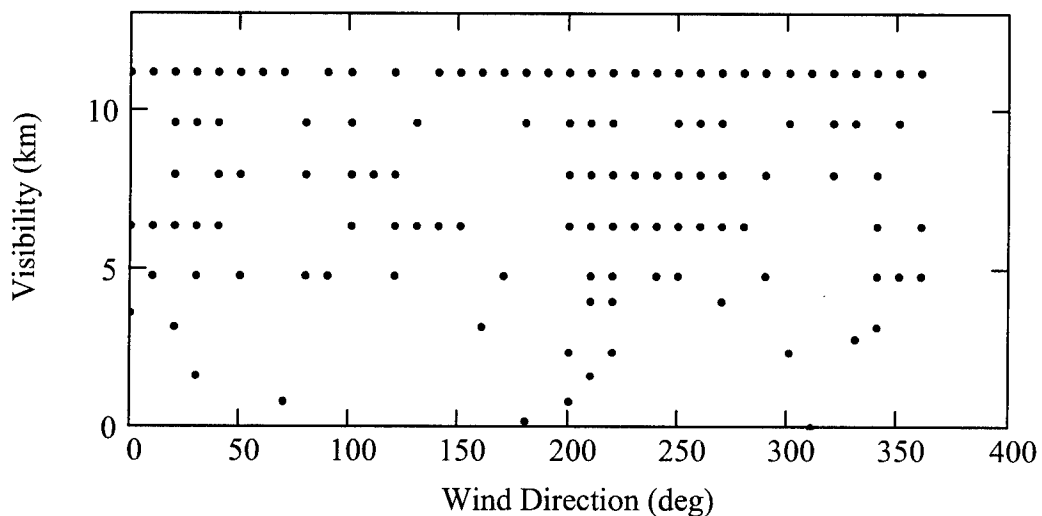


Figure 3.8. Scatter plot of 22 UTC wind direction versus 11 UTC visibility. Data from “synoptically calm” weather events selected from a ten year database of hourly surface weather observations from Pope AFB.

The current fog model does not include wind direction. The model assumes no moisture advection after initialization and strictly radiation conditions. Input of wind direction would only become important when attempting to parameterize moisture advection in the model. Addition of a parameterization of moisture advection to the model would expand the usefulness of this model for forecasting occurrences of advection fog in the Southeast. This, however, would restrict the portability of the model.

3.6 Regression Analysis of Fog Model Input Variables

Since most fog events occur during periods of low dewpoint depression, light winds, and, according to O'Sullivan (1996), high soil moisture, a multiple linear regression was performed using these three variables to show the proportion of observed variation in the reduction to visibility due to fog that can be explained by the fog model's input variables. This regression analysis produced a low coefficient of determination, $r^2 = 0.38$. This low coefficient of determination suggests that the fog model's input variables do not explain a significant amount of the observed variance in the reduction to visibility due to fog. Therefore, the fog model cannot be expected to accurately forecast the occurrence of fog with the current input variables. The fog model needs to include other input variables that affect visibility and the occurrence of fog so as to improve the amount of variance explained by the model's input parameters. Additional input variables that can affect fog formation include: availability of condensation nuclei, moisture and temperature advection, temperature, dewpoint, wind speed, and wind direction at significant levels in the lower atmosphere. While observation or forecasts of

condensation nuclei are not normally available for input into the model, temperature and dewpoint values from significant levels are readily available using synoptic scale model output. The 12hr forecasts of these variables can be used as initialization values for fog model. Wind speed and direction data can be obtained real time from the vertical azimuthal display product from Doppler radar observations. Use of this additional available information would greatly increase the applicability and accuracy of the fog model.

4. Verification and Sensitivity Study of the AWS Fog Model

A verification and sensitivity study was performed to determine the quality of forecasts and the sensitivities of the AWS Fog Model. First, a verification study was performed on the SLU version of the AWS Fog Model to establish a base line against which to gauge any changes made to fog model parameters to adapt the model to the Southeast United States. This verification study measures the relationship between a set of visibility forecasts and the corresponding observations of visibility. Secondly, a sensitivity study was performed on the fog model to measure the effects of various changes to model parameters on model output. Finally, a new visibility parameterization was added to the model and using the results of the sensitivity study, slight changes to fog model parameters were made and another verification study was performed.

4.1 Statistics used in Verification Study

The first statistic used to compare model output to actual observations is the hit rate or proportion correct (PC). It is defined as follows:

$$PC = \frac{X + W}{X + Y + Z + W} \quad (4.1)$$

where

X = the number of times the event was predicted and occurred,

Y = the number of times the event was not predicted but occurred,

Z = the number of times the event was predicted but did not occur, and,

W = the number of times the event was not predicted and did not occur.

The proportion correct is the fraction of the total forecasting occasions when the model correctly anticipated the fog event or non-fog event (Wilks 1995). The PC for perfect forecasts is one, and the worst PC is zero.

The second statistic used was the probability of detection (POD), defined as follows:

$$POD = \frac{X}{X + Y} \quad (4.2)$$

where X and Y are defined in equation 4.1. The POD is the likelihood that the event would be forecast, given that it occurred (Wilks 1995). The POD for perfect forecasts is one, and the worst POD is zero.

The third statistic used was the false-alarm rate (FAR), defined as follows:

$$FAR = \frac{Z}{X + Z} \quad (4.3)$$

where X and Z are defined in equation 4.1. The FAR is that proportion of forecast events that fail to materialize (Wilks 1995). The FAR has a negative orientation, so that smaller values of FAR are preferred. The best possible FAR is zero, and the worst possible FAR is one.

The fourth statistic used was the bias (B), defined as follows:

$$B = \frac{(X + Z)}{(X + Y)} \quad (4.4)$$

where X, Y, and Z are defined in equation 4.1. The bias is the ratio of the number of times fog was forecast to the number of times fog occurred (Wilks 1995). A bias less than one indicates that the event was underforecast, while a bias greater than one indicates that the event was overforecast. Our goal would be an unbiased forecast ($B = 1$), indicating that the event was forecast the same number of times that it was observed.

The fifth statistic used was the skill score (SS), defined as follows:

$$SS = \frac{(PC - PC_{per})}{(1 - PC_{per})} \quad (4.5)$$

where PC is defined in equation 4.1 and PC_{per} is proportion correct based on persistence forecasts from the observations taken at the same hour on the night before each fog event. If PC equal one, the skill score attains it maximum value of one. If PC equal PC_{per} , then SS equal zero, indicating no improvement over the persistence forecasts. If SS is less than zero then the model forecasts are inferior to the persistence forecasts (Wilks, 1995).

4.2 SLU Version Verification

Two types of verification studies were performed on the AWS Fog Model. First, the model was verified using the averaged results of 61 summer and 61 fall “synoptically calm” events. For the summer events, 40 were fog events and 21 were non-fog events at 11 UTC, the time of maximum fog occurrences. For the fall events, 22 were fog events and 39 were non-fog events at 12 UTC, the time of maximum fog occurrences. An attempt was made to verify the fog model for each season in the Southeast United States, but insufficient “synoptically calm” fog events were available for the winter and spring seasons. Secondly, the model was verified using one summer fog event that occurred on

28 - 29 August 1985 and one fall non-fog event that occurred on 9 - 10 November 1985 at Pope AFB North Carolina.

The model forecasts temperature, dewpoint, and, based on saturation of a layer (dewpoint equal to or greater than temperature), the occurrence of fog. The soil type parameter of the model was set to moist sand and the soil wetness was assumed to be 50% relative humidity (RH). The lapse rate was set to 90 % adiabatic. A fog event was declared if the hourly observation reported a reduction in visibility due to fog. A fog event was declared predicted if the model fog indicated saturated conditions at the 10 meter level for a given time in the model run.

4.2.1 SLU Version Verification Results for Summer Season

It can be seen from the computed bias that the fog model underforecasts fog events in the summer months (Table 4.1). The fog model underforecasted radiation fog each hour that fog was observed except 13 UTC. It missed over half the fog occurrences each hour. At the time of maximum fog occurrence (11 UTC), the fog model forecasted 14 of 40 fog events, but only forecasted 2 events that did not occur, for a percent correct of 54%. For the same hour, the persistence forecast percent correct was 63%. This gave a negative skill score (-0.24), which indicates that it would be better to use persistence forecasts than model output. The model beat persistence from 22 UTC until 9 UTC, then persistence beat the model during the critical hours of 10 UTC through 12 UTC, then the model once again beat persistence from 13 UTC on. The false alarm rate was low during most forecast hours, but this was due to the underforecasting bias with the model.

Figure 4.1 shows that the model on average cools the nocturnal boundary layer (NBL) at the 10 meter level during the night by around 1.5 °C more than observed. The computed standard deviation for the difference in cooling at the 10 meter level was between 1 and 2 °C during the night. Overcooling the NBL by 1.5 °C in the model is not of concern because the layer must become saturated before fog is predicted.

In a previous verification study verifying the model in California, O'Sullivan (1996) declared a fog event if the temperature and dewpoint were within 2.2 °C (4.0 °F) of each other. This method of verification was reviewed but rejected for two reasons. First, the calculations of visibility that were turned off in the model require a completely saturated level before reduced visibilities are computed. Second, declaring a fog event if the dewpoint depression was less than 2.2 °C results in the model forecasting fog for every event in the verification study. The large mean temperature difference (8 °C) after sunrise is of concern because it appears that the model does not warm the 10 meter layer sufficiently. This will cause the 10 meter layer to remain saturated longer than what is observed. If the model is tuned to have no underforecast bias during the critical fog hours of 10 and 11 UTC, the result of continued saturation will be invalid forecasts of low visibilities during the hours of 12, 13, 14, and 15 UTC.

Figure 4.2 shows that the mean dewpoint difference has a sinusoidal nature. The mean 10 meter model dewpoints are lower than the mean observed dewpoints during the first part of the night and then increases to about 1 °C greater than the mean observed dewpoints at around 10Z. The sinusoidal nature of Figure 4.2 is an artifact of nocturnal

changes in observed dewpoints. On a typical radiational cooling night after sunset, the dewpoint initially increases slightly due to reduced mixing with dryer air aloft. Then, as the temperature drops during the night, the dewpoint drops due to condensation in the form of dew or fog. The model does not reflect either of these processes; it simply reduces the initial input 22 UTC (sunset) dewpoint through a parameterization of turbulent mixing with the dryer surface and 200 meter levels.

The visibility errors between observed visibility and 10 meter model visibility are large. The average error at 11 UTC for the 61 summer events was 4.9 km. Part of this large error is due to the model the not predicting fog events that occurred and part is due to an error in the model's calculation of visibility. The SLU version, along with the Mathematica version, uses the total water content (vapor plus liquid) to compute visibility as soon as the layer becomes saturated. This is unrealistic as only the excess water vapor above saturation should be used in visibility calculations. This error causes the fog model to compute visibilities of around 50 meters as soon as the layer becomes saturated. The adapted model condenses out the excess water vapor and uses this value for visibility calculations in the method by Bergot and Guedalia (1994) (see Equation 2.21). While this is a slight improvement, more accurate calculations cannot be added until the vertical resolution of the model is increased. Increasing the vertical resolution will allow the additional parameterization of droplet settling to the model.

Table 4.1 SLU Version Verification Results for Summer Season.

Time UTC	X #	Y #	Z #	W #	PC	POD	FAR	Bias	SS
22	0	0	0	61	1	-	-	-	1
23	0	0	0	61	1	-	-	-	1
0	0	0	0	61	1	-	-	-	1
1	0	0	0	61	1	-	-	-	1
2	0	0	1	60	.98	-	1	-	.80
3	0	1	1	59	.97	0	1	1	.80
4	0	3	2	56	.92	0	1	.67	.60
5	1	6	1	53	.89	.14	.50	.29	.56
6	1	10	3	47	.79	.09	.75	.36	.28
7	5	11	2	43	.79	.31	.29	.44	.30
8	6	15	2	38	.72	.29	.25	.38	.07
9	8	21	3	29	.61	.28	.27	.38	0
10	13	24	3	21	.56	.35	.19	.43	-.22
11	14	26	2	19	.54	.35	.12	.40	-.24
12	12	19	4	26	.62	.39	.25	.52	-.19
13	4	3	6	48	.85	.57	.60	1.43	.44
14	0	3	0	58	.95	0	-	0	.64
15	0	2	0	59	.97	0	-	0	.40
16	0	1	0	60	.98	0	-	0	.33
17	0	1	0	60	.98	0	-	0	0
18	0	1	0	60	.98	0	-	0	0
19	0	1	0	60	.98	0	-	0	0
20	0	0	0	61	.98	-	-	-	0

X = the number of times the event was predicted and occurred

Y = the number of times the event was not predicted but occurred

Z = the number of times the event was predicted but did not occur

W = the number of times the event was not predicted and did not occur

PC = the proportion correct $PC = (X+W)/(X+Y+Z+W)$

POD = the probability of detection $POD = X/(X+Y)$

FAR = the false alarm rate $FAR = Z/(X+Z)$

Bias = the ratio of the number of times fog was forecasted to the number of times fog occurred $Bias = (X+Z)/(X+Y)$

SS = persistence based skill score $SS = (PC - PC_{per})/(1-PC_{per})$
where PC_{per} is proportion correct based on persistence forecasts

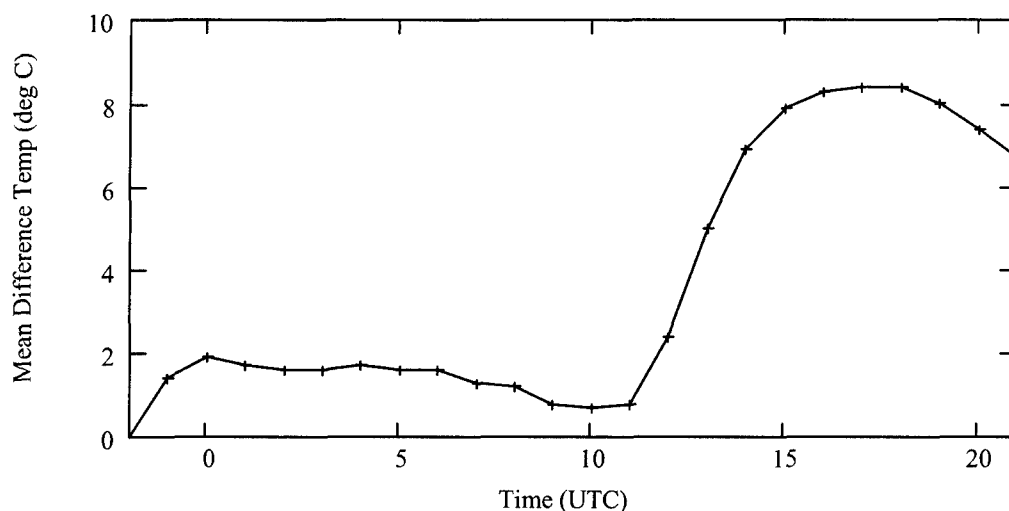


Figure 4.1. Mean temperature difference between observed temperature and model 10 meter temperature (—+) using SLU version, for 61 summer radiation cooling events. Positive values indicate that the observed temperature is greater than the model 10 meter temperature.

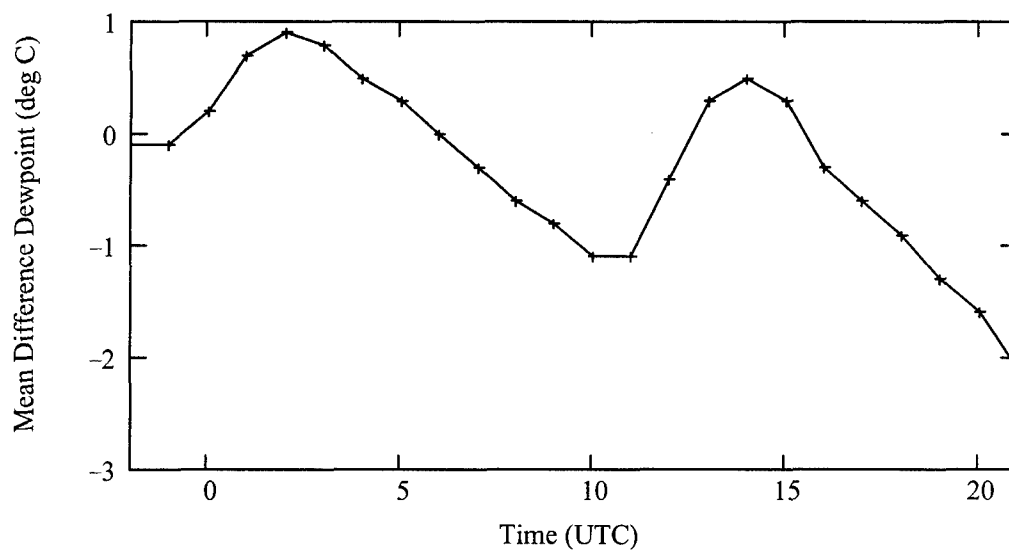


Figure 4.2. Mean dewpoint difference between observed dewpoint and 10 meter model dewpoint (—+) using SLU version, for 61 summer radiation cooling events. Positive values indicate that the observed dewpoint is greater than the model 10 meter dewpoint.

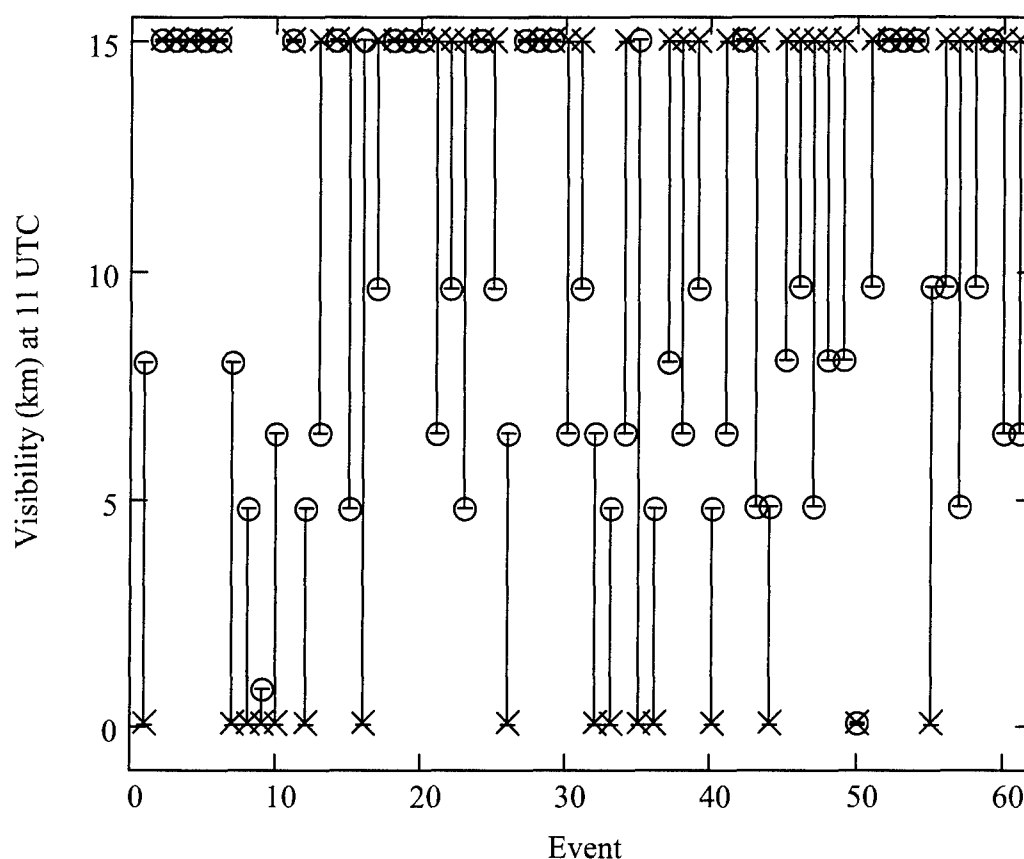


Figure 4.3. Visibility at 11 UTC: observed visibility (Θ) and 10 meter model visibility (X) using SLU version, for 61 summer radiation cooling events.

4.2.2 SLU Version Verification Results for Fall Season

It can be seen from the computed bias that the fog model overforecasts fog events in the fall months. The fog model overforecasted radiation fog during the critical fog hours of 8 UTC through 14 UTC. At the time of maximum fog occurrence (12 UTC), the fog model forecasted 15 of 22 fog events, but also forecasted 17 events that did not occur, for a percent correct of 61%. For the same hour, the persistence forecast percent correct was 78%. This gives a negative skill score (-0.77), which indicates that it would be better

to use persistence forecasts than model output. The model did beat persistence from 22 UTC until 7 UTC. Persistence forecasts beat model forecasts after 9 UTC. The false alarm rate was high each hour with over one half of the model forecasted fog events being false alarms.

Figure 4.4 shows that the model on average cools the NBL at the 10 meter level during the night by about the same amount as observed. The computed standard deviation for the difference in cooling at the 10 meter level was the same as in the summer study, between 1 and 2 °C during the night. The large mean temperature difference, 8 °C, after sunrise that showed up in the summer study also shows up in the fall study.

Figure 4.5 shows that, on average, the model does not decrease the dewpoint during the night as much as is observed. The difference approaches -3 °C at 11 UTC, which is a significant difference. This difference is most likely the cause of the overforecasting bias that appears in the fall verification study, as the 10 meter level of the model is generally more moist than observed.

The visibility error between observed visibility and 10 meter model are large. The average error at 11 UTC for the 61 fall events was 5.9 km. Part of this large error is due to the model the predicting fog events that did not occurred and part is due to an error in the model's calculation of visibility, that was described in the previous section.

Table 4.2. SLU Version Verification Results for Fall Season.

Time UTC	X #	Y #	Z #	W #	PC	POD	FAR	Bias	SS
22	0	0	0	61	1	-	-	-	1
23	0	0	0	61	1	-	-	-	1
0	0	0	0	61	1	-	-	-	1
1	0	0	0	61	1	-	-	-	1
2	0	0	0	61	1	-	-	-	1
3	0	2	0	59	.97	0	-	0	.81
4	0	4	0	57	.93	0	-	0	.56
5	0	5	0	56	.92	0	-	0	.60
6	1	4	0	56	.93	.20	0	.20	.65
7	4	5	1	51	.90	.44	.20	.56	.38
8	5	4	6	46	.84	.56	.55	1.22	0
9	7	4	8	42	.80	.64	.53	1.36	0
10	8	5	15	33	.67	.62	.65	1.77	-.65
11	11	7	16	27	.62	.61	.59	1.50	-1
12	15	7	17	22	.61	.68	.53	1.45	-.77
13	9	7	21	24	.54	.56	.70	1.88	-.40
14	4	4	18	35	.64	.50	.82	2.75	-.80
15	0	1	13	47	.77	0	1	-	-1
16	0	0	7	54	.89	-	1	-	-1
17	0	0	1	60	.98	-	1	-	-1
18	0	0	0	61	1	-	-	-	1
19	0	0	0	61	1	-	-	-	1
20	0	0	0	61	1	-	-	-	1

X = the number of times the event was predicted and occurred

Y = the number of times the event was not predicted but occurred

Z = the number of times the event was predicted but did not occur

W = the number of times the event was not predicted and did not occur

PC = the proportion correct $PC = (X+W)/(X+Y+Z+W)$

POD = the probability of detection $POD = X/(X+Y)$

FAR = the false alarm rate $FAR = Z/(X+Z)$

Bias = the ratio of the number of times fog was forecasted to the number of times fog occurred $Bias = (X+Z)/(X+Y)$

SS = persistence based skill score $SS = (PC - PC_{per})/(1 - PC_{per})$

where PC_{per} is proportion correct based on persistence forecasts

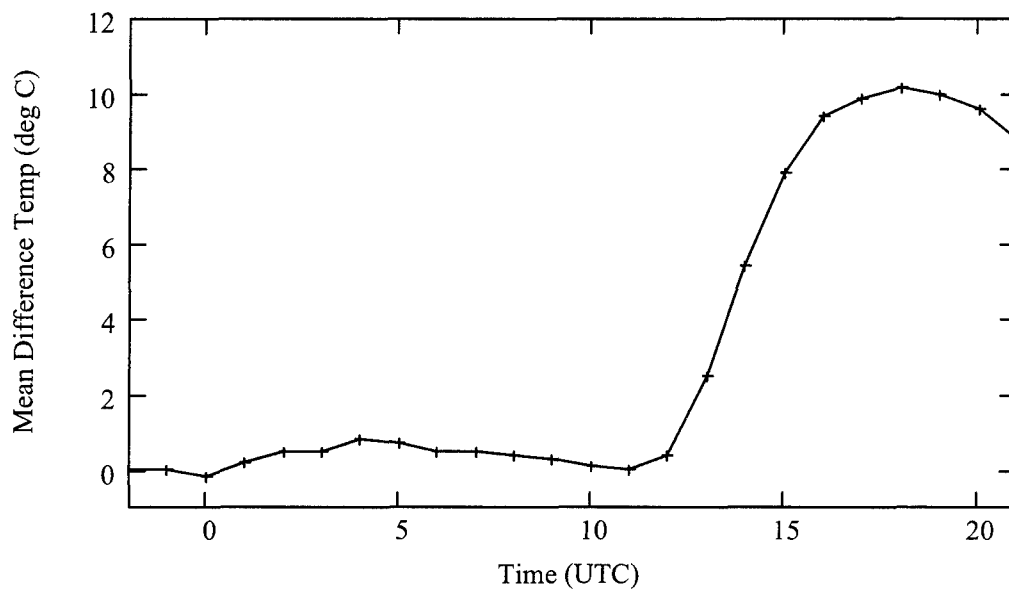


Figure 4.4. Mean temperature difference between observed temperature and model 10 meter temperature (—+) using SLU version, for 61 fall radiation cooling events. Positive values indicate that the observed temperature is greater than the model 10 meter temperature.

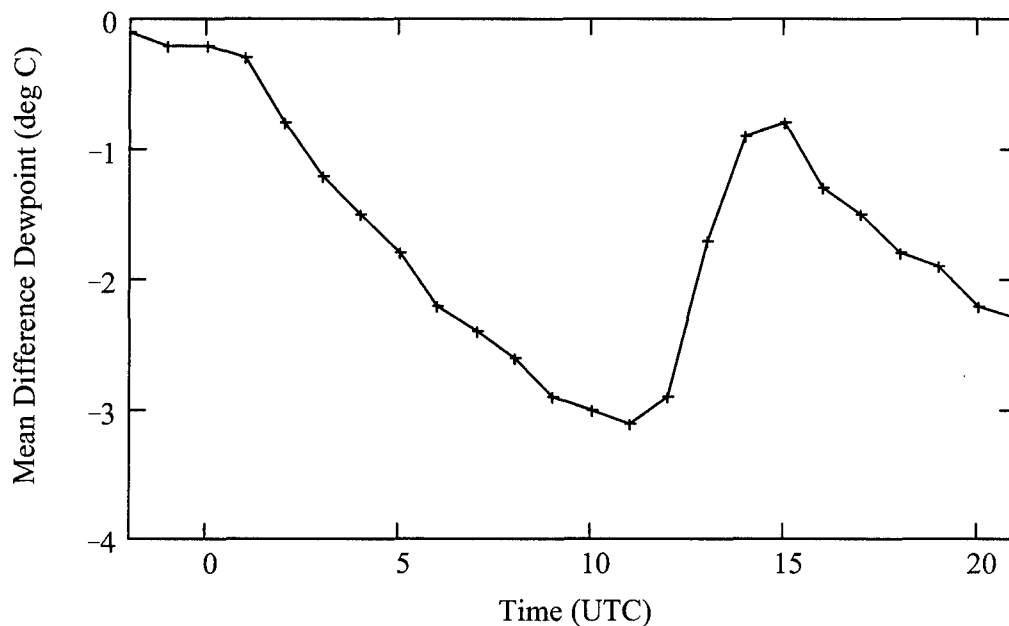


Figure 4.5. Mean dewpoint difference between observed dewpoint and 10 meter model dewpoint (—+) using SLU version, for 61 fall radiation cooling events. Positive values indicate that the observed dewpoint is greater than the model 10 meter dewpoint.

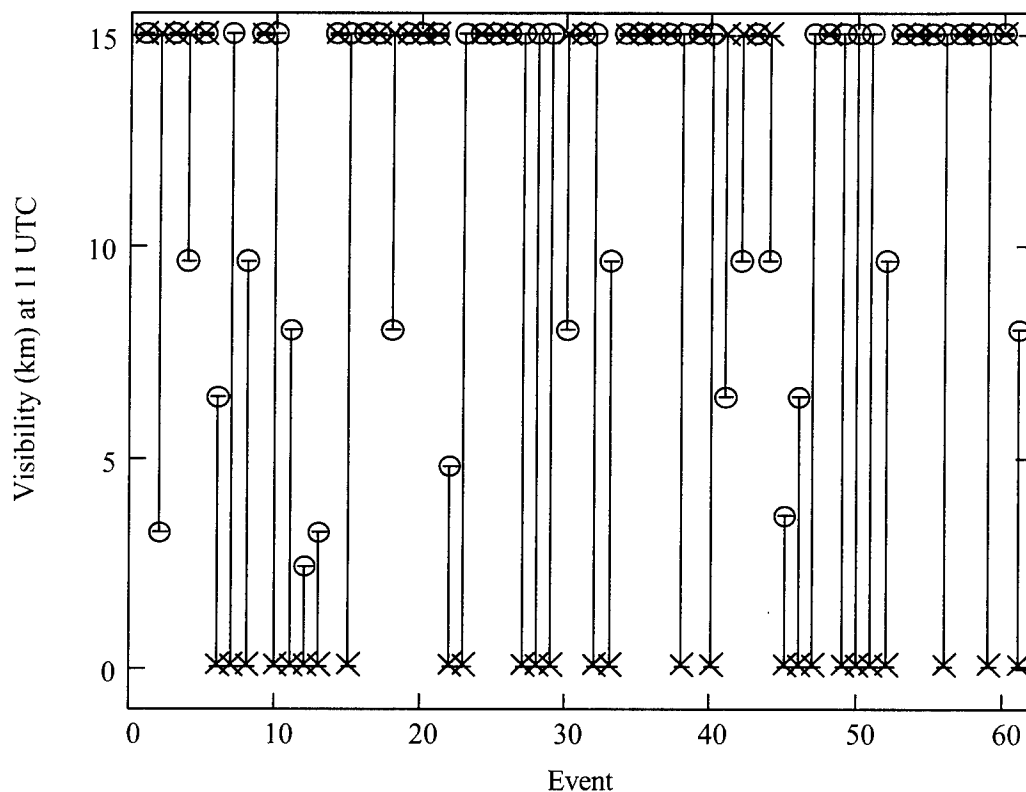


Figure 4.6. Visibility at 11 UTC: observed visibility (Θ) and 10 meter model visibility (X) using SLU version, for 61 fall radiation cooling events.

4.2.3 SLU Version Verification Results of a Single Summer Fog Event

In addition to looking at the averaged results of 61 summer radiational cooling events, it is also helpful to compare the observations of a single summer fog event to the output of the fog model. The initial data chosen for this single event was from observations taken on 28 and 29 August 1985 at Pope AFB. The 22 UTC observation taken on 28 August 1985 recorded a dry-bulb temperature of 28 °C (82.4 °F) and a dew-point temperature of 20.2 °C (68.4 °F). Winds at the time were observed to be 2.6 m s⁻¹ (5 knots). The soil type parameter of the model was set to moist sand and the soil wetness

was assumed to be 50% relative humidity (RH). The lapse rate was set to a value of 90% adiabatic.

The observed temperature and dewpoint traces from Pope AFB are shown in Figure 4.7. The minimum temperature occurred at 10 UTC 29 Aug 1985. The minimum temperature occurs at the same time in the model's minimum temperature for the surface level (Figure 4.8) and the minimum temperature for the 10 meter level occurred just after this time (Figure 4.9). Figure 4.9 also shows the model produced a period of saturation at the 10 meter level over the period 7 UTC to 14 UTC on 29 August 1985. The fog actually forms two hours before the model shows saturation at the 10 meter level. The observations from Pope AFB reported reduced visibility due to fog from 05 UTC to 15 UTC on 29 August 1985 (Figure 4.14). Upon saturation, the model immediately computes a visibility of around 50 meters. This is due to the model using the total water content (vapor plus liquid) in the visibility calculations. The lowest observed visibility of 800 meters was reported at 11 UTC(Figure 4.14). No stratus clouds were observed during this event nor would any be predicted based on the 200 meter temperature and dewpoint as shown in Figure 4.10.

Figure 4.11 is a direct comparison of observed temperature at Pope AFB during the night of 28 - 29 August 1985 and the predicted surface temperature based on 22 UTC 28 August 1985 Pope AFB data. The ground cools faster than the air due to emittance of longwave radiation. Therefore, the predicted surface temperature should be less than the observed temperature as shown in Figure 4.11. The results shown in the comparison of observed temperature at Pope AFB and predicted 10 meter temperature based on 22 UTC

28 August 1985 Pope AFB data (Figure 4.12) are also realistic. The predicted 10 meter temperature closely matches the observed temperature curve. The predicted 10 meter temperature ranges from 1 °C to 2 °C less than the observed temperature for each hour until sunrise (11 UTC). After 11 UTC, the observed temperature increases rapidly due to solar heating, but the 10 meter model temperature does not start increasing until 14 UTC and then by an insufficient amount. This result matches the results of the means of the difference of temperatures as shown in Figure 4.1. During this event, the observed dewpoint initially increased by around 1 °C during the first three hours (Figure 4.13) and then slowly decreased to a low at 10 UTC. In comparison, the predicted 10 meter dewpoint started decreasing immediately after initialization and decreased by around 1 °C more than observed at 10 UTC (Figure 4.13).

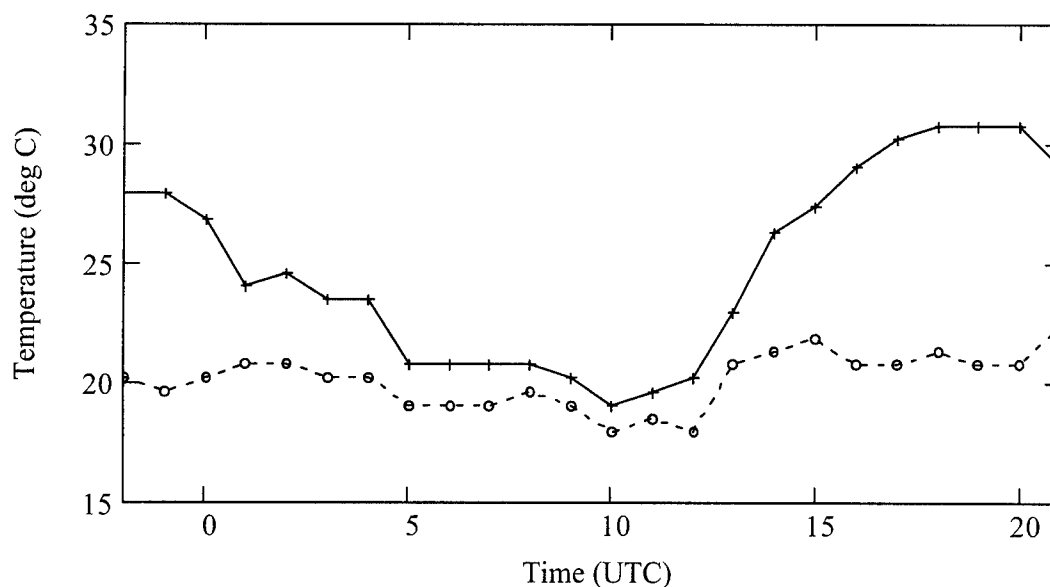


Figure 4.7. Hourly observations of temperature (—+—) and dewpoint (---o---) from 28 - 29 August 1985.

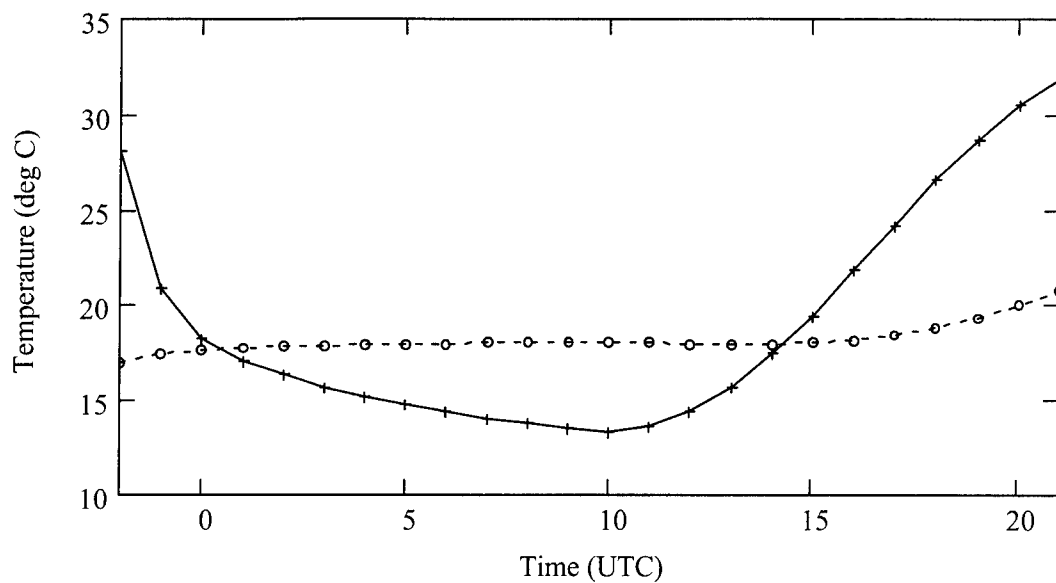


Figure 4.8. Predicted surface temperature (—+—) and dewpoint (---o---) based on 22 UTC 28 August 1985 data using SLU version of model.

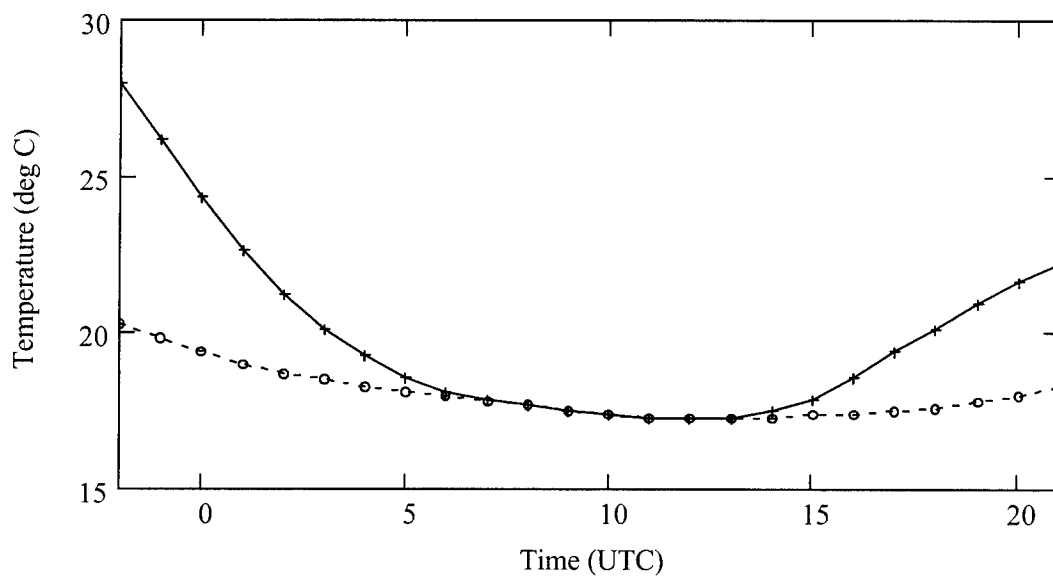


Figure 4.9. Predicted 10 meter temperature (—+—) and dewpoint (---o---) based on 22 UTC 28 August 1985 data using SLU version of model.

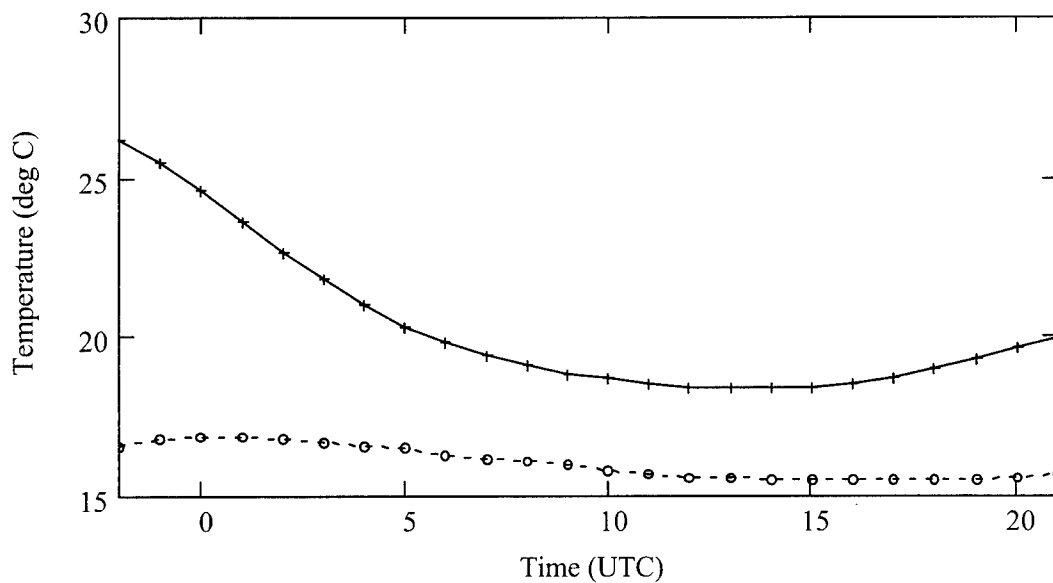


Figure 4.10. Predicted 200 meter temperature (—+—) and dewpoint (---o---) based on 22 UTC 28 August 1985 data using SLU version of model.

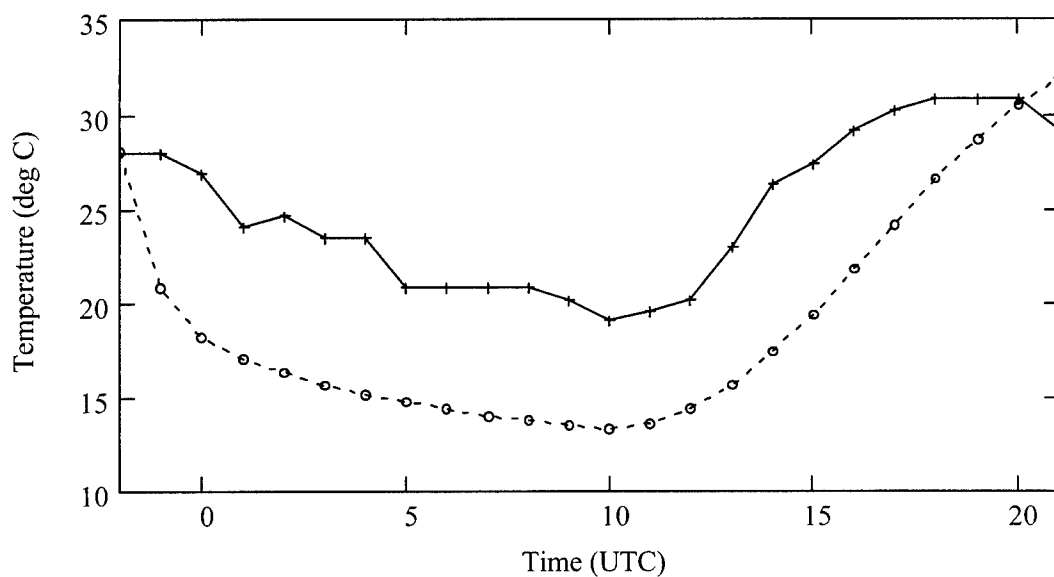


Figure 4.11. Comparison of observed temperature (—+—) and predicted surface temperature (---o---) based on 22 UTC 28 August 1985 data using SLU version of model.

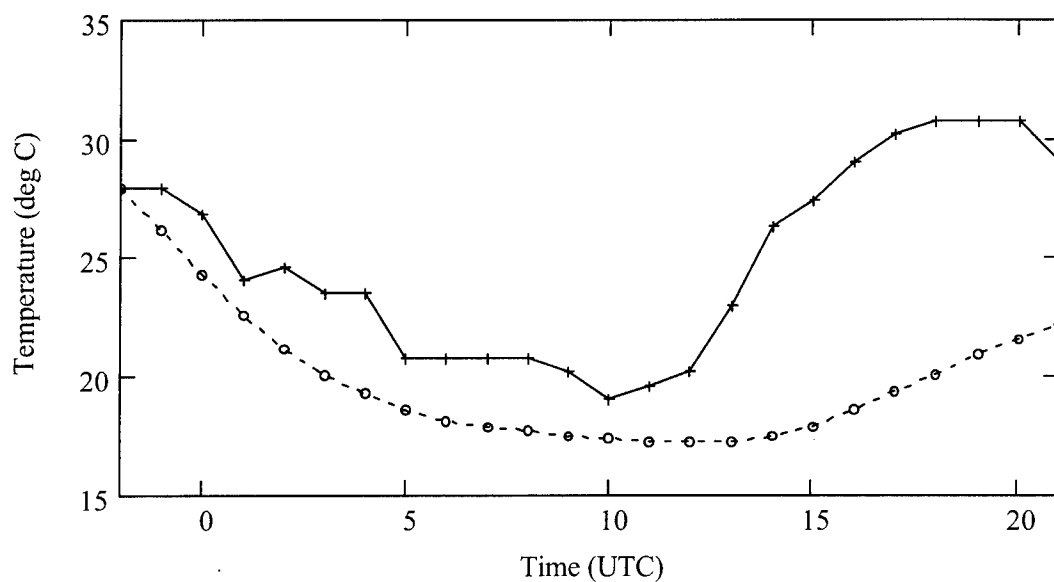


Figure 4.12. Comparison of observed temperature (—+—) and predicted 10 meter temperature (---o---) based on 22 UTC 28 August 1985 data using SLU version of model.

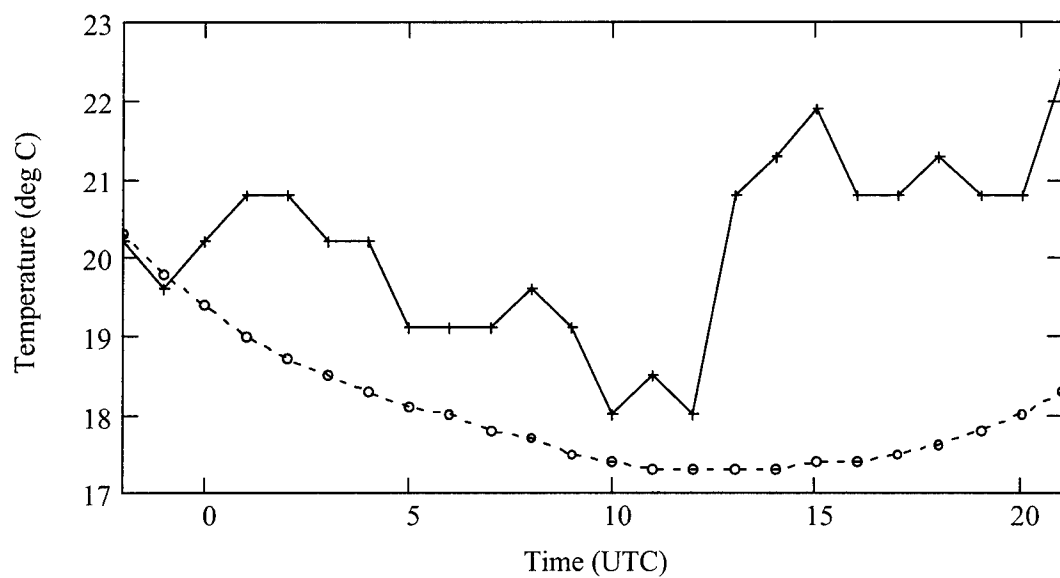


Figure 4.13. Comparison of observed dewpoint (—+—) and predicted 10 meter dewpoint (---o---) based on 22 UTC 28 August 1985 data using SLU version of model.

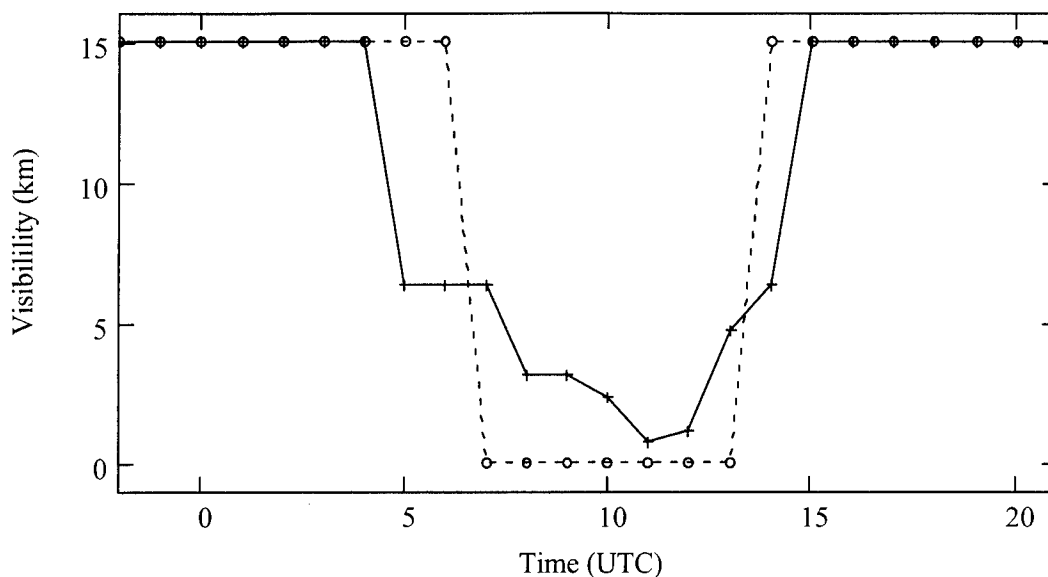


Figure 4.14. Comparison of observed visibility (—+—) and predicted 10 meter visibility (---o---) based on 22 UTC 28 August 1985 data using SLU version of model..

4.2.4 SLU Version Verification Results of a Single Fall Non-Fog Event

Now lets look at one of the events from the fall dataset where the model forecasted fog but no fog as observed. The initial data chosen was from observations taken on 9 and 10 November 1985 at Pope AFB. The 22 UTC observation taken on 9 November 1985 recorded the dry-bulb temperature of 20.2 °C (68.4 °F) and a dewpoint of 8.5 °C (47.3 °F). Winds at the time were observed to be 3.1 m s⁻¹ (6 knots). The soil type parameter of the model was set to moist sand and the soil wetness was assumed to be 50% relative humidity (RH). The lapse rate was set to a value of 90% adiabatic.

The minimum temperature occurred at 8 UTC 10 November 1985 as shown in Figure 4.15. The minimum temperature occurs at 11 UTC for both the surface (Figure

4.16) and 10 meter levels (Figure 4.17) of the model. Figure 4.17 also shows the model produced a period of saturation at the 10 meter level over the period 10 UTC to 15 UTC on 10 November 1985. The observations from Pope AFB reported no reduced visibility due to fog on 10 November (Figure 4.21). No stratus clouds were observed during this event nor would any be predicted based on the 200 meter temperature and dewpoint as shown in Figure 4.18. The results shown in the direct comparison of observed temperature at Pope AFB during the night of 9 - 10 November 1985 and the predicted 10 meter temperature based on 22 UTC November 1985 Pope AFB (Figure 4.19) are realistic until after sunrise. The predicted 10 meter temperature closely follows the observed temperature curve until 9 UTC. After 9 UTC, the observed temperature increased slowly until 12 UTC, when the observed temperature starts increasing rapidly due to solar heating, but the 10 meter model temperature does not start increasing until 15 UTC and then by an insufficient amount. This result matches the results from the summer verification study. During this event, the observed dewpoint slowly decreased by about 1 °C to a low from 8 and 13 UTC. In comparison, the predicted 10 meter dewpoint stayed almost constant throughout the period (Figure 4.20).

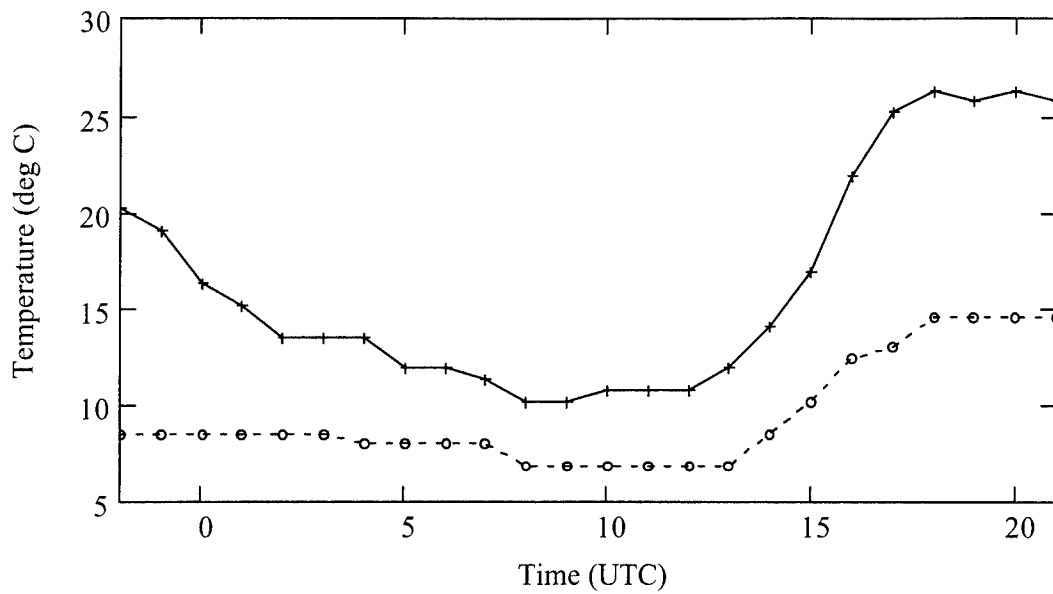


Figure 4.15. Hourly observations of temperature (—+—) and dewpoint (---o---) from 9 - 10 November 1985.

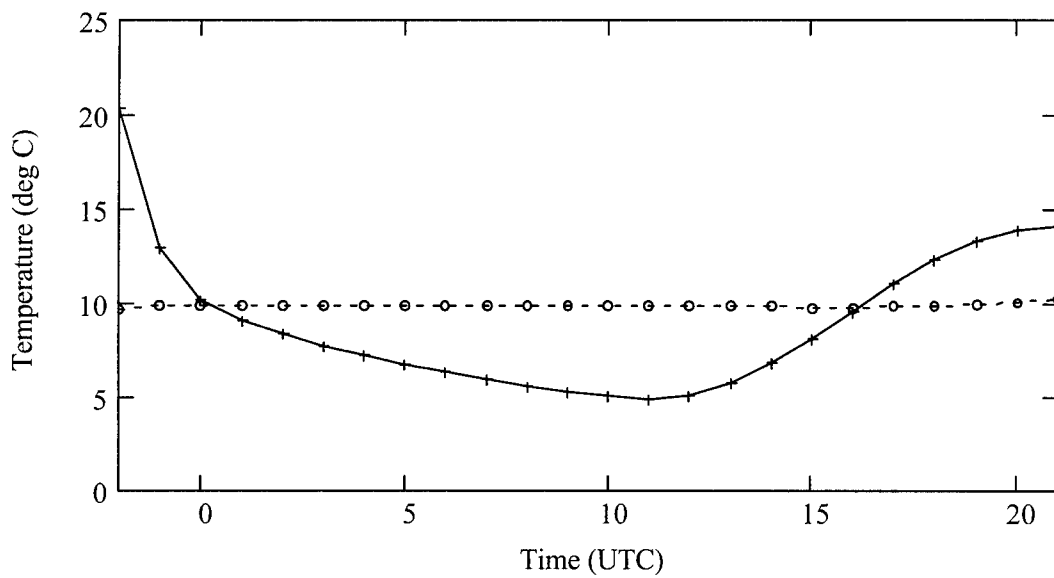


Figure 4.16. Predicted surface temperature (—+—) and dewpoint (---o---) based on 22 UTC 9 November 1985 data using SLU version of model.

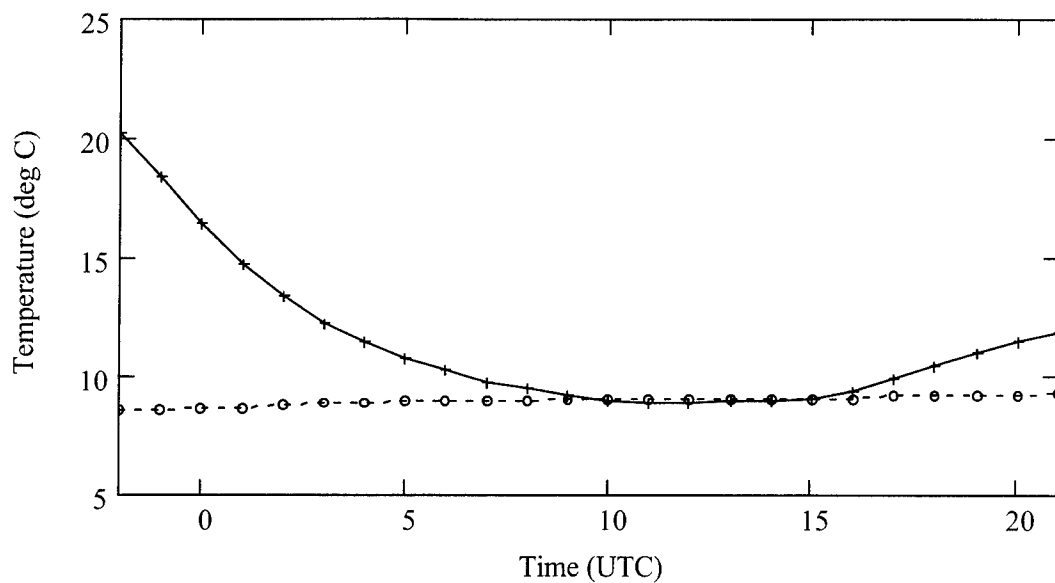


Figure 4.17. Predicted 10 meter temperature (—+—) and dewpoint (---o---) based on 22 UTC 9 November 1985 data using SLU version of model.

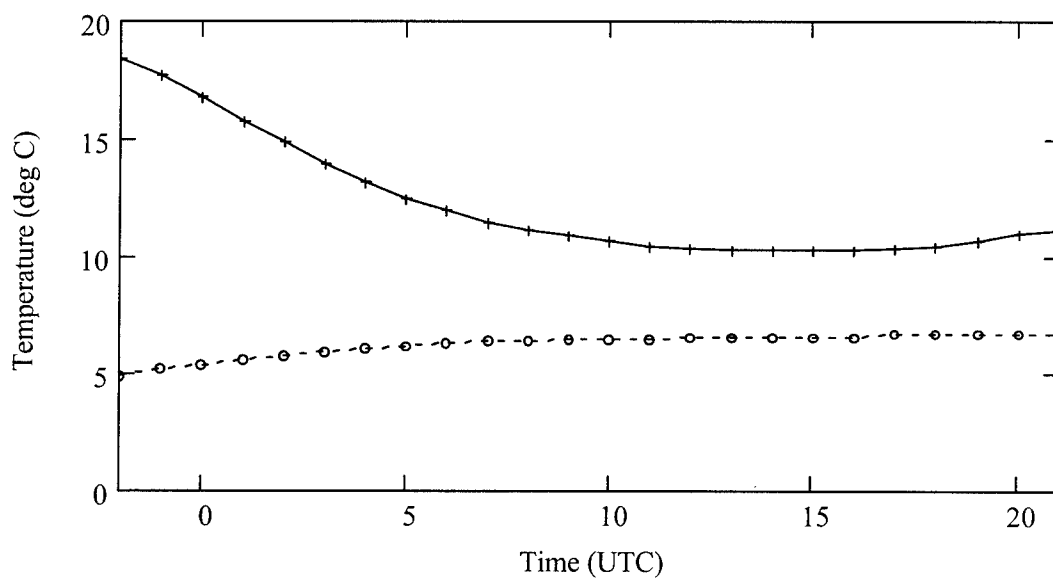


Figure 4.18. Predicted 200 meter temperature (—+—) and dewpoint (---o---) based on 22 UTC 9 November 1985 data using SLU version of model.

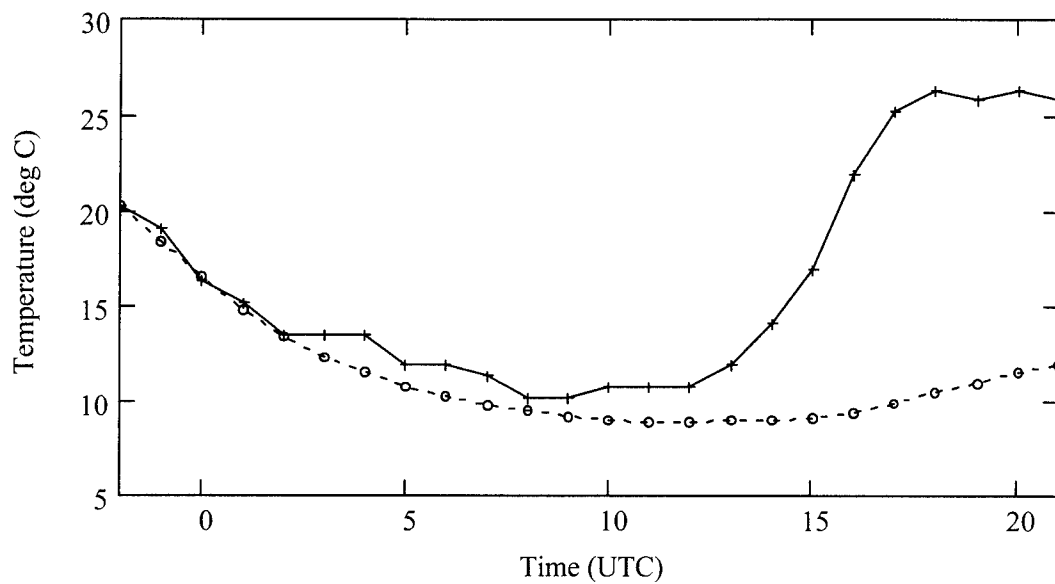


Figure 4.19. Comparison of observed temperature (—+—) and predicted 10 meter temperature (---o---) based on 22 UTC 9 November 1985 data using SLU version of model.

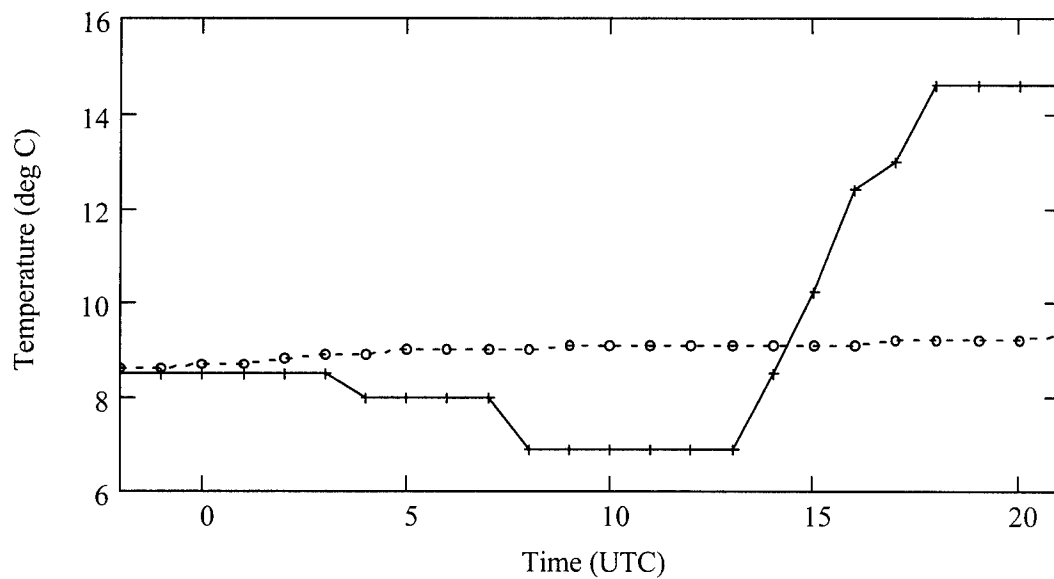


Figure 4.20. Comparison of observed dewpoint (—+—) and predicted 10 meter dewpoint (---o---) based on 22 UTC 9 November 1985 data using SLU version of model.

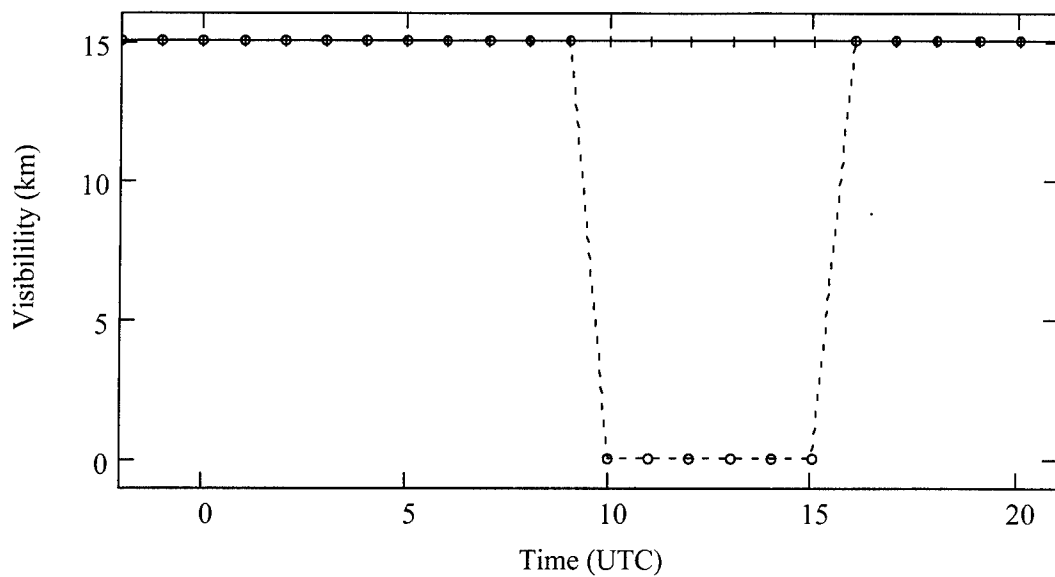


Figure 4.21. Comparison of observed visibility (—+—) and predicted 10 meter visibility (---o---) based on 22 UTC 9 November 1985 data using SLU version of model.

4.3 Sensitivity Study

Sensitivity tests were performed on the SLU version of the AWS Fog Model.

These sensitivity tests served two purposes. First, it is necessary to show what changes to the parameters and initial conditions affect fog model output. Second, they served as a basis for comparison with the adjusted fog model.

The results listed in Table 4.3 are valid for 11 UTC (7 L) and are for the same 61 summer “synoptically calm” events as used in the previous verification study. The results of each sensitivity test will be discussed in detail in the following sections.

4.3.1 Sensitivity Tests on Soil Type

The fog model is very sensitive to the soil type parameter. Because the fog model does not have explicit soil physics, several parameterizations have been included to account for the influence of soil characteristics in the development of the NBL and the onset of radiation fog (O'Sullivan 1996). Soil type has been parameterized following the results of Haltiner and Martin (1957). This parameterization allows for three different soil types, moist sand ($810.6 \text{ J K}^{-1} \text{ m}^{-2} \text{ s}^{-1/2}$), clay soil ($2215.6 \text{ J K}^{-1} \text{ m}^{-2} \text{ s}^{-1/2}$), and snow ($163.1 \text{ J K}^{-1} \text{ m}^{-2} \text{ s}^{-1/2}$). Soil type parameterization is important because it affects the amount of longwave cooling at the surface, which is the primary mechanism responsible for cooling the NBL.

The results of the sensitivity study show the model does not sufficiently cool the NBL with the Soil RH parameter set to clay soil. The average observed temperatures were over 2.5°C warmer than the 10 meter predicted temperatures. With the parameter set to snow, a very unrealistic scenario for summer in the Southeast, the NBL cools by about the right amount. The average observed temperatures were almost identical to the 10 meter predicted temperatures. As discussed in the previous verification study, this cooling is insufficient to completely saturate the 10 meter level. This leads to a bias much less than one ($B = 0.00$ to 0.03) for the snow and clay soil types, respectively, compared to bias of 0.40 for the moist sand soil type. SLU is currently working to incorporate a soil model into the fog model which should replace this crude parameterization of the soil physics. Until the current parameterization is replaced, the best value to use for the parameterization of soil type in the Southeast United States is moist sand.

4.3.2 Sensitivity Tests on Soil Relative Humidity (RH)

The fog model is overly sensitive to the soil RH in that there is almost no correlation between visibility and soil moisture as described in Chapter 3, but the fog model is very, very sensitive to the parameterization of soil RH. This is because the model uses the soil RH to calculate the surface dewpoint.

With soil RH set to 40%, the fog model predicted only 2 fog events out of 40. With soil RH set to 60%, the fog model predicted fog for almost every event in the study. The mean temperature error for forecasts with the soil RH equal to 40% showed that the model 10 meter temperature was on average 1.5 °C colder than the observed temperatures. The mean dewpoint error for forecasts with the soil RH equal to 40% showed that the model 10 meter dewpoint was on average 1.0 °C less than the observed dewpoints. This created higher dewpoint depressions at the 10 meter level and thus few predictions of fog when soil RH is set to 40%. The mean temperature error for soil RH equal to 60% showed that the model 10 meter temperature was on average 0.3 °C warmer than the observed temperatures. The mean dewpoint error for forecasts with the soil RH equal to 60% showed that the model 10 meter dewpoint was on average 3.0 °C greater than the observed dewpoints. This caused lower dewpoint depressions at the 10 meter level and thus fog prediction for almost every event when soil RH is set to 60%.

4.3.3 Sensitivity Tests on Wind Speed

The fog model is sensitive to the value input for wind speed, but in a way opposite to what is commonly observed. As shown in Table 4.3, the fog model predicts more fog events as the wind speed is increased. For the first test of model sensitivity, the observed winds that were generally around 5 to 8 knots or less were used for each event. Using these winds, the fog model predicted 14 out of 40 events at 11 UTC, while also predicting two fog events that did not occur. For the second test, the observed winds were disregarded and the wind speed was set to 10 knots for each event. Using 10 knots for the wind speed, the fog model predicted 23 out of 40 events at 11 UTC, while predicting three fog events that did not occur. For the third test, the observed winds were disregarded and the wind speed was set to 20 knots for each event. Using 20 knots for the wind speed, the fog model predicted 38 out of 40 events at 11 UTC, while predicting 20 fog events that did not occur. This result is not only counter intuitive but also runs counter to every observational study done to date. All observational studies have shown that as surface winds increase, fog is less likely to occur. This is because strong winds allow excess water that is condensed out due to radiational cooling to be deposited on the ground as dew through turbulent fluxes (Monteith 1957). This is a very significant problem that should be corrected before this model is used operationally.

4.3.4 Sensitivity Tests on Temperature and Dewpoint

Sensitivity tests were performed on temperature and dewpoint (Table 4.3). Decreasing the initial temperature by 2 °C or increasing the initial dewpoint by 2 °C gives

almost identical results. Decreasing the temperature by 2 °C gave the best results of the sensitivity study with 27 out of 40 fog events predicted, while only predicting 3 events that did not occur. This gives a percent correctly forecast of 75% and a bias of 0.75.

Increasing the dewpoint by 2 °C yields similar results with 23 out of 40 fog events predicted, while only predicting 3 events that did not occur. These results suggest that the model would perform better with additional cooling or by including a parameterization of the slight increase (1 to 2 °C) in dewpoint after sunset that was noted in the verification study.

4.3.5 Results of Sensitivity Study of Longwave Parameter, Shortwave Parameter, and Height of Observation Level

Sensitivity tests were also performed on the longwave radiation parameter, the shortwave radiation parameter and the height of observation level. The results are not shown in Table 4.3 because changes to these parameters did not affect the model output. The model is not sensitive to the longwave radiation parameter or the shortwave radiation parameter because calculations using these parameters are turned off in the SLU version. These parameters would become important if the effects of latent heat release and longwave radiation emittance from the fog layer were included in the model.

The height of the observation level was set to 10 meters in the SLU version. Bringing the observation level down to the standard observation level of 2 meter for temperature and dewpoint had no noticeable effect on model output. The two meter level will be used in the adapted version because most observations of visibility are taken at the

two meter level. This will allow for a better comparison of observed visibilities to model visibilities in future verification studies.

4.3.6 Results of Sensitivity Study of Lapse Rate

Sensitivity tests were also performed on changes in the lapse rate used for computing the initial temperatures and dewpoints at 200 and 1000 meters. The verification study was performed with the lapse rate set to 90 % of adiabatic (0.9×9.77 °C km⁻¹). Two other lapse rates were tested in the sensitivity study (Table 4.3). First, the lapse rate was set to 50% of adiabatic (0.5×9.77 °C km⁻¹). Secondly, the lapse rate was set to isothermal (0.0×9.77 °C km⁻¹). For both lapse rates, the results were the same. Fog was not predicted for any of the 61 events.

Table 4.3. Results of sensitivity tests using SLU version of the AWS Fog Model.

Parameter		Mean			Temp			Mean			DP			Mean			Visibility		
		Temp			Standard			Error			DP			Error			Standard		
		°C			°C			°C			°C			°C			meters		
		Bias			PC			W			Z			Y			X		
		#			#			#			#			#			#		
		%			%			%			%			%			%		
		°C			°C			°C			°C			°C			meters		
		meters			meters			meters			meters			meters			meters		
		meters			meters			meters			meters			meters			meters		
		meters			meters			meters			meters			meters			meters		
		meters			meters			meters			meters			meters			meters		
		meters			meters			meters			meters			meters			meters		
		meters			meters			meters			meters			meters			meters		
		meters			meters			meters			meters			meters			meters		
		meters			meters			meters			meters			meters			meters		
		meters			meters			meters			meters			meters			meters		
		meters			meters			meters			meters			meters			meters		
		meters			meters			meters			meters			meters			meters		
		meters			meters			meters			meters			meters			meters		
		meters			meters			meters			meters			meters			meters		
		meters			meters			meters			meters			meters			meters		
		meters			meters			meters			meters			meters			meters		
		meters			meters			meters			meters			meters			meters		
		meters			meters			meters			meters			meters			meters		
		meters			meters			meters			meters			meters			meters		
		meters			meters			meters			meters			meters			meters		
		meters			meters			meters			meters			meters			meters		
		meters			meters			meters			meters			meters			meters		
		meters			meters			meters			meters			meters			meters		
		meters			meters			meters			meters			meters			meters		
		meters			meters			meters			meters			meters			meters		
		meters			meters			meters			meters			meters			meters		
		meters			meters			meters			meters			meters			meters		
		meters			meters			meters			meters			meters			meters		
		meters			meters			meters			meters			meters			meters		
		meters			meters			meters			meters			meters			meters		
		meters			meters			meters			meters			meters			meters		
		meters			meters			meters			meters			meters			meters		
		meters			meters			meters			meters			meters			meters		
		meters			meters			meters			meters			meters			meters		
		meters			meters			meters			meters			meters			meters		
		meters			meters			meters			meters			meters			meters		
		meters			meters			meters			meters			meters			meters		
		meters			meters			meters			meters			meters			meters		
		meters			meters			meters			meters			meters			meters		
		meters			meters			meters			meters			meters			meters		
		meters			meters			meters			meters			meters			meters		
		meters			meters			meters			meters			meters			meters		
		meters			meters			meters			meters			meters			meters		
		meters			meters			meters			meters			meters			meters		
		meters			meters			meters			meters			meters			meters		
		meters			meters			meters			meters			meters			meters		
		meters			meters			meters			meters			meters			meters		
		meters			meters			meters			meters			meters			meters		
		meters			meters			meters			meters			meters			meters		
		meters			meters			meters			meters			meters			meters		
		meters			meters			meters			meters			meters			meters		
		meters			meters			meters			meters			meters			meters		
		meters			meters			meters			meters			meters			meters		
		meters			meters			meters			meters			meters			meters		
		meters			meters			meters			meters			meters			meters		
		meters			meters			meters			meters			meters			meters		
		meters			meters			meters			meters			meters			meters		
		meters			meters			meters			meters			meters			meters		
		meters			meters			meters			meters								

Table 4.3 Continued. Results of sensitivity tests using SLU version of the AWS Fog Model.

Parameter	Mean Temp				Mean DP				Mean Visibility			
	X #	Y #	Z #	W #	PC	Bias	Temp Error °C	Standard Deviation °C	DP Error °C	DP Variance °C	Visibility Error meters	Visibility Variance meters
n = 61	14	26	2	19	.54	.40	0.83	1.0	-1.1	1.0	-1500	910
Lapse Rate	0	40	0	21	.34	0	-1.2	1.5	-1.3	1.4	-5500	405
0.9 Adiabatic	0	40	0	21	.34	0	-1.5	1.8	-1.8	1.9	-5500	500
X	= the number of times the event was predicted and occurred at 11 UTC											
Y	= the number of times the event was not predicted but occurred at 11 UTC											
Z	= the number of times the event was predicted but did not occur at 11 UTC											
W	= the number of times the event was not predicted and did not occur AT 11 UTC											
PC	= the percent correctly forecasted $PC = (X+W)/(X+Y+Z+W)$											
Bias	= the ratio of the number of times fog was forecasted to the number of times fog occurred $Bias = (X+Z)/(X+Y)$											
Mean Temp Error	= The mean temperature difference between the observed temperature and the 10 meter model temperature at 11 UTC. Minus values indicate that the 10 meter model temperature is warmer than the observed temperature.											
Temp Standard Deviation	= The standard deviation of the difference between the observed temperature and the 10 meter model temperature at 11 UTC.											
Mean DP Error	= The mean dewpoint difference between the observed dewpoint and the 10 meter model dewpoint at 11 UTC. Minus values indicate that the 10 meter model dewpoint is warmer than the observed dewpoint.											
DP Standard Deviation	= The standard deviation of the difference between the observed dewpoint and the 10 meter model dewpoint at 11 UTC.											
Mean Visibility Error	= The mean visibility difference between the observed visibility and the 10 meter model visibility at 11 UTC. Minus values indicate that the 10 meter model visibility is higher than the observed visibility.											
Visibility Standard Deviation	= The variance of the difference between the observed visibility and the 10 meter model visibility at 11 UTC.											

4.4 Verification Study of Adapted Version

Using the results of the verification and sensitivity study done on the SLU version of the fog model, the fog model was adapted to forecast fog in the Southeast United States. The goal of this adaptation process was to remove any overforecasting and underforecasting bias from the model. In the verification of the SLU version, the fog model showed an underforecasting bias for the summer season and a overforecasting bias for the fall season. Many different parameter changes were tested to remove these biases. For the summer season, the underforecasting bias was removed by increasing the soil relative humidity parameter from 50 % to 53 %. For the fall season, the overforecasting bias was removed by decreasing the soil relative humidity parameter from 50% to 43%. Also, the minimum dewpoint depression reached before declaring a predicted fog event was changed from 0.1 to 0.5 °C for both seasons. The dewpoint depression of 0.5 °C was chosen to indicate the occurrences of light radiation fog, fogs with minimum visibilities greater than 4800 meters.

4.4.1 Adapted Version Verification Results for Summer Season

The adapted version shows a significant improvement over the standard SLU version for the summer verification study. Table 4.4 shows that during the critical hours of 10 and 11 UTC the model beat persistence with a skill score of 0.30. At 11 UTC, the model predicted 34 of 40 fog events, while predicted 9 that did not occur, for a percentage correct of 75 %. The bias at 11 UTC, 1.08, was close to one. The model now

has an overforecasting bias from 12 to 15 UTC. This is due to the insufficient warming at the 10 meter level after sunrise that was identified in the SLU version verification study.

The 10 meter predicted temperature during the 28 - 29 August 1985 event is slightly less than the observed temperature (Figure 4.24). After 12 UTC, the observed temperature increases rapidly, but the 10 meter predicted temperature does not start increasing until 15 UTC and then not as rapidly. Figure 4.25 shows that the 10 meter predicted dewpoint for the 28 - 29 August 1985 event closely matches the observed dewpoint at 10 and 12 UTC. The predicted visibility during the 28 - 29 August 1985 event closely matches the observed visibility (Figure 4.26). Both predicted and observed visibilities are 6400 meters at 5 UTC, the first hour of fog formation. Both the predicted and observed visibilities decrease to around 800 meters at 11 UTC. The fog model indicates no fog at 15 UTC, which is one hour later than observed. Figure 4.22 shows large differences in observed visibility versus predicted visibility at 11 UTC for most of the other events studied. The average error in predicted visibilities for the 61 summer events was 3.9 km, which is a one km reduction from the SLU version average error for the summer events.

4.4.2 Adapted Version Verification Results for Fall Season

The adapted version does not show as significant improvement over the standard SLU version for the fall verification study as it did for the summer events. Table 4.5 shows that during the critical hours of 11 and 12 UTC, the model still did not beat persistence with a skill score of -0.62 to -0.50, respectively. At 12 UTC, the model

predicted 9 of 20 fog events, but also predicting 7 that did not occur, for a percentage correct of 67 %. The bias at 12 UTC was 0.73. The model still has an overforecasting bias from 12 to 15 UTC. This overforecasting bias is due to the insufficient warming at the 10 meter level after sunrise that was identified in the SLU version verification study.

The predicted temperature during the 9 - 10 November 1985 event is slightly less than the observed temperature during the night (Figure 4.27). After 12 UTC, the observed temperature increases rapidly, but the 10 meter predicted temperature does not start increasing until 15 UTC and then not rapidly. Figure 4.28 shows that the 10 meter predicted dewpoint for the 9 - 10 November 1985 event closely matches the observed dewpoint until 3 UTC. After 3 UTC, the predicted dewpoint remains almost constant while the observed dewpoint decreases significantly. The model predicted a light fog (6400 meters) from 12 to 14 UTC for the 9 - 10 November 1985 event, but no visibility reduction was observed as shown in Figure 4.29. This visibility difference was mainly due to the model not decreasing the dewpoint at night as was observed and to insufficient warming after sunrise. Figure 4.23 shows differences in observed visibility versus predicted visibility at 11 UTC for most of the other events studied. The average error in predicted visibilities for the 61 fall events was 2.2 km. This is a 3.7 km reduction in average visibility error from the SLU version average error for the fall events.

Table 4.4. Adapted Version Verification Results for Summer Season.

Time UTC	X #	Y #	Z #	W #	PC	POD	FAR	Bias	SS
22	0	0	0	61	1	-	-	-	1
23	0	0	0	61	1	-	-	-	1
0	0	0	0	61	1	-	-	-	1
1	0	0	1	60	.98	-	1	-	.80
2	0	0	1	60	.98	-	1	-	.80
3	0	1	2	58	.95	0	1	2	.67
4	0	3	3	55	.90	0	1	1	.50
5	3	4	4	50	.87	.43	.57	1	.50
6	3	8	8	42	.74	.27	.73	1	.10
7	6	10	10	35	.67	.38	.62	1	-.10
8	8	13	11	29	.61	.38	.58	.90	-.30
9	19	10	10	22	.67	.66	.34	1	.15
10	29	8	6	18	.77	.78	.17	.95	.36
11	34	6	9	12	.75	.85	.21	1.08	.32
12	26	5	17	13	.64	.84	.40	1.39	-.13
13	7	0	26	28	.57	1	.79	4.71	-.59
14	3	0	15	43	.75	1	.83	6.00	-.79
15	0	2	3	56	.92	0	1	1.5	-.60
16	0	1	0	60	.98	0	-	0	.33
17	0	1	0	60	.98	0	-	0	0
18	0	1	0	60	.98	0	-	0	0
19	0	1	0	60	.98	0	-	0	-
20	0	0	0	61	.98	-	-	-	-

- X = the number of times the event was predicted and occurred
 Y = the number of times the event was not predicted but occurred
 Z = the number of times the event was predicted but did not occur
 W = the number of times the event was not predicted and did not occur
 PC = the proportion correct $PC = (X+W)/(X+Y+Z+W)$
 POD = the probability of detection $POD = X/(X+Y)$
 FAR = the false alarm rate $FAR = Z/(X+Z)$
 Bias = the ratio of the number of times fog was forecasted to the number of times fog occurred $Bias = (X+Z)/(X+Y)$
 SS = persistence based skill score $SS = (PC - PC_{per})/(1-PC_{per})$
 where PC_{per} is proportion correct based on persistence forecasts

Table 4.5. Adapted Version Verification Results for Fall Season.

Time UTC	X #	Y #	Z #	W #	PC	POD	FAR	Bias	SS
22	0	0	0	61	1	-	-	-	1
23	0	0	0	61	1	-	-	-	1
0	0	0	0	61	1	-	-	-	1
1	0	0	0	61	1	-	-	-	1
2	0	0	0	61	1	-	-	-	1
3	0	2	0	59	.97	0	-	0	.81
4	0	4	0	57	.93	0	-	0	.56
5	0	5	0	56	.92	0	-	0	.60
6	0	5	0	56	.92	0	-	0	.60
7	1	8	0	52	.87	.11	0	.11	.19
8	3	6	0	52	.90	.33	0	.33	.38
9	5	6	2	48	.87	.45	.29	.64	.35
10	5	8	3	45	.82	.38	.38	.62	.10
11	7	11	5	38	.74	.39	.42	.67	-.62
12	9	13	7	32	.67	.41	.44	.73	-.50
13	7	9	10	35	.69	.44	.59	1.06	.06
14	3	5	12	41	.72	.38	.80	1.88	-.40
15	0	1	8	52	.85	0	1	8.00	-1
16	0	0	5	56	.92	-	1	-	-1
17	0	0	0	61	1	-	-	-	1
18	0	0	0	61	1	-	-	-	1
19	0	0	0	61	1	-	-	-	1
20	0	0	0	61	1	-	-	-	1

- X = the number of times the event was predicted and occurred
 Y = the number of times the event was not predicted but occurred
 Z = the number of times the event was predicted but did not occur
 W = the number of times the event was not predicted and did not occur
 PC = the proportion correct $PC = (X+W)/(X+Y+Z+W)$
 POD = the probability of detection $POD = X/(X+Y)$
 FAR = the false alarm rate $FAR = Z/(X+Z)$
 Bias = the ratio of the number of times fog was forecasted to the number of times fog occurred $Bias = (X+Z)/(X+Y)$
 SS = persistence based skill score $SS = (PC - PC_{per})/(1-PC_{per})$
 where PC_{per} is proportion correct based on persistence forecasts

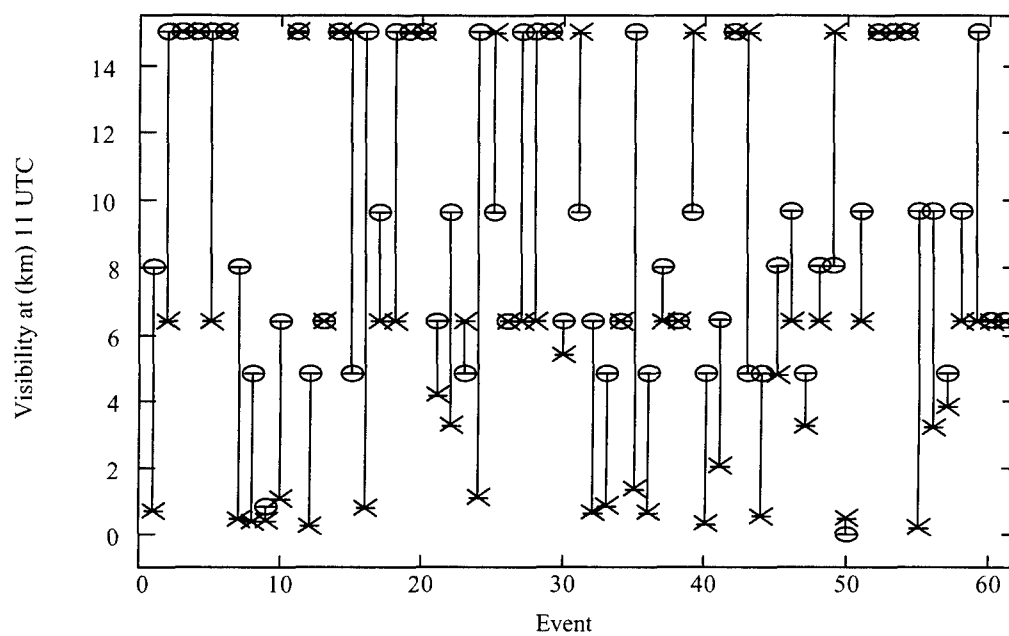


Figure 4.22. Visibility at 11 UTC: observed visibility (Θ) and 10 meter model visibility (X) using adapted version, for 61 summer radiation cooling events.

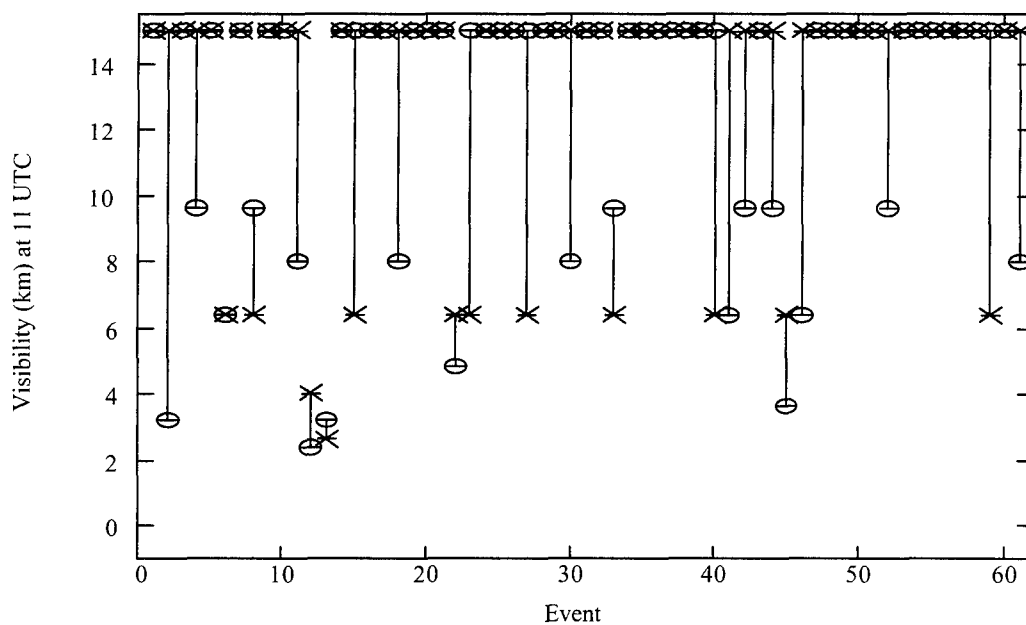


Figure 4.23. Visibility at 11 UTC: observed visibility (Θ) and 10 meter model visibility (X) using adapted version, for 61 fall radiation cooling events.

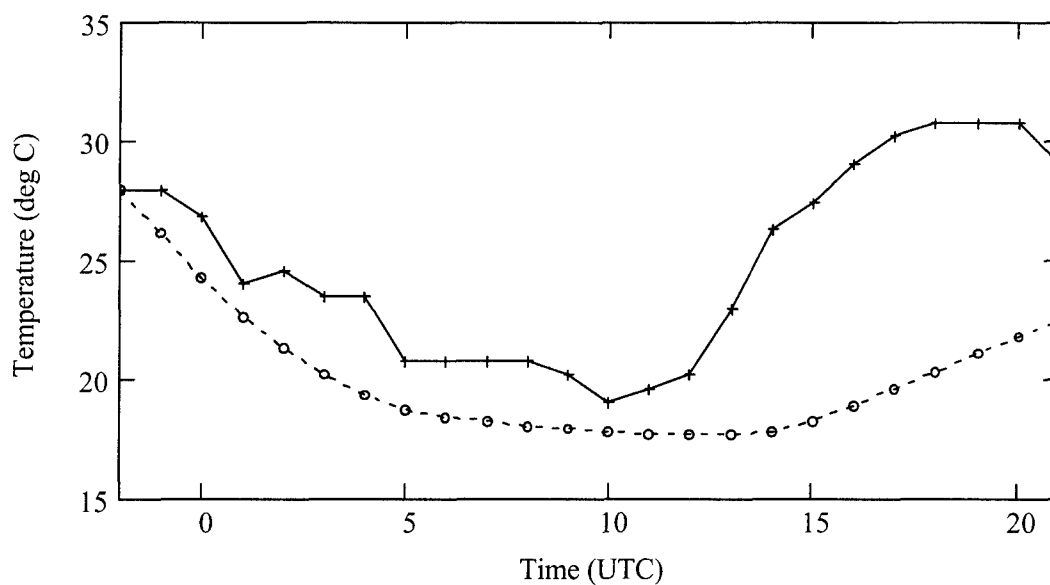


Figure 4.24. Comparison of observed temperature (—+—) and predicted 10 meter temperature (---o---) based on 22 UTC 28 August 1985 data using adapted version of model.

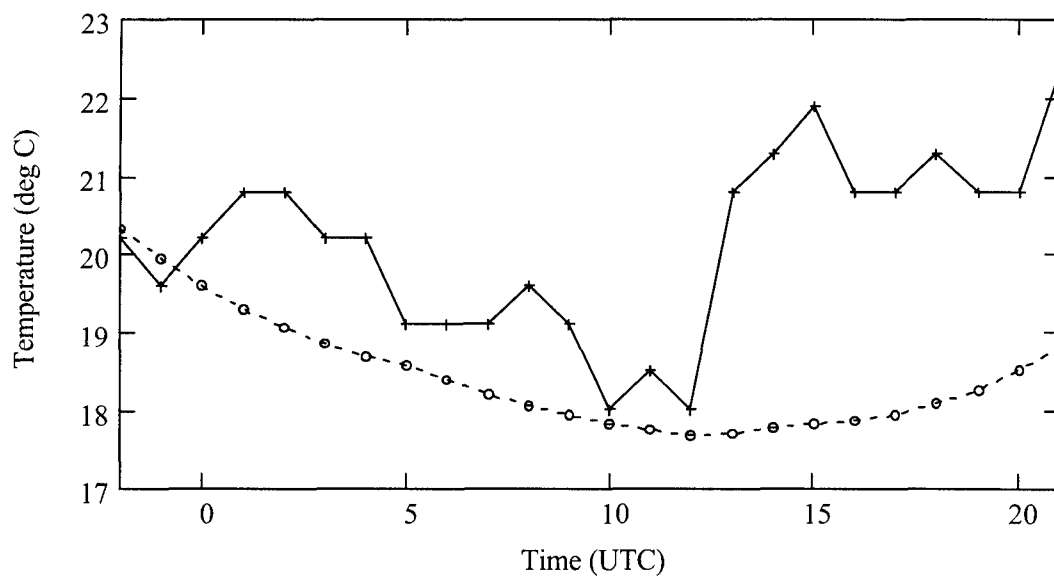


Figure 4.25. Comparison of observed dewpoint (—+—) and predicted 10 meter dewpoint (---o---) based on 22 UTC 28 August 1985 data using adapted version of model.

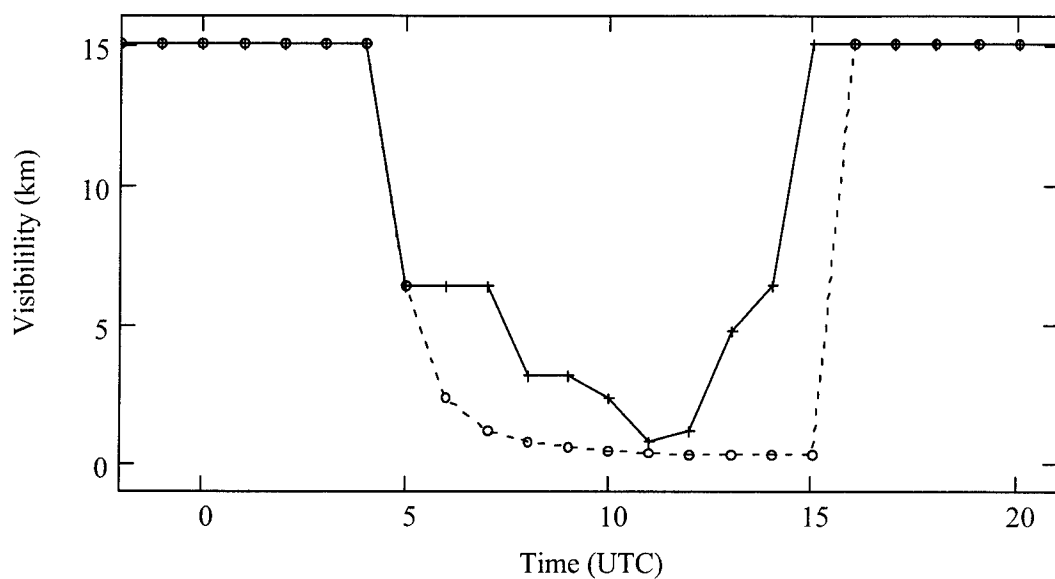


Figure 4.26. Comparison of observed visibility at Pope AFB (—+—) and predicted 10 meter visibility (---o---) based on 22 UTC 28 August 1985 data using adapted version of model.

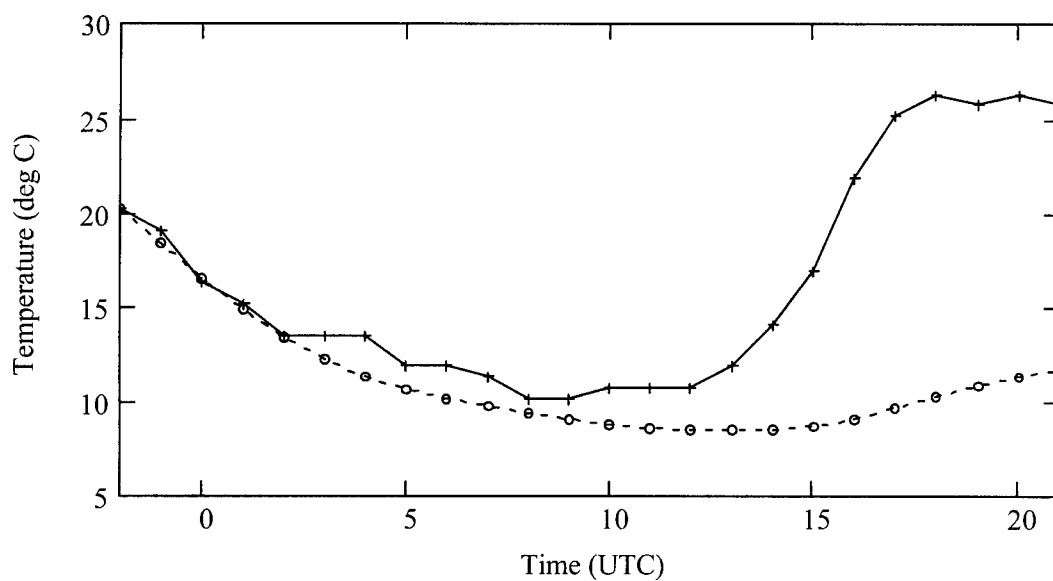


Figure 4.27. Comparison of observed temperature (—+—) and predicted 10 meter temperature (---o---) based on 22 UTC 9 November 1985 data using adapted version of model.

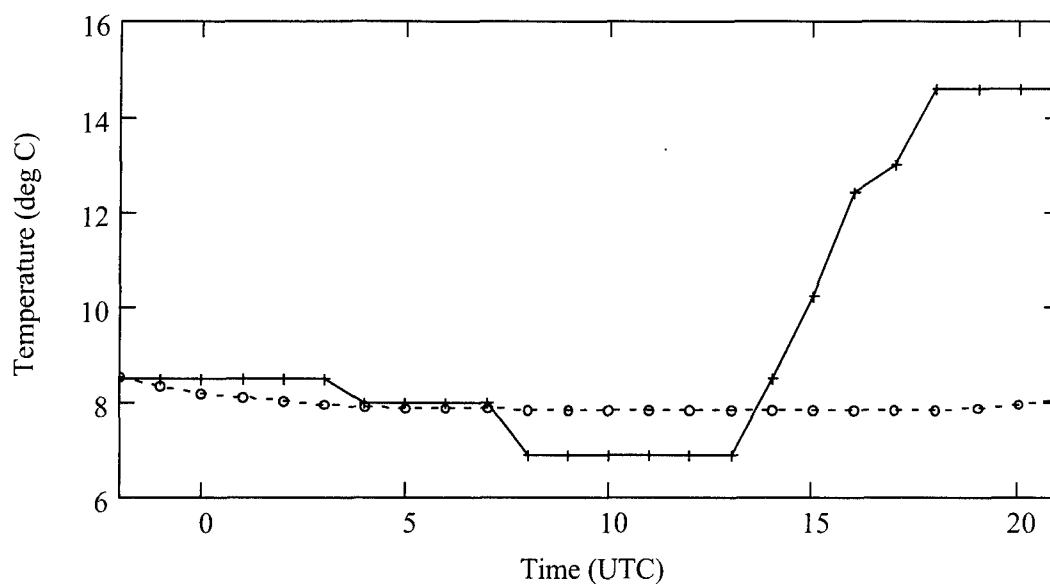


Figure 4.28. Comparison of observed dewpoint (—+—) and predicted 10 meter dewpoint (---o---) based on 22 UTC 9 November 1985 data using adapted version of model.

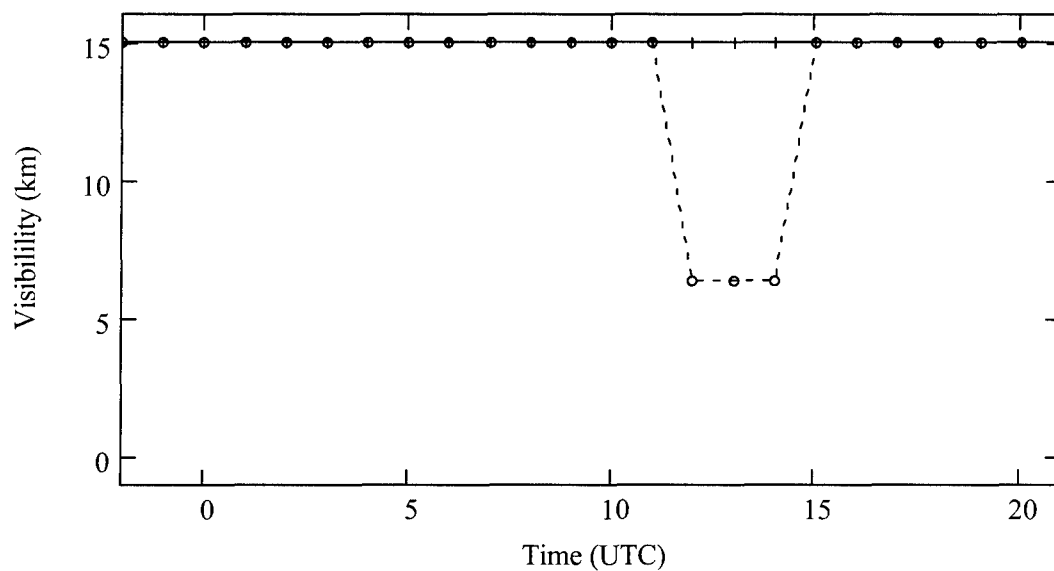


Figure 4.29. Comparison of observed visibility at Pope AFB (—+—) and predicted 10 meter visibility (---o---) based on 22 UTC 9 November 1985 data using adapted version of model.

4.5 Suggestions for Operational Use of the AWS Fog Model

Successful use of this fog model in operational forecasting is possible if the user is aware of model limitations. This section defines these limitations, presents suggestions for the user to consider when entering the model input variables, and gives some helpful insights in interpreting the model output.

This model is designed to predict radiation fog only. The user must decide if conditions are right for radiational cooling before using the fog model. The model assumes no cloud cover, therefore the model user should not expect accurate model output in cases where more than scattered clouds are present during the evening and early morning hours. The presence of clouds inhibits cooling in the nocturnal boundary layer. The model will overforecast fog occurrences in this situation. Also, the model assumes no advection of temperature or moisture after the 22 UTC initialization time. The user should be observant to increases in surface temperature and to large increases or decreases in surface dewpoint after model initialization. It may be necessary to run the model again with the new temperature or dewpoint values. The model should not be used in the presence of changing synoptic scale weather patterns. Frontal passage, rain events, and advection of fog or stratus clouds over the forecast area will completely invalidate model results.

The fog model is sensitive to the value input for wind speed, but in a way opposite to what is observed. The user should be aware that increasing the value input for wind speed will increase the model prediction of fog. Typical radiational cooling events occur

under very light wind conditions. Strong winds will invalidate model results. The soil type of moist sand should be used in most locations. Use the clay soil and new snow soil type only after performing a verification study for the desired location. This model has not been verified at any location with clay soil or new snow soil types. Also, the model is very sensitive to the soil moisture input variable. For Pope AFB a value of 53% produced the least biased results for the summer season, while a value of 43% produced the least biased results for the fall season. Lower soil moisture values will produce lower model prediction of fog, while higher values will produce higher model prediction of fog. The model allows the user to input surface temperature and dewpoint, in addition, the 200 meter and 1000 meter temperature and dewpoint can be entered, if desired. Inputting 200 and 1000 meter temperatures and dewpoints provides better model output over using 90% adiabatic lapse rate.

The model provides predictions of visibility along with temperature and dewpoint predictions. If the predicted observation level temperature is within 0.5 °C of the dewpoint, the model will predict a visibility equal to 6400 meters (4 miles). If the observation level temperature is less than or equal to the dewpoint, the model will compute a visibility based on available water above saturation. If using the model to forecast minimum temperature, increase the model minimum temperature by 1.0 °C to account for warming due to condensation at the surface. Be aware that the model does not sufficiently warm the observation level after sunrise, this allows the level to remain saturated longer than typically observed. Use normal rules of thumb and previous

experience to forecast fog dissipation; do not use model fog dissipation time as it will almost always be two to three hours later than observed.

5. Conclusions and Recommendations for Future Work

5.1 Summary of Conclusions

In this research, the performance of the AWS Fog Model was verified. The SLU version was also adapted for use in predicting radiation fog events in the Southeast United States. This task was accomplished through four separate steps. First, a correlation study was performed by comparing the different variables in observations that met certain radiational cooling conditions to the observed visibility. This correlation study established the importance of each input variable of the model. Second, a verification study was conducted on the SLU version of the AWS Fog Model. This verification study established the forecast accuracy of the SLU version in predicting fog in the Southeast United States. Third, a sensitivity study was conducted on the SLU version of the AWS Fog Model. This sensitivity study was used to adjust and revise the SLU version of the fog model for application in the Southeast United States. Finally, the SLU version of the fog model was revised using the results of the sensitivity and verification study and another verification study was conducted.

In the correlation study, the correlation between the parameterization of soil moisture and observed visibility was very low. This low correlation suggests that the development of fog does not depend significantly on the moisture of the soil. The results of the sensitivity study of soil moisture shows that while the fog model is very sensitive to the soil relative humidity parameter, this sensitivity is not reflected in real world observations. This results call into question the physics of the parameterization of soil

moisture used in the AWS Fog Model. SLU is currently working to replace this parameterization with a soil model that should correct this problem.

Low correlation (0.13) was also calculated between the 11 UTC dewpoint depression and the 11 UTC observed visibility. This result suggests that even though all occurrences of fog are at dewpoint depressions of 2.2 °C or less, not all occurrences of dewpoint depressions of 2.2 °C or less are accompanied by an occurrence of fog. The fog model does a good job of computing the diurnal changes in temperature and dewpoint, but it lacks the necessary physics to accurately distinguish between occurrences of fog and dew. The correlation between the 22 UTC dewpoint depression and 11 UTC visibility was 0.60, which was slightly greater than the forecasting accuracy of the SLU version of the fog model. It is this correlation that the fog model uses to forecast fog. In general, if the 22 UTC dewpoint depression is low, then the fog model will indicate saturated conditions at 11 UTC. If the 22 UTC dewpoint depression is high, then the fog model will not indicate saturated conditions at UTC.

The correlation of wind speed versus visibility was low, but this low correlation is most likely due to imprecise measurements of wind speed that were used in the correlation study. Standard airfield observations were used in the correlation study and more accurate wind speed measurements were not available. In correlation studies of wind speed versus visibility where more accurate wind speed measurements were available, a strong correlation was observed between visibility and wind speed (Monteith 1957). Monteith noted that strong winds allow excess water that is condensed out due to radiational cooling to be deposited on the ground as dew through turbulent fluxes. In the

sensitivity study performed on this model, the occurrence of fog increased as wind speed increased. This result is opposite to what is commonly observed and is one of the biggest problems with the model. The problem seems to come from the method of computing temperature that neglects cooling by longwave radiation of the air and assumes all cooling is due to turbulent mixing with the cooler surface level. Increasing wind speed allows more turbulent mixing and hence more cooling at the 10 meter level. More cooling at the 10 meter level leads to a lower dewpoint depression and more occurrences of saturation at that level. Another problem is the unlimited supply of moisture at the surface. The increased wind speed allows more turbulent mixing of moisture between the 10 meter level and the surface. The model does not condense water at the surface and therefore the surface becomes a source of water vapor, when in fact under high wind conditions it should be a water vapor sink leading to the formation of dew.

A verification study was performed for two seasons on the SLU version of the AWS Fog Model. The results of the summer season verification study showed that the model has a underforecasting bias at all hours except 13 UTC. At the time of maximum fog occurrence (11 UTC), the fog model forecasted 14 of 40 fog events, but only forecasted 2 events that did not occur, for a percent correct of 54%. For the same hour the persistence forecast percent correct was 63%. This gives a negative skill score of -0.24, which indicates that it would be better to use persistence forecasts than model output. The model on average cooled the nocturnal boundary layer at the 10 meter level during the night by around 1.5 °C more than observed. However, a large mean temperature difference, 8 °C, after sunrise was observed in every case. This causes the 10

meter layer to remain saturated longer than what is observed. The visibility errors between observed visibility and 10 meter visibility are large. The average error at 11 UTC for the 61 summer events was 4.9 km. Part of this large error is due to the model not predicting fog events that occurred and part is due to an error in the model's calculation of visibility. The SLU version, along with the Mathematica version, uses the total water content (vapor plus liquid) to compute visibility as soon as the layer becomes saturated. This is unrealistic as only the excess water vapor above saturation should be used in visibility calculations. This error causes the fog model to compute visibilities of around 50 meters as soon as the layer becomes saturated. The adapted model condenses out the excess water vapor and uses this value for visibility calculations in the method by Bergot and Guedalia (1994). While this is a slight improvement, more accurate calculations cannot be added until the vertical resolution of the model is increased. Increasing the vertical resolution will allow the additional parameterization of gravitational settling of fog droplets to the surface.

The results of the fall season verification study showed that the fog model overforecasted fog events in the fall months. The fog model overforecasted radiation fog during the critical fog hours of 8 UTC through 14 UTC. At the time of maximum fog occurrence (12 UTC), the fog model forecasted 15 of 22 fog events, but forecasted 17 events that did not occur, for a percent correct of 61 %. For the same hour the persistence forecast percent correct was 78 %. This gives a negative skill score, -0.77, which again indicates that it would be better to use persistence forecasts than model output. The false alarm rate was high for each hour with over one half of the model

forecasted fog events being false alarms. The most likely cause of the overforecasting bias that appears in the fall verification study is that the model does not decrease the dewpoint during the night as much as is observed.

The underforecasting for the summer season and a overforecasting bias for the fall season were removed by making slight changes in fog model parameters. For the summer season, the underforecasting bias was removed by increasing the soil relative humidity parameter from 50% to 53% and by declaring a predicted fog event when the 10 meter temperature came within 0.5 °C of the 10 meter dewpoint. For the fall season, the overforecasting bias was removed by decreasing the soil relative humidity parameter from 50% to 43% and by declaring a predicted fog event when the 10 meter temperature came within 0.5 °C of the 10 meter dewpoint. The adapted version shows a significant improvement over the standard SLU version for the summer verification study. During the critical hours of 10 and 11 UTC, the model beat persistence with a skill score of 0.30. At 11 UTC, the model predicted 34 of 40 fog events, while predicting 9 that did not occur, for a percentage correct of 75%. The bias at 11 UTC, 1.08, was close to one. The model now has an overforecasting bias from 12 to 15 UTC, but this is due to the insufficient warming at the 10 meter level after sunrise. The adapted version does not show as significant improvement over the standard SLU version for the fall verification study as it did for the summer events. During the critical hours of 11 and 12 UTC, the model still did not beat persistence with a skill score of -0.62 and -0.50, respectively. At 12 UTC the model predicted 9 of 20 fog events, while predicting 7 events that did not

occur, for a percentage correct of 67%. The bias at 12 UTC was 0.73. The model still has a overforecasting bias from 13 to 15 UTC due to insufficient warming.

5.2 Recommendations for Future Research

The following changes to the model should be considered as recommendations for future work. The staggered four level vertical structure of the model limits the accuracy of calculations of exchange coefficient in the model and does not allow adequate representation of the NBL. The staggered vertical structure of the model should be changed from 4 levels to 40 levels. The new staggered vertical structure should place the first grid point above the surface (z_2) at 0.03 m ($z_1 = 0$) and expand away from the surface to 1000 meters.

The wind parameterization of the fog model should be completely changed, in favor of the method used in Turton and Brown (1987). Turton and Brown (1987) used the following one-dimensional momentum equations to calculate the change of wind with time at each level based on changes in stability.

$$\frac{\partial u}{\partial t} = f v + \frac{\partial}{\partial z} \left(K_m \frac{\partial u}{\partial z} \right) \quad (5.6)$$

$$\frac{\partial v}{\partial t} = -f u + \frac{\partial}{\partial z} \left(K_m \frac{\partial v}{\partial z} \right) \quad (5.7)$$

where K_m and K_h are the exchange coefficients and are functions of the local gradient Richardson number (Ri).

The initial input observed wind speed should be modified to include wind speed at four levels - the surface observation wind, and the 1000 ft, 2000 ft and 3000 ft winds as

observed on the Doppler Radar. The SLU version did not include longwave radiation to or from any fog or stratus that formed at the fog level (10 meters) or at the stratus level (200 meters). Parameterization of these processes as well as latent heating due to evaporation at the surface should be added. A parameterization of the cooling of the lowest layers of air by radiative exchange with the surface in the strongly absorbing bands of water vapor and carbon dioxide should also be added.

BIBLIOGRAPHY

- Bergot, T., and D. Guedalia, 1994: Numerical Forecasting of Radiation Fog. Part I: Numerical Model and Sensitivity Tests. *Mon. Wea. Rev.*, **122**, 1218-1230.
- Dyer R. M., and F. L. Gerald, 1989: Rule Based Systems for Visibility Forecasts. *Environmental Research Papers*, **1030**, Geophysics Laboratory, Hanscom AFB, MA 01731.
- Fisher, E. L., and P. Caplan, 1963: An experiment in numerical prediction of fog and stratus. *J. Atmos. Sci.*, **20**, 425-437.
- Fitzjarrald, D. R., and G. G. Lala, 1989: Hudson valley fog environments. *J. Appl. Meteor.*, **28**, 1303-1328.
- Fleagle, R. G., and J. A. Businger, 1980: *An Introduction to Atmospheric Physics*. Academic Press, 432
- Guedalia D., and T. Bergot, 1994: Numerical Forecasting of Radiation Fog. Part II: A Comparison of Model Simulation with Several Observed Fog Events. *Mon. Wea. Rev.*, **122**, 1231-1246
- Haltiner, G. J., and F. L. Martin, 1957: *Dynamical and Physical Meteorology*. McGraw-Hill Book Company, 470 pp.
- Holton, J. R., 1992: *An Introduction to Dynamic Meteorology*. 3rd Ed., Academic Press, 511 pp.
- Mahrt, L., M. Ek, J. Kim, and A. A. M. Holtslag, 1991: Boundary Layer Parameterization of a Global Spectral Model. *US Air Force Phillips Laboratory Technical report 91-2031*. 204 pp.
- Meyer, W. D., and G. V. Rao, 1995: A Hybrid Model For Predicting Fog and Stratus Clouds, *Sixth Conference on Aviation Weather Systems*, Dallas, TX, Amer. Meteor. Soc., 441-444
- Mellor, G. L. and T. Yamada, 1974: A hierarchy of turbulence closure models for planetary boundary layers, *J. Atmos. Sci.*, **31**, 1791-1806
- Monteith, J. L., 1957: Dew. *Quart. J. Roy. Meteor. Soc.*, **83**, 322-341

- O'Sullivan, J. M., 1996: *A simple model for the prediction of environmental conditions leading to the onset and evolution of radiation fog*. MS Thesis, Saint Louis University
- Roach, W. T., R. Brown, S. J. Caughey, J. A. Garland, and C. J. Readings, 1976: The physics of radiation fog: I—a field study. *Quart. J. Roy. Meteor. Soc.*, **102**, 313-333.
- Turton, J. D., and R. Brown, 1987: A comparison of a numerical model of radiation fog with detailed observations. *Quart. J. Roy. Meteor. Soc.*, **113**, 37-54.
- Wallace, J. M., and P. V. Hobbs, 1977: *Atmospheric Science: An Introductory Survey*. Academic Press, 350
- Zdunkowski, W., and B. Neilsen, 1969: A preliminary prediction analysis of radiation fog. *Pure Appl. Geophy.*, **19**, 45-66.
- , and A. Barr, 1972: A radiative-convective model for the prediction of radiation fog. *Bound.-Layer Meteor.*, **3**, 152-157

Appendix

PROGRAM AFITFOG

```
*****
*           AFIT VERSION OF HQ AWS FOG Model           *
*           Capt Andrew Goodnite                       *
* Version created from 30 September 1996 to 12 January 1997, adapted *
* from code provided from St. Louis University.        *
* The major changes are as follows:                    *
*   1. Array size errors were fixed - there were many array *
*      out of bounds errors.                            *
*   2. Output file output.dat added to record output data in *
*      the same format as climo data.                   *
*   3. Added code to allow Temperature and Dewpoint to be input *
*      at 200 meters, and 1000 meters.                  *
*   5. Visibility calculations added                    *
*****
*****
*           Variable Descriptions                      *
*
*   year   = output year of the data
*   month  = output month of the data
*   day    = output day of the data
*   hour   = output hour of the data
*   tair1  = 1000 meter temperature
*   tair2  = tair1, 1000 meter temperature
*   tair0  = 10 meter temperature
*   tsfc   = surface temperature
*   fcori  = coriolis force
*   zair   = 66, used in wind computation
*   z0     = .2, Surface roughness in meters
*   zsfc   = 30.0, Top of Surface Layer in meters
*   v0     = windspeed observation after conversion of m/s
*   vss    = 22Z windspeed observation in knots
*   grav   = gravity (9.8 m/s2)
*   p      = Surface Pressure in mb (set to 1000 mb)
*   rd     = 287 Dry Air Gas Constant
*   cp     = 1004 Specific heat at constant pressure
*   emiss  = .95 Surface Emissivity
*   dz     = 1000 meters change in height
*   mv     = 18.015 Molecular Wt Water Vapor
*   md     = 28.97 Molecular Wt Dry Air
*   lewice = 2850000 w/s*ton Latent Heat Ice
```

```

*   le      = 2500000 W/s*ton Latent Heat Water
*   rstar   = 8314 Universal gas constant
*   radsunst = 104.65 W/m2 Radiation Sunset
*   netlwrad = .21 Climo value given by W and H pg 321
*   pi      = 3.1415927
*   soiltype = 810.6 (Moist Sand)
*   zri     = 300.0 Characteristic Model Pbl
*   tri     = Adjustment to tair1 for Ri Calculation
*   intug   = Initial geostrophic wind
*   stddev  = The standard deviation of wind speed
*   locnoon = Local time of solar noon
*   v0stddev = The standard deviation of wind speed
*   ustar   = Computed wind
*   lat     = Latitude of Station
*   long    = Longitude of Station
*   srh     = Sunrise Hour
*   ssh     = Sunset Hour
*   minsr   = Sunrise minute
*   minss   = Sunset minute
*   modelhrs = Output model hours of data
*   srmodhrs = Sunrise model hrs
*   ssmodhrs = Sunset model hrs
*   tss     = Input 22Z Surface temperature in F
*   tdss    = Input 22Z Surface dewpoint in F
*   vss     = Input 22Z 10 meter wind speed in Knots
*   adjlr   = Lapse rate
*****

```

IMPLICIT NONE

```

INTEGER year,month,day,hour,T
PARAMETER(T=1450)
common/com1/tair1,tair0,tsfc
real tair1,tair0,tsfc
common/com2/fcori,zair,z0,zsfc,v0,grav
real fcori,zair,z0,zsfc,v0
common/com3/p,rd,cp,emiss,sigwatt
real p,rd,cp,emiss,sigwatt
common/com4/dz
real dz,diffvar(30)
common/com6/mv,md,lewice,le,rstar
real mv,md,lewice,le,rstar
common/com7/radsunst,netlwrad,pi,soiltype
real radsunst,netlwrad,pi,soiltype
common/com8/zri,tri,intug
real zri,tri,intug

```



```

common/com9/tair2,stddev
real tair2,stddev
common/com10/locnoon,v0stddev,synv0cld,synv0fog
real locnoon,v0stddev,synv0cld,synv0fog
common/com11/ihess,ustar
real ihess,ustar,autowarm(T),autocon
real dtemhld,dtemsav,C10Td(T),C200Td(T)
real rad,yf,tsn,sigma,sindec,cosdec,lat,long,srh,ssh,locnoon
real gsr,gss,minsr,minss,dzero,ads,losr,loss,lohr(T),v0stddev
real shar(T),sirr(T),cosz(T),zenagl(T),abt,time
real dzone,modelhrs,dtnew,srmodhrs,ssmodhrs
real tss,tdss,vss,rhwet,rhsat,adjlr,tair1,dzsfc,dz,zair,zsfc
real p,z0,emiss,le,lewice,rd,secsr,secss,varyvsfc,v0clim
real rstar,mv,md,grav,cp,v0,tair0,tsfc,fcori,tdktop,varyvcld,au
real aw,av,as,tdkwet,bc,be,bd,ba,tdksat(T),er,eu,qsfcwet,vvcld(T)
real tdair0(T),es,ew,qair0wet,fk,fnsave,qsfcsat,fm,fr,vvsfc(T)
real qair1,qair0sat,qaircld,tdkcloud,rhwet
real adjsr,adjss,sfcoff,supersat,decpltd
real dQsat,zri,tri,iedcoeff,intug,wind(T)
real tempsfc(T),temp0(T),tempcld(T),tempclds(T)
real tempsfcs(T),zenagls(T),dtlong(T),zenasave(T)
real dtemlast,dQsats(T),sprhsfc(T),sprhair(T),v0vary
real sprhcld(T),qsfclrys(T),dtevpsat,dtlhfsat,clouds
real a,dzone,dzcloud,lwoff,swoff,dqcomsat,dtsol,dtgroen
real h2ofact,tcloud,swabsorp,sigwatt,dtsols(T)
real dqqsat,dqcldsats,dtlhssat,dtsolfog,dtsolstr
real dtlwfogu,dtlwfogd,dtlwstru,dtlwstrd,dtlwsfd,dtlwcad
real dtnewhld,dtnewcld,dtnewcom,dtlwrad,emill,dtsolar,dtnews(T)
real rhosfc,qs,dtemsav(T),qssfcs(T),tempcldh(T)
real sprhairh(T),sprhsfch(T),sprhcldh(T),tempsfch(T)
real temp0h(T),dewdep
real synv0fog,synv0cld
real vissat(T),liqh2o(T),cumh2o(T),denair(T)
real dewptsat(T),droprad,visber(30)
real TEMP600(T),DP600
real autocool(T)
real dtlwrad2,bulk
real fht,cht
real qlf(T),qlc(T)
real sfcbulk,extrah2o,sfclh
real dummy1,dummy2,dummy3
real p10,p200,kp,ewcld
real td0,cldtd0
real ihess,ustar

```

```

real ug,v0clim
real csfctd(T),sfccool(T)
integer i,month,x,num,jd,day,ilen,irec,chose
pi=3.1415927
rad= pi/180.0
do i=1,1450
sprhair(i)=0.0
sprhcld(i)=0.0
sprhsfc(i)=0.0
temp0(i)=0.0
tempcld(i)=0.0
tempsfc(i)=0.0
shar(i)=0.0
sirr(i)=0.0
cosz(i)=0.0
zenagl(i)=0.0
tempclds(i)=0.0
tempsfcs(i)=0.0
zenagls(i)=0.0
dtlong(i)=0.0
zenasave(i)=0.0
dqsats(i)=0.0
qsfclyrs(i)=0.0
dtsols(i)=0.0
dtnews(i)=0.0
dtemsave(i)=0.0
qssfcs(i)=0.0
sprhairh(i)=0.0
temp0h(i)=0.0
vissat(i)=0.0
dewptsat(i)=0.0
qlf(i)=0.0
qlc(i)=0.0
cumh2o(i) = 2.0*10.0** -5.0
enddo

do i=1,20
write(*,*)
enddo
write(*,*)'***** AFIT VERSION OF AWS FOG MODEL *****'

write(*,*)
*****
do while (x .eq. 0)

```

```

write(*,*)'Please enter the year (ex: 1995) : '
read(*,*) YEAR
write(*,*)'Please enter the month (1-12) : '
read(*,*) month
do i=1,12
  if(i .eq. month) x=1
enddo
if(x.eq.0) then
  write (*,*)'Month must be 1-12 !'
endif
enddo

x=0
do while(x.eq.0)
  write(*,*)'Enter the day (1-31) : '
  read(*,*) day
  if(month.eq.1) then
    if(day.le.31.)then
      num=0
      adjsr=-5.0
      adjss=6.0
      x=1
    endif
  endif
  if(month.eq.2) then
    if(day.le.28.)then
      num=31
      adjsr=-5.5
      adjss=6.0
      x=1
    endif
  endif
  if(month.eq.3) then
    if(day.le.31)then
      num=59
      adjsr=-6.0
      adjss=4.0
      x=1
    endif
  endif
  if(month.eq.4) then
    if(day.le.30.)then
      num=90
      adjsr=-5.0

```

```
adjss=5.0
  x=1
endif
endif
if(month.eq.5) then
  if(day.le.31.)then
    num=120
    adjsr=-5.5
    adjss=5.0
    x=1
  endif
endif
if(month.eq.6) then
  if(day.le.30.)then
    num=151
    adjsr=-5.5
    adjss=5.0
    x=1
  endif
endif
if(month.eq.7) then
  if(day.le.31.)then
    num=181
    adjsr=-4.0
    adjss=4.5
    x=1
  endif
endif
if(month.eq.8) then
  if(day.le.31.)then
    num=212
    adjsr=-3.5
    adjss=4.0
    x=1
  endif
endif
if(month.eq.9) then
  if(day.le.30.)then
    num=243
    adjsr=-2.5
    adjss=3.0
    x=1
  endif
endif
```

```

if(month.eq.10)then
  if(day.le.31.)then
    num=273
    adjsr=-2.5
    adjss=3.0
    x=1
  endif
endif
if(month.eq.11)then
  if(day.le.30.)then
    num=304
    adjsr=-4.0
    adjss=3.0
    x=1
  endif
endif
if(month.eq.12)then
  if(day.le.31.)then
    num=334
    adjsr=-5.0
    adjss=5.0
    x=1
  endif
endif
if(x.eq.0)then
  write(*,*) 'You have enter an invalid day !'
  write(*,*) ' double check your month.'
endif
enddo

jd=num+day
write(*,*) 'The date you entered was:',month,day
write(*,*) 'Which is Julian Date :',jd
dewdep=0.5
write(*,*) 'Please enter a Soil RH between 0 and 100 '
write(*,*) 'Values between 40 and 60 work best: '
READ(*,*) rhsat
do while (rhsat.gt.100)
  write(*,*) 'Soil RH must be between 0 and 100 !'
  write(*,*) 'Please reenter Soil RH :'
  read(*,*) rhsat
enddo

```

***** CALCULATING THE YEAR FRACTION *****

```

*   yf=ANGULAR FRACTION OF A YEAR
    yf=rad*(360.0*(jd-1.0)/365.242)

*   tsn = TRUE SOLAR NOON
    tsn=12.0+(0.12357*sin(yf))-(0.004289*cos(yf))+
    & (0.153809*sin(2.0*yf))+(0.06078*cos(2.0*yf))

*   CALCULATING SIGMA
    sigma=(yf*(1.0/rad))+279.9348+1.914827*sin(yf)-0.079525
    & *cos(yf)+0.019938*sin(2.0*yf)-0.001620*cos(2.0*yf)

*   CALCULATING SINDEC
    sindec=(sin(rad*23.4438))*(sin(sigma*rad))

*   CALCULATING COSDEC
    cosdec=abs(sqrt(1.0-(sindec**2.0)))

*   srh=PIELKE SUNRISE HOUR ANGLE
*   ssh=PIELKE SUNSET HOUR ANGLE
C   write(*,*)'Please enter your latitude , longitude'
C   write(*,*)'example: stl = 38,90 :'
C   read(*,*)lat,long
    lat=35.0
    long=79.0
    lat=abs(lat)
    long=abs(long)
    do while (lat.gt.90)
        write(*,*)'latitude must be btwn (0-90) !'
        write(*,*)'please reenter latitude : '
        read(*,*)lat
    enddo
    do while (long.gt.180)
        write(*,*)'longitude must be (0-180) !'
        write(*,*)'please reenter longitude : '
        read(*,*)long
    enddo
    srh=(-1/rad)*(acos((-sindec/cosdec)*tan(lat*rad)))
    ssh=(1/rad)*(acos((-sindec/cosdec)*tan(lat*rad)))

*   gsr=UTC SUNRISE (ZULU)
*   gss=UTC SUNSET (ZULU)
    gsr=srh/15.0+tsn+(long/15.0)+(adjsr/60.0)

```

```

gss=ssh/15.0+tsn+(long/15.0)+(adjss/60.0)
minsr=(gsr-int(gsr))*60.0
minss=(gss-int(gss))*60.0
secsr=(minsr-int(minsr))*60.0
secss=(minss-int(minss))*60.0
if(secsr.ge.30.0)minsr=minsr+1.0
if(secss.ge.30.0)minss=minss+1.0
losr=gsr-(int(long/15.0))
loss=gss-(int(long/15.0))
srmodhrs=losr
ssmodhrs=loss
locnoon=srmodhrs+(ssmodhrs-srmodhrs)/2.0
v0stddev=0.6*abs(ssmodhrs-srmodhrs)
*****
*   added v0vary calculation, it is the variance used in wind   *
*   calculation, it was missing, caused winds to be NaN       *
v0vary=v0stddev

*   ads = AVERAGE DISTANCE FROM SUN
dzero=2.0*3.1415927*jd/365
ads=1.00011+0.034221*cos(dzero)+0.00128*sin(dzero)+
& 0.000719*cos(2*dzero)+0.000077*sin(2*dzero)

*   lohr = LOCAL HOURS
time=18.0
do i=1,1440
    lohr(i)=time+(i/60.0)
    if(lohr(i).ge.24) time=-6.0
enddo

*   shar = SOLAR HOUR ANGLE RADIANS
do i=1,1440
    shar(i)=15.0*(lohr(i)-tsn)*rad
enddo

*****
*****   SETTING VARIABLES   *****

*   INPUT OBSERVATIONS
write(*,*)'Please enter temp at sunset (C):'
read(*,*)tss
x=0
write(*,*)'Please enter the dew point at sunset (C):'

```

```

do while (x.eq.0)
  read(*,*)tdss
  if (tdss.le.tss) then
    x=17
  else
    write(*,*)'Dew point needs to be less than or'
    write(*,*)'equal to the temperture, please reenter :'
  endif
enddo
write(*,*)'Please enter the wind speed (knots) : '
read(*,*)vss
if (vss.lt.5.0) then
  write(*,*)'For this model the min. wind speed will be'
  write(*,*)'set to 5 Knots, therefore wind speed = 5 '
  vss=5.0
endif
soiltype=0.0
do while(soiltype.eq.0)
  write(*,*)'Please enter soil type : '
  write(*,*)
  write(*,*)' 1) moist sand'
  write(*,*)' 2) clay soil'
  write(*,*)' 3) new snow'
  read(*,*)a
*   Following are in J*m-2*K-1*s-(1/2)
  if(a.eq.1)soiltype=810.6
  if(a.eq.2)soiltype=2215.6
  if(a.eq.3)soiltype=163.1
  if(soiltype.eq.0)write(*,*)'Invalid choice try again'
enddo

*****  MODEL CONSTANTS  *****
dzzone=1000.0
dzcloud=200.0
lwoff=1.0
swoff=1.0
sfcoff=1.0
supersat=1.012835

*****  HEIGHT CONSTANTS  *****
fht=500.0
cht=495.0

*****  INTIAL PBL MOISTURE *****

```



```

    rhwet=70.0
    h2ofact=0.2
    decpbld=2.0
    synv0fog=1.0
    synv0cld=1.0
    WRITE(*,*) 'Press 1 to enter temperatures and dewpoints aloft'
    WRITE(*,*) 'Press 2 to use 90% of adiabatic lapse rate'
    WRITE(*,*) 'Press 1 or 2 now:'
    READ(*,*) chose
*****  INTIAL LAPSE RATE  *****
    IF (chose .eq. 2) then
        adjlr=0.9
        tair1=tss-adjlr*((9.8/1004.0)*dzone)
        tair2=tair1
        tcloud=tss-adjlr*((9.8/1004.0)*dzcloud)
*****
*****  Added to allow for inputting temperatures aloft *****
    ELSE
        WRITE(*,*) 'Please enter temp at 200 meters (C):'
        READ(*,*) tcloud
        WRITE(*,*) 'Please enter temp at 1000 meters (C):'
        READ(*,*) tair1
    ENDIF
    tair2=tair1

*****

*****  BOUNDARY LAYER GEOMETRY  *****
    dzsfc=10.0
    dz=1000.0
*    dz is changed on Apr 10, 95 to tune the warming. was 500 m
    zair=66.0
    zsf=30.0

*****  METEOROLOGICAL VARIABLES  *****
*    Following p values are in mb. p10 and p200 are from
*    Brutsaert p138 and kp is in m-1.
    p=1000.0
    kp=0.00013
    p10=p*(exp(-kp*dzsfc))
    p200=p*(exp(-kp*dzcloud))
    z0=0.2
*    Above is surface roughness parameter
    emiss=0.95

```

swabsorp=0.03

***** METEOROLOGICAL CONSTANTS *****

le=2500000.0

lewice=2850000.0

rd=287.0

* UNIVERSAL GAS CONSTANT

rstar=8314.0

mv=18.015

md=28.97

grav=9.8

cp=1004.0

* cp and cpv are in J per K per kg.

v0=vss/1.94

tair0=tss

tsfc=tair0+(grav/cp)*dzsfc

tdair0(1)=273.16+tdss

fcori=2.0*0.0000729*sin(lat*rad)

* CHARACTERISTIC MODEL PBL

zri=300.0

* ADJUSTMENT TO TAIR1 FOR RI CALCULATION

tri=tair1-5.0

iedcoeff=10.0

* DEPTH OF PENETRATION

abt=0.4

do i=1,1440

cosz(i)=cos(lat*rad)*cosdec*cos(shar(i))+sindec*sin(lat*rad)

sirr(i)=(1-abt)*1376.*ads*cosz(i)

zenagl(i)=(acos(cosz(i)))/rad

if(abs(zenagl(i)).gt.90) sirr(i)=0

dtsol=60.*sirr(i)/(cp*rhosfc(tsfc)*dz)

enddo

ihess=sqrt(fcori/(2.0*iedcoeff))

ustar=0.1

intug=ug(dzcloud+150.0)

***** CACL Q FOR LEVEL 0 *****

es=(1.0/273.16)-1.0/tdair0(1)

ew=(6.11*exp(mv*(le/rstar)*es))

qair0sat=((mv/md)*ew)/(p10-(ew*(1.0-(mv/md))))

qair0wet=qair0sat

```
***** CACL DEW PT FOR TOP AND CLD LEVELS OF MODEL *****
      IF (chose .eq. 2) THEN
        tdktop=(1.0/((1.0/273.16)-(log((((6.11*exp(mv*(le/rstar)*
& (1.0/273.16-1.0/(tdss+273.16))))/(6.11*
& exp(mv*(le/rstar)*(1.0/273.16-1.0/(tss+273.16))))))
& *(6.11*exp(mv*(le/rstar)*(1/273.16-1.0/(tair1+273.16))))/
& 1.0)/6.11)/(mv*le/rstar)))-decpltd
        tdkcloud=(1.0/((1.0/273.16)-(log((((6.11*exp(mv*(le/rstar)*
& (1.0/273.16-1.0/(tdss+273.16))))/(6.11*
& exp(mv*(le/rstar)*(1.0/273.16-1.0/(tss+273.16))))))
& *(6.11*exp(mv*(le/rstar)*(1./273.16-1.0/(tcloud+273.16))))/
& 1.0)/6.11)/(mv*le/rstar)))-decpltd
*****
***** Turned off dew tp cACL in favor of entering actual values **
      ELSE
        WRITE(*,*) 'Please enter dew point at 200 meters (C): '
        READ(*,*) tdkcloud
        WRITE(*,*) 'Please enter dew point at 1000 meters (C): '
        READ(*,*) tdktop
        tdkcloud = tdkcloud + 273.16
        tdktop = tdktop + 273.16
      ENDIF
*****

***** CACL SFC LAYER DEW POINTS *****
      au=(1.0/273.16-1.0/(tsfc+273.16))
      aw=(0.611*exp(mv*(le/rstar)*au))
      av=(rhwet*aw/100.0)
      as=(log(av/0.611))/(mv*le/rstar)
      tdkwet=(1.0/((1.0/273.16)-as))
      bc=(1.0/273.16-1.0/(tsfc+273.16))
      be=(0.611*exp(mv*(le/rstar)*bc))
      bd=rhsat*be/100.0
      ba=(log(bd/0.611))/(mv*le/rstar)
      tdkSAT(1)=(1.0/((1.0/273.16)-ba))

***** DEFINE INITIAL SPECIFIC HUMIDITIES *****
      er=(1.0/273.16)-1.0/(tdkwet)
      eu=(6.11*exp(mv*(le/rstar)*er))
      qsfcwet=(mv/md)*(eu/p)
```

***** CALC FOR THE SAT SURFACE *****

```
fk=(1.0/273.16)-1.0/tdksat(1)
fnsave=(6.11*exp(mv*(le/rstar)*fk))
qsfcscat=(mv/md)*(fnsave/p)
fm=(1.0/273.16)-1.0/tdktop
fr=(6.11*exp(mv*(le/rstar)*fm))
qairl=(mv/md)*(fr/p)
ewcld=6.11*(exp(mv*(le/rstar)*((1.0/273.16)-(1.0/tdkcloud))))
qaircld=((mv/md)*ewcld)/(p200-(ewcld*(1.0-(mv/md))))
```

***** RADIATION CALCULATIONS *****

* LONG-WAVE RADIATION

* Following are in W/m2

radsunst= 104.65

sigwatt=6.57E-08

* Following is dimensionless

netlwrad=.21

***** INITILIZE VARIABLES *****

```
tempsfc(1)=tsfc
temp0(1)=tair0
tempcld(1)=tcloud
tempclds(1)=tcloud
tempsfc(2)=tsfc
temp0(2)=tair0
tempcld(2)=tcloud
tempsfcs(1)=tsfc
dtemsav(1)=0.0
zenagls(1)=100.0
qssfcs(1)=qs(tsfc)
dtlong(1)=0.0
dtemlast=0.0
dQsats(1)=0.0
sprhsfc(1)=qsfcscat
sprhsfc(2)=qsfcscat
sprhair(1)=qair0sat
sprhair(2)=qair0sat
sprhcld(1)=qaircld
sprhcld(2)=qaircld
wind(1)=vss/1.94
qsfclrys(1)=0.0
dtevpsat=0.0
```

```

dtlhfsat=0.0
dtlhssat=0.0
bulk=0.0
sfcbulk=0.0
sfclh=0.0
extrah2o=0.0
clouds= 1-swabsorp
varyvsfc=v0*2.0
varyvcld=v0*2.0
dtemsav=0
td0=0.0
cltd0=0.0
tdair0(2)=tdair0(1)
tdksat(2)=tdksat(1)

```

***** WRITING FIRST RECORD OF OUTPUT *****

```

open(400,file='output.dat',status='unknown')
CSFCtd(1)=tdksat(1)-273.16

```

***** BEGIN TIME INTEGRATION CALCULATIONS *****

```

do i=2,1440
  modelhrs=1+(i-1)/60.0

```

```

  dqqsat=dqcomsat(tair1,temp0(i-1),tempsfc(i-1),qaircld,
& sprhair(i-1),sprhsfc(i-1),dzsfc,modelhrs,ght)*60.0

```

- * The purpose of dqqsat is to calculate latent heat later
- * and also to extrapolate in time the humidity values
- * This was necessary to compute the Richardson number

```

  dqcldsat=dqcomsat(tair1,temp0(i-1),tempsfc(i-1),qair1,
& sprhcld(i-1),sprhair(i-1),dzcloud,modelhrs,cht)*60.0

```

- * dzsfc was introduced in stead of dzcloud on Dec 12, 1994
- * This was necessary also to compute Ri.Put back dzcloud on Mar 15,95
- * one time step was used on Mar 4,95

***** SURFACE EVAP TO UPPER LEVEL *****

```

sfcbulk=0.0
sfclh=0.0
extrah2o=0.0
if(qs(tempsfc(i-1)).gt.sprhsfc(i-1)) then

```

```

      sfcbulk=grav*rhosfc(tempsfc(i-1))*0.1*v0*(qs(tempsfc(i-1))-
&   sprhsfc(i-1))*60./(p*100.0)
      sfc1h=0.0
C   else
C   extrah2o=(sprhsfc(i-1)-(qs(tempsfc(i-1))))
C   sfc1h=(le/cp)*extrah2o
C   sfcbulk=0.0
      endif

***** Surface evaporation calculations *****

      bulk=0.0
      if(qs(tempsfc(i-1)).ge.sprhair(i-1))then
        bulk=grav*rhosfc(tempsfc(i-1))*0.01*v0*(qs(tempsfc(i-1))-
&   sprhair(i-1))*60./(p*100.0)
      endif

***** FOG LATENT HEAT AND H2O FALLOUT CALCS *****

      if(sprhair(i-1).ge.(supersat*qs(temp0(i-1)))) then
        qlf(i)=(sprhair(i-1)-(supersat*qs(temp0(i-1))))
        dtlhfsat=(le/cp)*qlf(i)
      else
        dtlhfsat=0.0
        qlf(i)=0.0
        cumh2o(i)=cumh2o(i-1)
      endif

***** Stratus latent heat and h2o fallout calc *****

      if(sprhcld(i-1).ge.(supersat*qs(tempcld(i-1))))then
        qlc(i)=(sprhcld(i-1)-(supersat*qs(tempcld(i-1))))
        dtlhssat=(le/cp)*qlc(i)
      else
        dtlhssat=0.0
        qlc(i)=0.0
      endif

***** Radiation calculations *****

      dtemhld=0.0
      a=i-1
      dtemhld=dtgroen(a,tempsfc(i-1))*emiss

```

***** Short wave calculations *****

```

    if(sprhcld(i-1).ge.qs(tempcld(i-1)).and.sprhair(i-1).ge.
    & qs(temp0(i-1))) then
      dtsolstr=swabsorp*sirr(i)*dtsolar(modelhrs,tempcld(i-1))
      dtsolfog=swabsorp*sirr(i)*dtsolar(modelhrs,temp0(i-1))
    else
      dtsolfog=0.0
      dtsolstr=0.0
    endif
  *   dtsolar depends on time of day through model hours

```

***** Longwave radiation up and down from fog w/o stratus *****

```

C   if(sprhcld(i-1).le.qs(tempcld(i-1)).and.sprhair(i-1).ge.
C   & qs(temp0(i-1)))then
C     dtlwfogu=dtlwrad(temp0(i-1))/190.0
C     dtlwfogd=1.24*(emill(temp0(i-1))/(273.16+temp0(i-1)))*(.143)*
C   &   dtlwrad2(temp0(i-1))/10.0
  *   source of these formulas and logic behind considering both u and
  *   d fluxes in fog warming. Source Brutsaert P138
C   else
C     dtlwfogu=0.0
C     dtlwfogd=0.0
C   endif

```

***** Longwave radiation up from stratus *****

```

    if(sprhcld(i-1).ge.qs(tempcld(i-1)))then
      dtlwstru=dtlwrad(tempcld(i-1))/800.0
    else
      dtlwstru=0.0
    endif

```

***** Longwave radiation down from stratus w/o fog *****

```

    if(sprhcld(i-1).ge.qs(tempcld(i-1)).and.sprhair(i-1).lt.
    & qs(temp0(i-1)))then

      dtlwstrd=1.24*(emill(tempcld(i-1))/(273.16+tempcld(i-1)))
      &   **(.143)*dtlwrad2(tempcld(i-1))/200.0
  *   the first expression denotes atm. emissivity. Although dtlwrad
  *   needs a division by dz dimensionally it was done so later
    else
      dtlwstrd=0.0
    endif

```

```

endif

***** Longwave radiation down from str w/ fog *****

    if(sprhcld(i-1).ge.qs(tempcld(i-1)).and.sprhair(i-1).ge.
    & qs(temp0(i-1)))then
        dtlwsfd=1.24*(emill(temp0(i-1))/(273.16+temp0(i-1)))**(.143)
    & *dtlwrad2(temp0(i-1))/190.0
    else
        dtlwsfd=0.0
    endif
***** Longwave radiation down from clear atmos *****

    dtlwcad=1.24*(emill(-55.0)/(-55.0+273.16))**0.143*dtlwrad2(-55.0)

***** HEAT FLUX CALCULATIONS *****
*   new Q values
*   heat fluxes for 1st step
    dtnewhld=0.0
    dtnewcld=0.0
    If (i.eq.2) then
        dtnewhld=dtnew(tair1,temp0(1),tempsfc(1),fht)*60.0
        dtnewcld=dtnew(tair1,tempcld(1),temp0(1),cht)*60.0
        sprhsfc(i)=sprhsfc(i-1)-h2ofact*dQsat(tair1,temp0(i-1),
    & tempsfc(i-1),qair1,qair0sat,qsfcsat,fht)*60.+1.0*sfcbulk-
    & extrah2o
        sprhair(i)=sprhair(i-1)+dQsat(tair1,temp0(i-1),tempsfc(i-1),
    & qair1,qair0sat,qsfcsat,fht)*60.+0.0*bulk+0.0*sfcbulk
        sprhcld(i)=sprhcld(i-1)+dQsat(tair1,temp0(i-1),tempsfc(i-1),
    & qair1,qair0sat,qsfcsat,cht)*60.+0.0*bulk+0.0*sfcbulk

        temp0(i)=temp0(i-1)+dtnewhld+(swoff*dtolfog)-(0.0*dtemhld)+
    & dtlhfsat-lwoff*(dtlwfogu-dtlwsfd)
        tempcld(i)=tempcld(i-1)+dtnewcld+(swoff*dtolfog)+dtlhfsat-
    & (0.0*dtemhld)-lwoff*(dtlwstru-dtlwfogu)
        tempsfc(i)= tempsfc(i-1)-sfcff*dtemhld-0.2*dtnewhld+clouds*
    & dtsolar(modelhrs,tempsfc(i-1))*sirr(i)-lwoff*(dtlwfogd+
    & dtlwstrd)
    endif
    if(sprhcld(i-1).ge.supersat*qs(tempcld(i-1)).or.sprhair(i-1)
    & .ge.supersat*qs(temp0(i-1))) then
        clouds=(1-swabsorp)
    endif
    qssfcs(modelhrs)=qs(tempsfc(i))

```



```

zenasave(modelhrs)=abs(zenagl)
qssfcs(modelhrs)=qs(tempsfc(i))
dQsats(i)=dqqsat
dtnews(i)=dtnewhld
tempsfcs(i)=tempsfc(i)
tempclds(i)= tempcld(i)
dtsols(modelhrs)=dtsolar(modelhrs,tempsfc(i))
vvsfc(modelhrs)=v0clim(modelhrs,locnoon,v0vary,dzsfc)
vvclld(modelhrs)=v0clim(modelhrs,locnoon,v0vary,dzsfc)
if(i.eq.2) then
a=i
dtemhld=dtgroen(a,tempsfc(i))*emiss

if ((dtlwfogd+dtlwstrd).eq.(0.0)) then
  tempsfc(i+1)=tempsfc(i-1)-sfcoff*dtemhld-2.*.2*dtnewhld+clouds*
& (sirr(i)*dtsolar(modelhrs,tempsfc(i))+sirr(i-1)*dtsolar(
& modelhrs,tempsfc(i-1)))+sfcldh
else
  tempsfc(i+1)=tempsfc(i-1)-2.*.2*dtnewhld+clouds*
& (sirr(i)*dtsolar(modelhrs,tempsfc(i))+sirr(i-1)*dtsolar(
& modelhrs,tempsfc(i-1)))-2.0*lwoff*(-dtlwfogd-dtlwstrd)+sfcldh
endif

*   dtnewhld was over one time step; hence multiplied by 2
*   twice the time step added on Mar 22,95
*   sirr(i) was added on Oct 28
dtnewhld=(dtnewcom(tair1,temp0(i),tempsfc(i),dzsfc,modelhrs,fht)
& +dtnew(tair1,temp0(i-1),tempsfc(i-1),fht))*60.0

*   This formulation was added on Mar 8, 95
dtnewcld=(dtnewcom(tair1,tempcld(i),temp0(i),dzcloud,modelhrs,cht)
& +dtnew(tair1,tempcld(i-1),tempsfc(i-1),cht))*60.

sprhsfc(i+1)=sprhsfc(i-1)-h2ofact*(dQsat(tair1,temp0(i-1),
& tempsfc(i-1),qaircld,qair0sat,qsfcSAT,fht)+dqcomsat(tair1,
& temp0(i),tempsfc(i),sprhclld(i),sprhair(i),sprhsfc(i),dzsfc,
& modelhrs,fht))*60.0+1.0*sfcbulk+0.0*bulk-extrah2o

sprhair(i+1)=sprhair(i-1)+(dQsat(tair1,temp0(i-1),tempsfc(i-1),
& qaircld,qair0sat,qsfcSAT,fht)+dqcomsat(tair1,temp0(i),
& tempsfc(i),sprhclld(i),sprhair(i),sprhsfc(i),dzsfc,modelhrs,
& fht))*60.0+0.4*bulk+0.0*sfcbulk

sprhclld(i+1)=sprhclld(i-1)+(dQsat(tair1,temp0(i-1),tempsfc(i-1),

```

```

& qair1,qair0sat,qsfcscat,cht)+dqcomsat(tair1,temp0(i),tempsfc(i),
& qair1,sprhcld(i),sprhair(i),dzcloud,modelhrs,cht))*60.0+
& 0.1*bulk+0.0*sfcbulk

```

```

dummy1=(dQsat(tair1,temp0(i-1),tempsfc(i-1),qair1,qair0sat,
& qsfcscat,fht)*60.0)
dummy2=(dqcomsat(tair1,temp0(i),tempsfc(i),sprhcld(i),sprhair(i),
& sprhsfc(i),dzsfc,modelhrs,fht)*60.0)
dummy3=((dQsat(tair1,temp0(i-1),tempsfc(i-1),qaircld,qair0sat,
& qsfcscat,fht)+dqcomsat(tair1,temp0(i),tempsfc(i),sprhcld(i),
& sprhair(i),sprhsfc(i),dzsfc,modelhrs,fht))*60.0)

```

```

if ((dtlwfogu+dtlwsfd).eq.(0.0)) then
  temp0(i+1)=temp0(i-1)+dtnewhld+2.*swoff*dtsolfog+(dtlhfsat)-
& 0.0*(dtemhld-dtgroen((a-1),tempsfc(a-1))*emiss)
else
  temp0(i+1)=temp0(i-1)+2.*swoff*dtsolfog+(dtlhfsat)-
& -2.0*lwoff*(dtlwfogu-dtlwsfd)
endif

```

- * dtsolfog should be multiplied by 2 . lwoff should be multiplied by 2
- * This multiplication is necessary because dtlhfsat is extrapolated over
- * twice the time step. Also examine why dtlwfogd and
- * dtlwfogu were added without minding their sign. One is up so must be
- * negative and the other down so must be positive.

```

if ((dtlwstru+dtlwfogu).eq.(0.0)) then
  tempcld(i+1)=tempcld(i-1)+dtnewcld+2.*swoff*dtsolstr+
& (dtlhssat)-0.0*(dtemhld-dtgroen((a-1),tempsfc(a-1))*emiss)
else
  tempcld(i+1)=tempcld(i-1)+2.*swoff*dtsolstr+(dtlhssat)-
& -2.0*lwoff*(dtlwstru+dtlwfogu)
endif

```

```

endif

```

```

if (sprhcld(i-1).ge.supersat*qs(tempcld(i-1)).or.sprhair(i-1)
& .ge.supersat*qs(temp0(i-1))) then
  clouds=(1-swabsorp)
endif

```

```

if(i.ge.3) then
  if (qs(tempsfc(i)).le.sprhsfc(i)) then
    sfccoeff=0.5

```

```

    elseif (qs(tempsfc(i)).gt.sprhsfc(i)) then
      sfcoff=1.0
    endif

    a=i
    dtemhld=dtgroen(a,tempsfc(i))*emiss

    if ((dtlwfogd+dtlwstrd).eq.(0.0)) then
      tempsfc(i+1)=(tempsfc(i-1)+0.25*(tempsfc(i-2)-2.0*tempsfc(i-1)+
&   tempsfc(i)))-sfcoff*(dtemhld-dtgroen((a-2),
&   tempsfc(i-2))*emiss)-.2*dtnewhld+clouds*(sirr(i)*
&   dtsolar(modelhrs,tempsfc(i))+sirr(i-1)*dtsolar(modelhrs,
&   tempsfc(i-1)))+sfclh
    else
      tempsfc(i+1)=(tempsfc(i-1)+0.25*(tempsfc(i-2)-2.0*tempsfc(i-1)+
&   tempsfc(i)))-.2*dtnewhld+clouds*(sirr(i)*
&   dtsolar(modelhrs,tempsfc(i))+sirr(i-1)*dtsolar(modelhrs,
&   tempsfc(i-1)))-2.0*lwoff*(-dtlwfogd-dtlwstrd)+sfclh
    endif

```

- * 2 added to show 2 time steps: April 30, 1995
- * dtnewhld was over two timesteps; hence not multiplied by 2
- * the above formulation on Mar 22, and 23, 95

```

    dtnewhld=(dtnewcom(tair1,temp0(i-1),tempsfc(i-1),dzsfc,modelhrs,
& fht)+dtnewcom(tair1,temp0(i),tempsfc(i),dzsfc,modelhrs,
& fht))*60.

```

- * dtnewcom has a trap in it; tair1-tsfc(temp0 or temsfc) cannot be
 - * less than 0.5. Be aware of this
- ```

 dtnewcld=(dtnewcom(tair1,tempcld(i-1),temp0(i-1),dzcloud,modelhrs,
& cht)+dtnewcom(tair1,tempcld(i),temp0(i),dzcloud,modelhrs,
& cht))*60.0

```

```

 if ((dtlwfogu+dtlwsgd).eq.(0.0)) then
 temp0(i+1)=(temp0(i-1)+0.25*(temp0(i-2)-2.0*temp0(i-1)+
& temp0(i)))+dtnewhld+2.*swoff*dtsolfog+2.0*(dtlhfsat)
& -0.0*(dtemhld-dtgroen((a-2),tempsfc(i-2))*emiss)
 else
 temp0(i+1)=(temp0(i-1)+0.25*(temp0(i-2)-2.0*temp0(i-1)+
& temp0(i)))+dtnewhld+2.*swoff*dtsolfog+2.0*(dtlhfsat)
& -2.0*lwoff*(dtlwfogu+dtlwsgd)
 endif

```

\*\*\*\*\* Code to warm 10 meter level due to condensation \*\*\*\*\*

```

* and to decrease dewpoint due to loss of water vapor *
* into liquid water (cumh2o)
 if ((temp0(i+1)).le.C10td(i-1)).and.(sprhair(i).gt.(0.01)))
$ then
 autocool(i)=autocon(sprhair(i))*60.0
 autowarm(i)=autocon(sprhair(i))*(1e*60.0/cp)
 temp0(i+1)=temp0(i)+autowarm(i)
 cumh2o(i)=autocool(i)+cumh2o(i-1)
 endif

 sprhair(i+1)=(sprhair(i-1)+0.25*(sprhair(i-2)-2.0*sprhair(i-1)+
& sprhair(i)))+(dqcomsat(tair1,temp0(i-1),tempsfc
& (i-1),sprhcl(i-1),sprhair(i-1),sprhsfc(i-1),dzsfc,modelhrs,
& fht)+dqcomsat(tair1,temp0(i),tempsfc(i),sprhcl(i),
& sprhair(i),sprhsfc(i),dzsfc,modelhrs,fht))*
& 60.0-autocool(i)+0.0*bulk+0.0*sfcbulk

 sprhsfc(i+1)=(sprhsfc(i-1)+0.25*(sprhsfc(i-2)-2.0*sprhsfc(i-1)+
& sprhsfc(i)))-h2ofact*(dqcomsat(tair1,temp0(i-1),
& tempsfc(i-1),sprhcl(i-1),sprhair(i-1),sprhsfc(i-1),dzsfc,
& modelhrs,fht)+dqcomsat(tair1,temp0(i),tempsfc(i),sprhcl(i),
& sprhair(i),sprhsfc(i),dzsfc,modelhrs,fht))*60.+1.0*sfcbulk-
& extrah2o-sfccool(i)

 sprhcl(i+1)=(sprhcl(i-1)+0.25*(sprhcl(i-2)-2.0*sprhcl(i-1)+
& sprhcl(i)))+(dqcomsat(tair1,temp0(i-1),tempsfc
& (i-1),qair1,sprhcl(i-1),sprhair(i-1),dzcloud,modelhrs,
& cht)+dqcomsat(tair1,temp0(i),tempsfc(i),qair1,sprhcl(i),
& sprhair(i),dzcloud,modelhrs,cht))*60.+0.0*bulk+0.0*sfcbulk

 dummy1=(dqcomsat(tair1,temp0(i-1),tempsfc(i-1),sprhcl(i-1),
& sprhair(i-1),sprhsfc(i-1),dzsfc,modelhrs,fht)*60.0)
 dummy2=(dqcomsat(tair1,temp0(i),tempsfc(i),sprhcl(i),sprhair(i),
& sprhsfc(i),dzsfc,modelhrs,fht)*60.0)
 dummy3=(dqcomsat(tair1,temp0(i-1),tempsfc(i-1),sprhcl(i-1),
& sprhair(i-1),sprhsfc(i-1),dzsfc,modelhrs,fht)+dqcomsat(tair1,
& temp0(i),tempsfc(i),sprhcl(i),sprhair(i),sprhsfc(i),dzsfc,
& modelhrs,fht))*60.0

* 2times swoff, 2 times lwoff and +dtlwfogu were done on Mar 27

 if ((dtlwstru+dtlwfogu).eq.(0.0)) then
 tempcld(i+1)=(tempcld(i-1)+0.25*(tempcld(i-2)-2.0*tempcld(i-1)+
& tempcld(i)))+dtnewcld+2.*swoff*dtlwfogu+

```

```

& 2.*(dtlhssat)-0.0*(dtemhld-dtgroen((a-2),tempsfc(i-2))*emiss)
else
tempcld(i+1)=(tempcld(i-1)+0.25*(tempcld(i-2)-2.0*tempcld(i-1)+
& tempcld(i)))+dtnewcld+2.*swoff*dtsofstr+
& 2.*(dtlhssat)-2.0*lwoff*(dtlwstru+dtlwfogu)
endif

* Put in dtsofstr on 12/13/95

endif
qssfcs(modelhrs)=qs(tempsfc(i))
zenasave(modelhrs)=abs(zenagl)
qssfcs(modelhrs)=qs(tempsfc(i))

c10td(i)=(((1.0/((1.0/273.16)-log((sprhair(i)
& *p10/(mv/md))/6.11)/(mv*le/rstar)))-273.16))
c200td(i)=(((1.0/((1.0/273.16)-log((sprhld(i)
& *p200/(mv/md))/6.11)/(mv*le/rstar)))-273.16))
csfctd(i)=(((1.0/((1.0/273.16)-log((sprhsfc(i)
& *p/(mv/md))/6.11)/(mv*le/rstar)))-273.16))

wind(i)=v0clim(modelhrs,locnoon,v0stddev,dzsf)
enddo

***** END OF TIME INTEGRATION LOOP *****

***** Visibility Calculations *****

do i=1,1440,60
modelhrs= 1+(i-1)/60.0
sprhsfch(modelhrs)=sprhsfc(i)
sprhairh(modelhrs)=sprhair(i)
liqh2o(modelhrs)=cumh2o(i)
sprhldh(modelhrs)=sprhld(i)
tempsfch(modelhrs)=tempsfcs(i)
tempcldh(modelhrs)=tempclds(i)
temp0h(modelhrs)=temp0(i)
vvsfc(modelhrs)=wind(i)

***** Corrected error in the next calucation added 1/273.16 *****
***** per mathematica version page 32 *****

```

```

 dewptsat(modelhrs)=(((1/((1/273.16)-log((sprhairh
& (modelhrs)*p/(mv/md))/6.11)/(mv*le/rstar)))-273.16))
 droprad=5.0*10.0**-.6
 denair(modelhrs)=p/(rd*(273.16+temp0h(modelhrs)))
 visber(modelhrs)=15000.0
 diffvar(modelhrs)=dewptsat(modelhrs)-
$ (temp0h(modelhrs))

***** Visibility as computed from Bergot and Guedalia 1994 *****
***** The first if statement allows for a small reduction in
***** visibility before the model shows complete saturation.
***** The sensitivity tests for the AFIT version shows that
***** based on the Pope AFB data 0.5 deg C is the
***** best value to use in the Southeast United States.
 if((c10td(i)+dewdep) .ge. temp0(i)) then
 visber(modelhrs)=3.9/(144.7*(denair(modelhrs)*
& liqh2o(modelhrs)**.88)
 if (visber(modelhrs) .gt. 6400) then
 visber(modelhrs)=6400
 endif
 else
 visber(modelhrs)=15000
 endif
enddo

**** WRITING OUTPUT.DAT DATA FILE *****
hour=21
open(450,file='mod00Z.dat')
open(500,file='mod12Z.dat')
WRITE(*,*) ' Model Output '
WRITE(*,33) 'TIME', 'TEMPERATURE', 'DEWPOINT','VISIBILITY',
$ 'WIND'
do i=1,1440,60
 modelhrs=1+(i-1)/60
 hour=hour+1
 IF (hour .EQ. 24) then
 hour=0
 write(450,*) ' 0 ',' 10 ',' 200 ',' 600 ',' 1000 '
 write(450,*) tempsfc(i),temp0(i),tempcld(i),temp600(i),tair1
 write(450,*) Csfctd(i),C10td(i),C200td(i),DP600,
$ (tdktop-273.)
 endif
 if (hour .eq. 12) then
 write(500,*) ' 0 ',' 10 ',' 200 ',' 600 ',' 1000 '

```

```

 write(500,*) tempsfc(i),temp0(i),tempcld(i),temp600(i),tair1
 write(500,*) Csfctd(i),C10td(i),C200td(i),DP600,
$ (tdktop-273.)
 endif
 C10td(1)=C10td(2)
 C200td(1)=C200td(2)
 write(400,*) year,month,day,hour,visber(modelhrs),tempsfc(i),
& Csfctd(i),temp0(i),C10td(i),tempcld(i),C200td(i),Temp600(i),
& DP600,tair1,(tdktop-273.)

* *****OUTPUT TO SCREEN *****
 WRITE(*,34) hour,'00',temp0(i), C10td(i),visber(modelhrs),
$ wind(i)
 enddo
33 FORMAT(A4,4X,A11,4X,A8,4X,A10)
34 FORMAT(I2,A2,8X,F4.1,9X,F4.1,4X,F10.0,4X,F10.0)
 close(400)
 close(450)
 close(500)

** Grads output code
 ILEN=4
 OPEN(550,FILE='~/fogmodel/fogout.dat',ACCESS='direct',
& FORM='unformatted',RECL=ILEN)
 IREC=1
 DO i=1,1440,60
 modelhrs=1+(i-1)/60
 WRITE(550,REC=IREC)tempsfc(i)
 IREC=IREC+1
 WRITE(550,REC=IREC)temp0(i)
 IREC=IREC+1
 WRITE(550,REC=IREC)tempcld(i)
 IREC=IREC+1
 WRITE(550,REC=IREC)Temp600(i)
 IREC=IREC+1
 WRITE(550,REC=IREC)tair1
 IREC=IREC+1
 WRITE(550,REC=IREC)Csfctd(i)
 IREC=IREC+1
 WRITE(550,REC=IREC)C10td(i)
 IREC=IREC+1
 WRITE(550,REC=IREC)C200td(i)
 IREC=IREC+1
 WRITE(550,REC=IREC)DP600

```

```

IREC=IREC+1
WRITE(550,REC=IREC)(tdktop-273.16)
IREC=IREC+1
WRITE(550,REC=IREC)visber(modelhrs)
IREC=IREC+1
WRITE(550,REC=IREC)vvsfc(modelhrs)
IREC=IREC+1
WRITE(550,REC=IREC)vvsfc(modelhrs)
IREC=IREC+1
ENDDO
CLOSE(550)
end

FUNCTION dqcomsat(tair1,tair0,tsfc,qair1,qair0sat,qsfcsat
& ,zeters,modelhrs,hgt)
real dqcomsat,tair1,tair0,tsfc,qair1,qair0sat,qsfcsat
& ,zeters,modelhrs,hgt
real modelhrs,locnoon,v0stddev,zeters

common/com2/fcori,zair,z0,zsfc,v0,grav
real fcori,zair,z0,zsfc,v0,grav
common/com10/locnoon,v0stddev,synv0cld,synv0fog
real locnoon,v0stddev,synv0cld,synv0fog,v0clim
xx1a=0.4*0.4*(synv0cld+v0clim(modelhrs,locnoon,v0stddev,
& zeters))
xx1=(1.0/3.0)*xx1a
xx2= abs(tair1-tair0)
xx3= 273.16+tsfc
xxx1=v0clim(modelhrs,locnoon,v0stddev,zeters)
xxrib1= exp(-grav*zsfc*xx2/(xx3*(xxx1**2)))
xx4= xx1*xxrib1
xx5= xx4/(log(zsfc/z0))**2
xx6= (xx5*(qair0sat- qair1))
xx7=0.4*0.4*(synv0fog+v0clim(modelhrs,locnoon,
& v0stddev,zeters))
xx8= abs(tair1-tair0)
xxrib2= exp(-grav*zsfc*xx8/(xx3*(v0clim(modelhrs,locnoon,
& v0stddev,zeters))**2))
xx9=xx7*xxrib2
xx10=xx9/(log (zsfc/z0))**2
xx11= (xx10*(qsfcsat-qair0sat))
xx12=xx6-xx11
dqcomsat= -xx12/hgt
return

```



end

\*\*\*\*\*

```
FUNCTION qssnow(tsfc)
real qssnow,tsfc
common/com6/mv,md,lewice,le,rstar
real mv,md,lewice,le,rstar
common/com3/p,rd,cp,emiss,sigwatt
real p,rd,cp,emiss,sigwatt
qssnow=(mv/md)*(6.11*exp(mv*(lewice/rstar)*((1.0/273.16)
& -1.0/(tsfc+273.16))))/p
end
```

\*\*\*\*\*

```
FUNCTION qs0(tsfc)
real qs0,tsfc
common/com6/mv,md,lewice,le,rstar
real mv,md,lewice,le,rstar
common/com3/p,rd,cp,emiss,sigwatt
real p,rd,cp,emiss,sigwatt
qs0=(mv/md)*(6.11*exp(mv*(le/rstar)*((1.0/273.16)-1.0/
& (tsfc+273.16))))/p
end
```

\*\*\*\*\*

```
FUNCTION qs(tsfc)
real qs,tsfc
common/com6/mv,md,lewice,le,rstar
real mv,md,lewice,le,rstar
common/com3/p,rd,cp,emiss,sigwatt
real p,rd,cp,emiss,sigwatt
common/com4/dz
if(tsfc.le.0.0)then
 qs=(mv/md)*(6.11*exp(mv*(lewice/rstar)*((1/273.16)-1/
& (tsfc+273.16))))/p
else
 qs=(mv/md)*(6.11*exp(mv*(le/rstar)*((1/273.16)-1/
& (tsfc+273.16))))/p
endif
end
```

\*\*\*\*\*

```
FUNCTION rhosfc(tsfc)
real rhosfc,tsfc
common/com3/p,rd,cp,emiss,sigwatt
real p,rd,cp,emiss,sigwatt
```

```

 rhosfc=(p/(rd*(273.16+tsfc))*100.0)
 end

 FUNCTION dtsolar(modelhrs,temp)
 real dtsolar,modelhrs,temp
 common/com3/p,rd,cp,emiss,sigwatt
 real p,rd,cp,emiss,sigwatt
 common/com4/dz
 real dz,rhosfc
 dtsolar=(60.0*modelhrs)/(cp*rhosfc(temp)*dz)
 dtsolar=dtsolar/modelhrs
 * dtsolar was divided by modelhrs on Mar 12,95,a
 * sirr has time included in it. Therefore it is
 * wrong to use time twice. This caused too much warming
 end

 FUNCTION rodger(temp)
 real rodger,temp
 common/com3/p,rd,cp,emiss,sigwatt
 real p,rd,cp,emiss,sigwatt
 common/com6/mv,md,lewice,le,rstar
 real mv,md,lewice,le,rstar
 rodger=(mv/md)*(6.11*exp(mv*(le/rstar)*((1.0/273.16)-1.0/
 & (temp+273.16))))/p
 end

 FUNCTION emill(temp)
 real emill,temp
 real rodger
 common/com3/p,rd,cp,emiss,sigwatt
 real p,rd,cp,emiss,sigwatt
 emill=(rodger(temp)*p)/0.622
 end

 FUNCTION tdrod(qew)
 real tdrod,qew
 common/com6/mv,md,lewice,le,rstar
 real mv,md,lewice,le,rstar
 tdrod=((((1.0/273.16)-rstar/(mv*le))*log((qew*p/(mv/md))/
 & 6.11))**(-1))
 end

 FUNCTION dtlwrad(tsfc)
 real dtlwrad,tsfc

```

```

common/com3/p,rd,cp,emiss,sigwatt
real p,rd,cp,emiss,sigwatt

dtlwrad=((60./((p*100.0)/(rd*(273.16+tsfc))*cp))*emiss
& *sigwatt*(273.16+tsfc)**4)
* 10 was changed to 600 on Mar 27,95 because it should be secs
end

FUNCTION dtlwrad2(tsfc)
real dtlwrad,tsfc
common/com3/p,rd,cp,emiss,sigwatt
real p,rd,cp,emiss,sigwatt

dtlwrad=((60./((p*100.0)/(rd*(273.16+tsfc))*cp))*
& sigwatt*(273.16+tsfc)**4)
* Added on 11/15 to correct emissivity problems.
end

FUNCTION dtnewcom(tair1,tair0,tsfc,zmet,modhrs,hgt)
real dtnewcom,tair1,tair0,tsfc,zmet,modhrs,hgt
common/com2/fcori,zair,z0,zsfc,v0,grav
real fcori,zair,z0,zsfc,v0,grav
common/com3/p,rd,cp,emiss,sigwatt
real p,rd,cp,emiss,sigwatt
common/com10/locnoon,v0stddev,synv0cld,synv0fog
real locnoon,v0stddev,synv0cld,synv0fog,v0clim
Xtair1=273.16+tair1
Xtair0=273.16+tair0
Xden1=(p*100.0)/(rd*Xtair1)
Xh1=Xden1*cp*0.4*0.4*(synv0cld+v0clim(modhrs,locnoon,v0std
& dev,zmet))
Xrib1=exp(-grav*zsfc*abs((tair1-tair0))/(Xtair0*(v0clim(modhrs,
$ locnoon,v0stddev,zmet))**2))
Xh2= Xh1*Xrib1
Xh3= Xh2/(log(zsfc/z0))**2
Xh4= Xh3*(tair0-tair1)
Xtsfc= 273.16+tsfc
Xden12=(p*100.0)/(rd*Xtsfc)
Xrib21=-grav*zsfc*abs(tair0-tsfc)
Xrib22=Xtsfc*(v0clim(modhrs,locnoon,v0stddev,zmet))**2
Xrib2= Xrib21/Xrib22
Xh22= Xden12*cp*0.4*0.4*(synv0fog+v0clim(modhrs,locnoon,
& v0stddev,zmet))*exp(Xrib2)
Xh32= Xh22/(log(zsfc/z0))**2

```

```

 Xh42= Xh32*(tsfc-tair0)
* Xh5 is the Flux Divergence numerator
 Xh5= Xh4-Xh42
 Xh103=cp*Xden1
 dtnewcom= -Xh5/(hgt*Xh103)
* minus sign was placed on mar 4, 95 so that -vdq/dz was shown
 end

 FUNCTION dtnew(tair1,tair0,tsfc,hgt)
 real tair1,tair0,tsfc,hgt
 common/com2/fcori,zair,z0,zsfc,v0,grav
 real fcori,zair,z0,zsfc,v0,grav
 common/com3/p,rd,cp,emiss,sigwatt
 real p,rd,cp,emiss,sigwatt
c dtnew=((-(p/(rd*(273.16+tair1))))*cp*0.4*0.4*v0*
c & (exp(-(10.0*zsfc*abs((tair1-tair0))/((273.16+tair0)*v0*v0))))/
c & (log(zsfc/z0))**2*(tair0-tair1)-(p/(rd*(273.16+tsfc)))
c & cp*0.4*0.4*v0*(exp((-10.0*zsfc*(tair0-tsfc))/((273.16+tsfc)*
c & v0*v0)))/(log(zsfc/z0))**2*(tsfc-tair0))/532.0/(cp*(p/(rd*
c & (273.16+tair1))))
* This function is only used when computing 2nd temps.

 xtair1= 273.16+tair1
 xtair0= 273.16+tair0
 xtsfc= 273.16+ tsfc
 xy1= (p*100.0)/(rd*xtair1)
 xy2= xy1*cp*0.4*0.4*v0
 ribb1=-grav*zsfc*abs((tair1-tair0))/(xtair0*v0*v0)
 xy3= xy2*exp(ribb1)/(log (zsfc/z0))**2
 xy4= xy3*(tair0-tair1)
 xy5= (p*100.0)/(rd*xtsfc)
 xy6= xy5*cp*0.4*0.4*v0
 ribb2= -grav*zsfc*abs(tair0-tsfc)/(xtsfc*v0*v0)
 xy7= xy6*exp(ribb2)/(log (zsfc/z0))**2
 xy8= xy7*(tsfc-tair0)
 xy10= cp*(p*100.0)/ (rd*xtair1)
 xy11=(xy4-xy8)/hgt
 xy12= xy11/ xy10
 dtnew=-xy12
* dtnew is now consistent with math -vdq/dz, Mar 4, 95
 end

 FUNCTION qfsfcsat(tair1,tair0,tsfc,qair0sat,qsfcsat)
 real qfsfcsat,tair1,tair0,tsfc,qair0sat,qsfcsat

```

```

common/com2/fcori,zair,z0,zsfc,v0,grav
real fcori,zair,z0,zsfc,v0,grav
common/com9/tair2,stddev
real tair2,stddev
qsfcsat=0.4*0.4*v0*(exp((-grav*zsfc*abs((tair1-tair0))/((273.16+
& tsfc)*v0*v0))))/(log(zsfc/z0))**2*(qsfcsat-qair0sat)
* qsfcsat-qair0sat was put in on Mar 4, 95
end

FUNCTION qfairsat(tair1,tair0,tsfc,qair1,qair0sat)
real qfairsat,tair1,tair0,tsfc,qair1,qair0sat
common/com2/fcori,zair,z0,zsfc,v0,grav
real fcori,zair,z0,zsfc,v0,grav
common/com9/tair2,stddev
real tair2,stddev
qfairsat=0.4*0.4*v0*(exp((-9.8*zsfc*abs((tair1-tair0))/((273.16+
& tsfc)*v0*v0))))/(log(zsfc/z0))**2*(qair0sat-qair1)
* qair0sat-qair1 was put in Mar 4, 95 to be consistent with math
end

*

FUNCTION dQsat(tair1,tair0,tsfc,qair1,qair0sat,qsfcsat,hgt)
real dQsat,tair1,tair0,tsfc,qair1,qair0sat,qsfcsat
common/com2/fcori,zair,z0,zsfc,v0,grav
real fcori,zair,z0,zsfc,v0,grav
real qfairsat, qsfcsat
dQsat=0.0
dQsat=-(qfairsat(tair1,tair0,tsfc,qair1,qair0sat)-
& qsfcsat(tair1,tair0,tsfc,qair0sat,qsfcsat))/hgt
* minus sign was put on Mar 4, 95 to be consistent with equations
end

FUNCTION dtbrunt(min)
real dtbrunt,min
common/com7/radsunst,netlwrad,pi,soiltype
real radsunst,netlwrad,pi,soiltype
dtbrunt=(2.0/sqrt(pi))*(radsunst/5.972)*sqrt(min)
* 5.972 above is equal to radsunst in Haltiner & Martin
end

FUNCTION fn(min,tsfc)
real fn,min,tsfc
common/com7/radsunst,netlwrad,pi,soiltype
real radsunst,netlwrad,pi,soiltype,sigwatt

```

```

sigwatt=5.67E-08
fn=radsunst-(2./sqrt(pi))*(radsunst/810.62)*
& sqrt(min)*netlwrad*(4.0*sigwatt*((tsfc+273.16)**3.0))
end

FUNCTION dtgroen(n,tempsfc)
real dtgroen,n,tempsfc
common/com7/radsunst,netlwrad,pi,soiltype
real radsunst,netlwrad,pi,soiltype
dtgroen=(2.0/sqrt(pi))*(fn(n*60.0,tempsfc)/soiltype)*
& sqrt(n*60.0)
end

FUNCTION kmclim(model,mean,variance)
real kmclim,model,mean,variance
c if (model.lt.(6.0)) then
c kmclim=10.0*(1./((variance*sqrt(6.28)))*exp
c & -(abs((mean-18.0)-model)**2.5)/(2.0*variance**2))
c else
c kmclim=10.0*(1./((variance*sqrt(6.28)))*exp
c & -(abs(((model-6.0)-mean))**2.5)/(2.0*variance**2))
c endif

kmclim=10.0*(1./((variance*sqrt(6.28)))*exp
& -(abs((model-mean))**2.5)/(2.0*variance**2))
c in the above model-mean was raised to 2.5. Used to be 2.0
c This change took place mar 20, 1995.
c if (kmclim.le.0.1) then
c kmclim=0.1
c endif
end

FUNCTION ribulk(tair1,tair0)
real ribulk,tair1,tair0
common/com8/zri,tri,intug
real zri,tri,intug
common/com2/fcori,zair,z0,zsfc,v0,grav
real fcori,zair,z0,zsfc,v0,grav
ribulk=(grav*zri*((tri)-tair0)/((273.16+tair0)*v0*v0))
end

FUNCTION ahesscl(modelhrs,mean,stddev)
real ahesscl,modelhrs,mean,stddev
common/com2/fcori,zair,z0,zsfc,v0,grav

```

```

real fcori,zair,z0,zsfc,v0,grav
ahesscl=sqrt(fcori/(2.0*abs(kmclim(modelhrs,mean,stddev))))
end

FUNCTION v0clim(modelhrs,mean,variance,dzsfc)
real v0clim,modelhrs,mean,variance,dzsfc,kmclim
common/com8/zri,tri,intug
real zri,tri,intug
c v0clim=(v0/(variance*(sqrt(6.28))))*exp(-abs((model-mean))**2.5/
c & (2.0*variance**2))
c v0clim=(intug*abs((1.0-exp(-abs(ahesscl
c & (modelhrs,mean,variance)
c & *dzsfc))*cos(ahesscl(modelhrs,mean,variance)*dzsfc))))
c
c v0clim=intug*((10.0/200.0)**(abs(kmclim(modelhrs,mean,
c & variance))))
c v0clim=intug**(abs(kmclim(modelhrs,mean,
c & variance)))
c
c if (v0clim.le.(4.0)) then
c v0clim=4.0
c endif
c end

FUNCTION autocon(sprh)
real autocon,sprh,critsprh,k1
k1=1.0E-4
critsprh=0.01
autocon=k1*(sprh-critsprh)
end

FUNCTION powerlog(wind,toplevel,botlevel)
real powerlog,power,wind,toplevel,botlevel,rough
rough=0.01
power=(1.0/(log(toplevel/rough)))
powerlog=(wind*((toplevel/botlevel)**power))
end

FUNCTION ug(zmeters)
real ug,zmeters
common/com8/zri,tri,intug
real zri,tri,intug
common/com11/ihess,ustar
real ihess,ustar

```

```

common/com2/fcori,zair,z0,zsfc,v0,grav
real fcori,zair,z0,zsfc,v0,grav

ug=v0/abs((sqrt(1.0+exp(-2.0*ihess*zometers)-
& 2.0*exp(-ihess*zometers)*cos(ihess*zometers))))
end

```



## *Vita*

Andrew Curtis Goodnite, the son of Ray and Mary Goodnite, was born on May 10, 1965, in Point Pleasant, West Virginia. He graduated from Wahama High School in June, 1983. After graduation, Andrew immediately married his high school sweetheart, the former Regina Lynn Clarke, daughter of Milton and Audrey Clarke of Letart, West Virginia.

In September 1983, Andrew enlisted in the United States Air Force as a personnel specialist. After graduating with honors from personnel specialist school, he was assigned to Wright Patterson Air Force Base Ohio. While assigned at Wright Patterson, Andrew was recognized in many ways, he received the John L. Levitow Honor Graduate award from both the Airman Leadership School and the Noncommissioned Officer Leadership School. Also, in February 1986, he received the Wright Patterson Air Force Base Airman of the Year award. On August 31, 1987, Jessica Elisabeth Goodnite was born to Andrew and Regina.

In May 1988, Andrew was selected to attend the University of Arizona to obtain a degree in Meteorology under the Airman Education and Commissioning Program (AECPP) program. While attending the University of Arizona on March 20, 1991, Amy Christine Goodnite was born to Andrew and Regina. In May 1992, Andrew graduated Magna Cum Laude from the University of Arizona with a Bachelor of Science Degree in Meteorology. In the summer of 1992, he attended the Officer Training School at Lackland AFB Texas and in September 1992 was commissioned as a second lieutenant in the Air Force.

*Vita*

Andrew Curtis Goodnite, [REDACTED]

[REDACTED] He graduated from Wahama High School in June, 1983. After graduation, Andrew immediately married his high school sweetheart, the former Regina Lynn Clarke, daughter of Milton and Audrey Clarke of Letart, West Virginia.

In September 1983, Andrew enlisted in the United States Air Force as a personnel specialist. After graduating with honors from personnel specialist school, he was assigned to Wright Patterson Air Force Base Ohio. While assigned at Wright Patterson, Andrew was recognized in many ways, he received the John L. Levitow Honor Graduate award from both the Airman Leadership School and the Noncommissioned Officer Leadership School. Also, in February 1986, he received the Wright Patterson Air Force Base Airman of the Year award. On August 31, 1987, Jessica Elisabeth Goodnite was born to Andrew and Regina.

In May 1988, Andrew was selected to attend the University of Arizona to obtain a degree in Meteorology under the Airman Education and Commissioning Program (AECPP) program. While attending the University of Arizona on [REDACTED] Amy Christine Goodnite was born to Andrew and Regina. [REDACTED] Andrew graduated Magna Cum Laude from the University of Arizona with a Bachelor of Science Degree in Meteorology. In the summer of 1992, he attended the Officer Training School at Lackland AFB Texas and in September 1992 was commissioned as a second lieutenant in the Air Force.

| REPORT DOCUMENTATION PAGE                                                                                                                                                                                                                                                                                                                                                                                                                                                                                                                                                                                                                                                                                                                                                                                                                                                                                                                                                                                                                                                                                                                                       |                                                |                                               | Form Approved<br>OMB No. 0704-0188               |                                           |
|-----------------------------------------------------------------------------------------------------------------------------------------------------------------------------------------------------------------------------------------------------------------------------------------------------------------------------------------------------------------------------------------------------------------------------------------------------------------------------------------------------------------------------------------------------------------------------------------------------------------------------------------------------------------------------------------------------------------------------------------------------------------------------------------------------------------------------------------------------------------------------------------------------------------------------------------------------------------------------------------------------------------------------------------------------------------------------------------------------------------------------------------------------------------|------------------------------------------------|-----------------------------------------------|--------------------------------------------------|-------------------------------------------|
| Public reporting burden for this collection of information is estimated to average 1 hour per response, including the time for reviewing instructions, searching existing data sources, gathering and maintaining the data needed, and completing and reviewing the collection of information. Send comments regarding this burden estimate or any other aspect of this collection of information, including suggestions for reducing this burden, to Washington Headquarters Services, Directorate for Information Operations and Reports, 1215 Jefferson Davis Highway, Suite 1204, Arlington, VA 22202-4302, and to the Office of Management and Budget, Paperwork Reduction Project (0704-0188), Washington, DC 20503.                                                                                                                                                                                                                                                                                                                                                                                                                                      |                                                |                                               |                                                  |                                           |
| 1. AGENCY USE ONLY (Leave blank)                                                                                                                                                                                                                                                                                                                                                                                                                                                                                                                                                                                                                                                                                                                                                                                                                                                                                                                                                                                                                                                                                                                                |                                                | 2. REPORT DATE<br>March 1997                  |                                                  | 3. REPORT TYPE AND DATES COVERED<br>Final |
| 4. TITLE AND SUBTITLE<br>Adaptation of the Air Weather Service Fog Model to Forecast Radiation Fog Events in the Southeast United States                                                                                                                                                                                                                                                                                                                                                                                                                                                                                                                                                                                                                                                                                                                                                                                                                                                                                                                                                                                                                        |                                                |                                               | 5. FUNDING NUMBERS                               |                                           |
| 6. AUTHOR(S)<br><br>Andrew C. Goodnite, Capt, USAF                                                                                                                                                                                                                                                                                                                                                                                                                                                                                                                                                                                                                                                                                                                                                                                                                                                                                                                                                                                                                                                                                                              |                                                |                                               |                                                  |                                           |
| 7. PERFORMING ORGANIZATION NAME(S) AND ADDRESS(ES)<br>AFIT/ENP (Bldg 640)<br>2950 P. Street<br>Wright Patterson AFB OH 45433-7765                                                                                                                                                                                                                                                                                                                                                                                                                                                                                                                                                                                                                                                                                                                                                                                                                                                                                                                                                                                                                               |                                                |                                               | 8. PERFORMING ORGANIZATION REPORT NUMBER         |                                           |
| 9. SPONSORING / MONITORING AGENCY NAME(S) AND ADDRESS(ES)<br>HQ AWS/XOX<br>102 W. Losey Street<br>Scott AFB IL 62225-5206<br>Dr W. Dale Meyer<br>DSN: 576-3350 Ext: 444                                                                                                                                                                                                                                                                                                                                                                                                                                                                                                                                                                                                                                                                                                                                                                                                                                                                                                                                                                                         |                                                |                                               | 10. SPONSORING / MONITORING AGENCY REPORT NUMBER |                                           |
| 11. SUPPLEMENTARY NOTES                                                                                                                                                                                                                                                                                                                                                                                                                                                                                                                                                                                                                                                                                                                                                                                                                                                                                                                                                                                                                                                                                                                                         |                                                |                                               |                                                  |                                           |
| 12a. DISTRIBUTION / AVAILABILITY STATEMENT<br><br>Unlimited                                                                                                                                                                                                                                                                                                                                                                                                                                                                                                                                                                                                                                                                                                                                                                                                                                                                                                                                                                                                                                                                                                     |                                                |                                               | 12b. DISTRIBUTION CODE                           |                                           |
| 13. ABSTRACT (Maximum 200 words)<br><br>This research examined the performance of the Air Weather Service (AWS) Fog Model and the potential for using it in the Southeast United States for predicting fog. A correlation study was performed by comparing different weather elements in observations that met radiational cooling conditions to the observed visibility. This correlation study showed that the 22 UTC dewpoint depression was correlated (0.60) with early morning fog and no other weather elements that are commonly observed had significant correlation with early morning fog. A verification study was conducted on the Saint Louis University (SLU) version of the fog model. This verification study showed that the fog model has an underforecasting bias in the summer season and an overforecasting bias in the fall season and that persistence forecasts beats fog model forecasts for both seasons. A sensitivity study was conducted on the fog model. The sensitivity study showed that the fog model is sensitive to the value input for wind speed; the fog model predicts more fog events as the wind speed is increased. |                                                |                                               |                                                  |                                           |
| 14. SUBJECT TERMS<br>Fog Forecasting, Boundary Layer Model, Fog Model Verification                                                                                                                                                                                                                                                                                                                                                                                                                                                                                                                                                                                                                                                                                                                                                                                                                                                                                                                                                                                                                                                                              |                                                |                                               | 15. NUMBER OF PAGES<br>137                       |                                           |
|                                                                                                                                                                                                                                                                                                                                                                                                                                                                                                                                                                                                                                                                                                                                                                                                                                                                                                                                                                                                                                                                                                                                                                 |                                                |                                               | 16. PRICE CODE                                   |                                           |
| 17. SECURITY CLASSIFICATION OF REPORT<br>Unclassified                                                                                                                                                                                                                                                                                                                                                                                                                                                                                                                                                                                                                                                                                                                                                                                                                                                                                                                                                                                                                                                                                                           | 18. SECURITY CLASSIFICATION OF THIS PAGE<br>UL | 19. SECURITY CLASSIFICATION OF ABSTRACT<br>UL | 20. LIMITATION OF ABSTRACT<br>UL                 |                                           |

## GENERAL INSTRUCTIONS FOR COMPLETING SF 298

The Report Documentation Page (RDP) is used in announcing and cataloging reports. It is important that this information be consistent with the rest of the report, particularly the cover and title page. Instructions for filling in each block of the form follow. It is important to *stay within the lines* to meet *optical scanning requirements*.

**Block 1. Agency Use Only (Leave blank).**

**Block 2. Report Date.** Full publication date including day, month, and year, if available (e.g. 1 Jan 88). Must cite at least the year.

**Block 3. Type of Report and Dates Covered.** State whether report is interim, final, etc. If applicable, enter inclusive report dates (e.g. 10 Jun 87 - 30 Jun 88).

**Block 4. Title and Subtitle.** A title is taken from the part of the report that provides the most meaningful and complete information. When a report is prepared in more than one volume, repeat the primary title, add volume number, and include subtitle for the specific volume. On classified documents enter the title classification in parentheses.

**Block 5. Funding Numbers.** To include contract and grant numbers; may include program element number(s), project number(s), task number(s), and work unit number(s). Use the following labels:

|                             |                                     |
|-----------------------------|-------------------------------------|
| <b>C</b> - Contract         | <b>PR</b> - Project                 |
| <b>G</b> - Grant            | <b>TA</b> - Task                    |
| <b>PE</b> - Program Element | <b>WU</b> - Work Unit Accession No. |

**Block 6. Author(s).** Name(s) of person(s) responsible for writing the report, performing the research, or credited with the content of the report. If editor or compiler, this should follow the name(s).

**Block 7. Performing Organization Name(s) and Address(es).** Self-explanatory.

**Block 8. Performing Organization Report Number.** Enter the unique alphanumeric report number(s) assigned by the organization performing the report.

**Block 9. Sponsoring/Monitoring Agency Name(s) and Address(es).** Self-explanatory.

**Block 10. Sponsoring/Monitoring Agency Report Number.** (If known)

**Block 11. Supplementary Notes.** Enter information not included elsewhere such as: Prepared in cooperation with...; Trans. of...; To be published in.... When a report is revised, include a statement whether the new report supersedes or supplements the older report.

**Block 12a. Distribution/Availability Statement.** Denotes public availability or limitations. Cite any availability to the public. Enter additional limitations or special markings in all capitals (e.g. NOFORN, REL, ITAR).

**DOD** - See DoDD 5230.24, "Distribution Statements on Technical Documents."

**DOE** - See authorities.

**NASA** - See Handbook NHB 2200.2.

**NTIS** - Leave blank.

**Block 12b. Distribution Code.**

**DOD** - Leave blank.

**DOE** - Enter DOE distribution categories from the Standard Distribution for Unclassified Scientific and Technical Reports.

**NASA** - Leave blank.

**NTIS** - Leave blank.

**Block 13. Abstract.** Include a brief (*Maximum 200 words*) factual summary of the most significant information contained in the report.

**Block 14. Subject Terms.** Keywords or phrases identifying major subjects in the report.

**Block 15. Number of Pages.** Enter the total number of pages.

**Block 16. Price Code.** Enter appropriate price code (*NTIS only*).

**Blocks 17. - 19. Security Classifications.** Self-explanatory. Enter U.S. Security Classification in accordance with U.S. Security Regulations (i.e., UNCLASSIFIED). If form contains classified information, stamp classification on the top and bottom of the page.

**Block 20. Limitation of Abstract.** This block must be completed to assign a limitation to the abstract. Enter either UL (unlimited) or SAR (same as report). An entry in this block is necessary if the abstract is to be limited. If blank, the abstract is assumed to be unlimited.